



US Army Corps
of Engineers®
Engineer Research and
Development Center

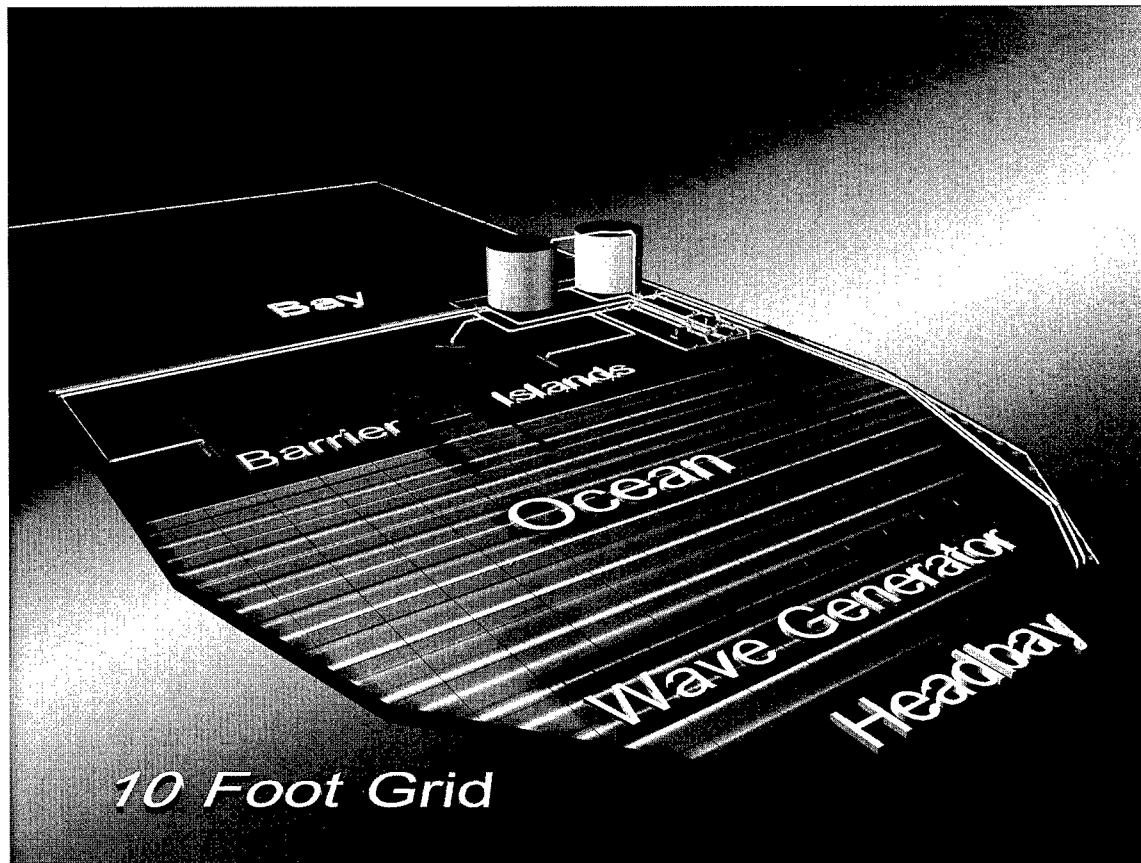
Coastal Inlets Research Program

Tidal Inlet Equilibrium Area Experiments, Inlet Laboratory Investigations

William C. Seabergh, David B. King, Jr.,
and Bettye E. Stephens

September 2001

**Coastal and Hydraulics
Laboratory**



The contents of this report are not to be used for advertising, publication, or promotional purposes. Citation of trade names does not constitute an official endorsement or approval of the use of such commercial products.

The findings of this report are not to be construed as an official Department of the Army position, unless so designated by other authorized documents.



PRINTED ON RECYCLED PAPER

Tidal Inlet Equilibrium Area Experiments, Inlet Laboratory Investigations

by William C. Seabergh, David B. King, Jr., and Bettye E. Stephens

Coastal and Hydraulics Laboratory
U.S. Army Engineer Research and Development Center
3909 Halls Ferry Road
Vicksburg, MS 39180-6199

Final report

Approved for public release; distribution is unlimited

20020114 154

Prepared for U.S. Army Corps of Engineers
Washington, DC 20314-1000

Under Inlet Laboratory Investigations Work Unit 32935

Contents

Preface.....	vi
1—Introduction	1
Background.....	1
Purpose of Model Investigation	2
2—Experiment Arrangement	4
Idealized Inlet Facility.....	4
Instrumentation	7
3—Experiment Procedures	8
Experiment Design.....	8
Description of Experiment Conditions and Measurements	8
4—Experiments and Results	11
Description of Experiments.....	11
Run 1.....	11
Run 2.....	13
Run 3.....	13
Run 4.....	14
Run 5.....	14
Run 6.....	17
Run 7.....	17
Run 8.....	17
Run 9.....	19
Discussion of Results	19
Inlet hydraulics	19
Inlet morphology	20
5—Conclusions.....	27
References	29
Appendix A: Detailed Experiment Data.....	A1

List of Figures

Figure 1.	Idealized inlet model research facility	5
Figure 2.	Idealized inlet entrance channel with oblique wave approaching inlet.....	5
Figure 3.	Grain size distributions of sands used in this study.....	9
Figure 4.	Location of cross-section measurement stations in the inlet.....	10
Figure 5.	Initial inlet channel at start of Run 1	13
Figure 6.	Hour 31 of Run 4 showing the widening of the inlet 15 hr after waves were initiated.....	15
Figure 7.	Hour 144 of Run 4, showing the inlet after migrating bayward and reaching equilibrium.....	15
Figure 8.	Ocean and bay tidal elevations for Runs 4 and 8, representing the two types of tidal conditions occurring for the 26- and 105-min tidal periods, respectively.....	16
Figure 9.	Hours 1 and 20 of Run 5. Hour 1 was at initiation of run, hour 20 at conclusion of tidal portion of run (no waves up to this point)	17
Figure 10.	The inlet at Run 8.....	18
Figure 11.	Tidal cycle 1 at start of Run 9 and tidal cycle 54 at the conclusion of the tidal current experiment (no waves).....	19
Figure 12.	Comparison of measured and calculated equilibrium areas.....	21
Figure 13.	Actual versus calculated area for Jarrett's tidal prism minimum equilibrium area relationship	22
Figure 14.	Actual versus calculated area for tidal prism – minimum equilibrium area relationship of this report	23
Figure 15.	Field and laboratory tidal prism and inlet minimum cross-section area plotted with Jarrett's equation	24
Figure 16.	Laboratory data for tidal prism versus minimum cross-section area for tide-only and tide-plus-wave conditions.....	25

List of Tables

Table 1.	Model-Prototype Scale Relations	6
Table 2.	Inlet Equilibrium Experiments: Conditions and Results	12
Table 3.	Widths, Depths, Areas, and Aspect Ratios for Runs 4, 5, 8, and 9.....	20
Table 4.	Calculation of Velocity in Laboratory and Field Inlet with Manning's Equation.....	26
Table B1.	CIRP Run 4.....	B2
Table B2.	CIRP Run 5.....	B10
Table B3.	CIRP Run 7.....	B11
Table B4.	CIRP Run 8.....	B12
Table B5.	CIRP Run 9.....	B13

Preface

The research investigation described herein was conducted as part of the Coastal Inlets Research Program (CIRP) under Work Unit 32935, "Inlet Laboratory Investigations." Overall program management for CIRP is directed by the Hydraulic Design Section of Headquarters, U.S. Army Corps of Engineers (HQUSACE). Program Monitors for the CIRP at HQUSACE are Messrs. Barry W. Holliday and Charles B. Chesnutt. The Program Manager was Mr. E. Clark McNair, Jr., Coastal and Hydraulics Laboratory (CHL), Vicksburg, MS, U.S. Army Engineer Research and Development Center (ERDC), followed by Dr. William McAnally, Technical Director, CHL. CIRP Technical Leader is Dr. Nicholas C. Kraus, Coastal Sediments and Engineering Division, CHL. Mr. William C. Seabergh, Harbors and Entrances Branch, Navigation and Harbors Division, CHL, is Principal Investigator of the Inlet Laboratory Investigations Work Unit.

The mission of CIRP is to conduct applied research to improve USACE capability to manage federally maintained inlets, which exist on all coasts of the United States (including Atlantic, Gulf, Pacific, and the Great Lakes regions). Objectives are to (a) make management of channels—design, maintenance, and operation—more effective to reduce the cost of dredging, and (b) preserve the adjacent beaches in a systems approach that treats the inlet and beach together. To achieve these objectives, CIRP includes work units on short-wave and circulation modeling, channels and adjacent shorelines, inlet scour, laboratory investigations, field investigations, and technology transfer.

The study was conducted by CHL personnel, under the general direction of Dr. James R. Houston, Director, and Mr. Thomas W. Richardson, Acting Director. Direct guidance was provided by Mr. Dennis Markle, Chief, Harbors and Entrances Branch. Experiments were conducted by Ms. Bettye E. Stephens and Mr. Hugh F. Acuff, Jr., Civil Engineering Technicians, Harbors and Entrances Branch, under the direction of Mr. William C. Seabergh, Principal Investigator, and Dr. David B. King, Prototype Measurement and Analysis Branch, Coastal Sediments and Engineering Division, CHL. Mr. Wallace Guy of the Information Technology Laboratory, ERDC, provided instrumentation support. This report was prepared by Mr. Seabergh, Dr. King, and Ms. Stephens. Word processing and formatting were completed by Ms. Holley Messing, Coastal Sediments and Engineering Division. Ms. Leonette J. Thomas, Harbors and Entrances Branch, contributed to preparation of figures.

At the time of publication of this report, Dr. James R. Houston was Director of ERDC, and COL John W. Morris III, EN, was Commander and Executive Director.

The contents of this report are not to be used for advertising, publication, or promotional purposes. Citation of trade names does not constitute an official endorsement or approval for the use of such commercial products.

1 Introduction

Background

The equilibrium area concept for a tidal inlet has been a useful approach to understand the adjustment of the minimum cross-sectional area of an entrance channel to the basic hydraulic and sedimentation characteristics of the inlet it serves. Based on a concept originated by LeConte (1905), O'Brien (1931, 1969) examined field data from tidal inlets through sandy barriers on the west coast of the United States and determined a relationship between the minimum cross-sectional flow area of the entrance channel and the tidal prism (the volume of water flowing into the bay during the flood tidal cycle or conversely, the volume of water flowing out of the bay during the ebb portion of the tidal cycle usually at spring tide conditions). This relationship defines the equilibrium area.

The form of this equation is

$$A_c = CP^n \quad (1)$$

where

A_c = the minimum inlet cross-sectional area in the equilibrium condition

C = an empirically determined coefficient

P = the tidal prism (typically during the spring tide)

n = an exponent usually slightly less than unity

C and n are usually determined by best fits to data sets. Many investigators have found regional differences in the values of C and n .

Jarrett (1976) refined Equation 1 and developed expressions for the east, west, and Gulf coasts of the United States based on additional field data. Others have examined this relationship with regard to reduced wave exposure of more protected shorelines (Riedel and Gourlay 1980) and relative to inlet channel area magnitude (Byrne, Gammisch, and Thomas 1980). Kraus (1998) developed a process-based model to calculate equilibrium area, and Hughes (1999) introduced a simple expression relating maximum discharge to depth of scour in a coastal inlet. Laboratory inlet work for equilibrium areas with movable beds has been

performed by McNair (1976), Mayor-Mora (1973, 1977), and Delmonte and Johnson (1971).

Purpose of Model Investigation

The purpose of the investigation was to generate equilibrium inlet areas where tide period, sediment size, and wave conditions were varied (including the situation of no waves present), creating differing hydraulic conditions. These data were then to be used to examine an analytical solution to O'Brien's tidal prism/minimum inlet cross-sectional area relationship:

$$A_c = \frac{\pi P}{T U_m} \quad (2)$$

where

T = tidal period

U_m = maximum velocity of water passing through the inlet

This relationship was analytically derived in O'Brien (1969) from the same continuity equation considered by Keulegan (1967) in arriving at his inlet hydraulics relationships. The standard simplifying assumptions made by Keulegan (1967) of constant bay surface area and inlet channel cross-section area during the tidal cycle were invoked. Also assumed was uniform rise and fall of bay level in a sinusoidal manner. Van de Kreeke (1992) discusses this development and also mentions that the derivation is based on a sinusoidal current in the channel. If the semidiurnal tide period of 44,712 sec and a rule-of-thumb current for large inlets in equilibrium of 3.28 ft/sec (1.0 m/sec) (van de Kreeke 1992) is substituted for U_m in Equation 2, the resultant equation (in units of feet),

$$A_c = 2.14 \times 10^{-5} P \quad (3)$$

is very close to O'Brien's (1969) relation,

$$A_c = 2.0 \times 10^{-5} P \quad (4)$$

developed from data for inlets without jetties. The value of the equilibrium current is dependent on the littoral climate (local wave and sediment characteristics) affecting the inlet, i.e., the current needed to maintain the inlet, scouring the incoming littoral sand.

An idealized tidal inlet physical model (described in Chapter 2) molded in concrete was constructed for the present study. It had a gorge or throat (region of minimum area) of a cross-sectional area large enough that it could be filled in with sand to create a movable-bed region, which could then respond to the action of tidal currents and waves. The cross-sectional area could then adjust to its equilibrium area, dependent on the tidal period and ocean tide range, which controlled the maximum velocity and the tidal prism.

The experiment was initiated with a relatively small pilot channel, which usually enlarged over time to an equilibrium area, i.e., an area that did not change significantly after a certain period of time. Initially, only tidal currents were the forcing function. However, for some tests, waves were generated after an equilibrium area was reached for the tidal-current-only condition, and testing continued until a second equilibrium occurred.

The experiments also provided valuable information for future phases of the study program on inlet stability. Appropriate equilibrium areas would be useful in the design of future laboratory work concerning ebb and flood shoals, for example.

2 Experiment Arrangement

This chapter describes the design of the idealized physical model inlet, arrangement of equipment, and measurement procedures.

Idealized Inlet Facility

An idealized inlet was designed to fit in a 46-m- (150-ft-) wide by 99-m- (325-ft-) long concrete basin with a 0.6-m- (2-ft-) high wall that is part of the Idealized Inlet facility (Seabergh 1999) of the Coastal Inlets Research Program (CIRP). The approach was to design an inlet with simplified bathymetry and fairly steep beach slopes so that additional features (such as an ebb shoal) could easily be added. Also, it was anticipated that a fine sand would serve as both a tracer and as a fully mobile bed that could be placed over the concrete bottom in a thick layer. A 1:50 undistorted scale was assumed to determine reasonable inlet dimensions to model; however, other scales can easily be assumed to accommodate the study of specific processes because of the simplified bathymetry.

Figure 1 shows the basin area. The ocean-side parallel contours were determined by following an equilibrium profile equation from Dean (1977):

$$h = Ax^{2/3} \quad (5)$$

where

h = still-water depth

A = coefficient determined by sediment characteristics

x = distance seaward from the shoreline

A value of $A = 0.24, \text{ m}^{1/3}$, was used as it represented a relatively steep beach. The contoured ocean beach slope extends to the 18.3-cm (0.6-ft) mean low water (mlw) depth (or 9.1-m (30-ft) depth if scaled by 1:50) and is linearly transitioned to the basin floor at a depth of 30.4 cm (1.0 ft) (or 15.2 cm (50-ft) depth if scaled by 1:50). The inlet throat region converges to a depth of 15.2 cm (or if scaled to 1:50, 7.6 m (25 ft)) relative to an mlw datum. The minimum width is 244 cm across the inlet between mlw contours (or if scaled by 1:50, it represents a width of 122 m (400 ft)). Figure 2 shows the inlet throat and entrance channel with

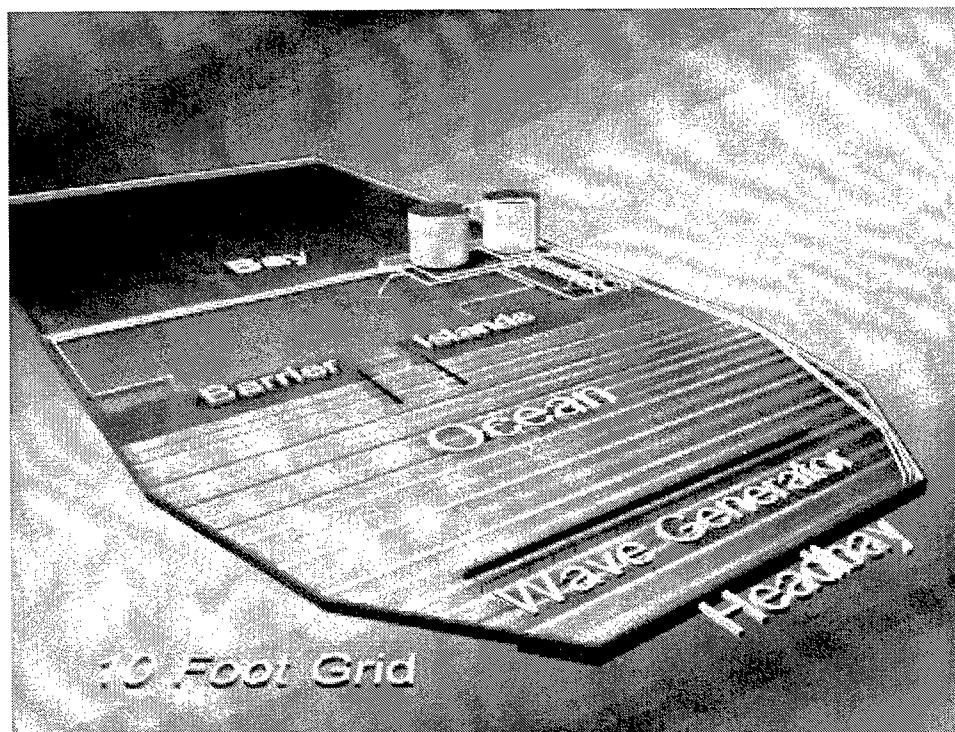


Figure 1. Idealized inlet model research facility

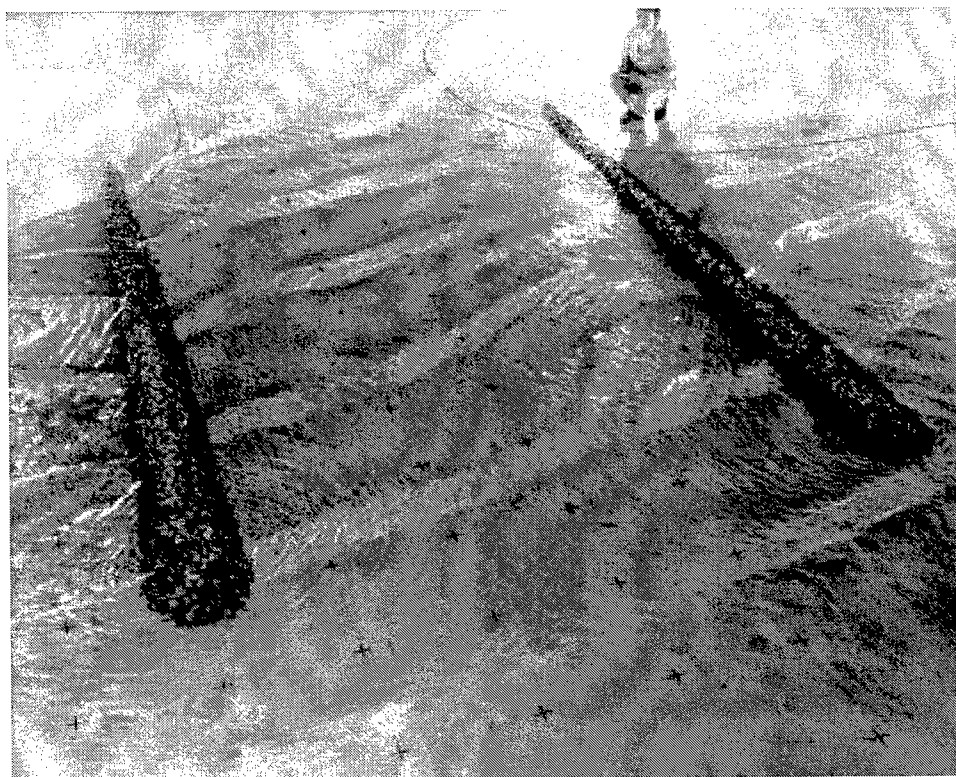


Figure 2. Idealized inlet entrance channel with oblique waves approaching inlet (spacing 62 cm between cross markings on research facility basin floor)

parallel jetties, which have a spacing of 3.66 m (12.0 ft) and extend 5.5 m (18 ft) offshore.

Based on Froude's model law (Stevens 1942; Hughes 1993) and the linear scale of 1:50, the model-prototype relations in Table 1 were derived. Dimensions are in terms of length L and time T . As mentioned previously, other scales may be assumed for the bathymetry, so different scaling relationships would apply other than those listed in Table 1.

Table 1 Model-Prototype Scale Relations		
Characteristic	Dimension	Model-Prototype Scale Relation
Length	L	1:50
Area	$A_r = L_r^2$	1:2,500
Volume	$V_r = L_r^3$	1:125,000
Time (tidal and short wave period)	$T_r = L_r^{1/2}$	1:7.07
Velocity	$V_r = L_r/T_r$	1:7.07

The Idealized Inlet Facility is connected to a large sump (volume of 1.98×10^6 L (523,000 gal)) for water exchange so that tides may be produced in the facility ocean to drive tidal currents into and out of the inlet bay. A constant inflow is introduced from the sump into the model ocean while a "rolling" gate either reduces or increases flow area over an exit pipe into the sump, which causes ocean rise or fall, respectively. The rolling gate is regulated by a controller connected to a feedback loop comparing actual to desired water level. The two cylindrical shapes in the upper middle of Figure 1 are storage tanks, each holding 182,000 L (48,000 gal) of water. They can be used to simulate a much larger bay area by storing flood tide water and releasing it back to the bay to flow to the ocean during ebb flow. They were not used in this study as the size of bay surface area relative to channel cross section was adequate. Pumps and control valves associated with this procedure are located adjacent to the storage tanks.

A steady-state flow may also be set up for ebbing or flooding currents. The piping system is shown in Figure 1. Water is either collected (flood flow) or distributed (ebb flow) through a system of manifolds in the bay, which may be adjusted for one, two, or three bay channels or a uniform flow across the bay. Water is either released (flood flow) or taken from (ebb flow) the ocean headbay to complete the circulation energized by the pumps located in front of the tanks in Figure 1.

A 24.4-m- (80-ft-) long wave generator (Figure 1) produced either irregular or monochromatic waves. Unscaled wave periods could be varied from 0.5 to about 3 sec and wave heights to 10 cm (at the generator location and for this particular setup of the generator). Wave angle could be varied for specific tests by moving the generator on its castors and orienting it at an angle to the beach.

Instrumentation

Wave height and period data were collected on electrical capacitance wave gauges calibrated daily with a computer-controlled procedure incorporating a least-square fit of measurements at 11 steps. This averaging technique, involving 21 voltage samples per gauge, minimizes the error of slack in the gear drives and hysteresis in the sensors. Typical calibration errors are less than 1 percent of full scale for the capacitance wave gauges. Wave signal generation and data acquisition were controlled by a Digital Equipment Corporation (DEC) MicroVax I computer.

Water velocity data were collected with a SonTek, Inc., two-dimensional Acoustic-Doppler Velocimeter (ADV) with a side-looking probe oriented to collect x-y velocity information in a horizontal plane. Samples were collected at 10 Hz, though the instrument makes 250 pings/sec and averages for each output sample. Accuracy is 0.5 percent of the measured velocity, with resolution of 0.1 mm/sec and threshold of 0.1 cm/sec. The probe samples a 0.25-cm³ volume located 5 cm from the sensor heads.

3 Experiment Procedures

This chapter discusses the procedures performed and measurements obtained in the inlet channel equilibrium area experiments.

Experiment Design

The purpose of this study was to examine tidal inlet equilibrium areas in a laboratory (physical model) facility. Determining, or evolving, an equilibrium area required a movable bed. The approach was to fill the inlet gorge area with sand, cut a small pilot channel, and initiate the simulation of tides, permitting tidal currents to widen and deepen the channel until it reached an equilibrium state. Once an equilibrium area was reached, waves with crests parallel to the shore were run with the tide, and the test was continued until there was no significant change in area. Periodic channel cross-section areas were measured to determine channel area change through the inlet gorge. To study the effect of tide period T (Equation 2), two tide periods were reproduced.

Description of Experiment Conditions and Measurements

Two tidal periods were reproduced: 105.4 min (which is equivalent to a semi-diurnal model tide period if a 1:50 scale is assumed) and a 26.35-min tide, or one fourth the first period chosen. These tidal periods are greater than the minimum period (25 min) that McDowell (1955) found was necessary to ensure well-developed velocity gradients near the bottom for physical model studies. The tide range for all tests was 30.5 mm (0.1 ft). Also, two sand sizes were used: median diameter D_{50} of 0.13- and 0.26-mm quartz sand. Gradation curves for each sand are shown in Figure 3. The finer sand was a packaged molding sand, and the larger sand was from a nearby natural sand source and was available from previous movable-bed models at the U.S. Army Engineer Research and Development Center. About 3,000 kg (7,000 lb) of each type of sand was spread in the model inlet and adjacent regions. The following measurements were obtained: one velocity station at the minimum cross-section area at the channel center line, measured with the SonTek ADV at about 2 cm (0.8 in.) below the low-tide level (tide range about 3 cm (1.18 in.)); tidal elevations for ocean and bay, measured well away from the influence of high-velocity flow in the inlet; and cross-sectional area

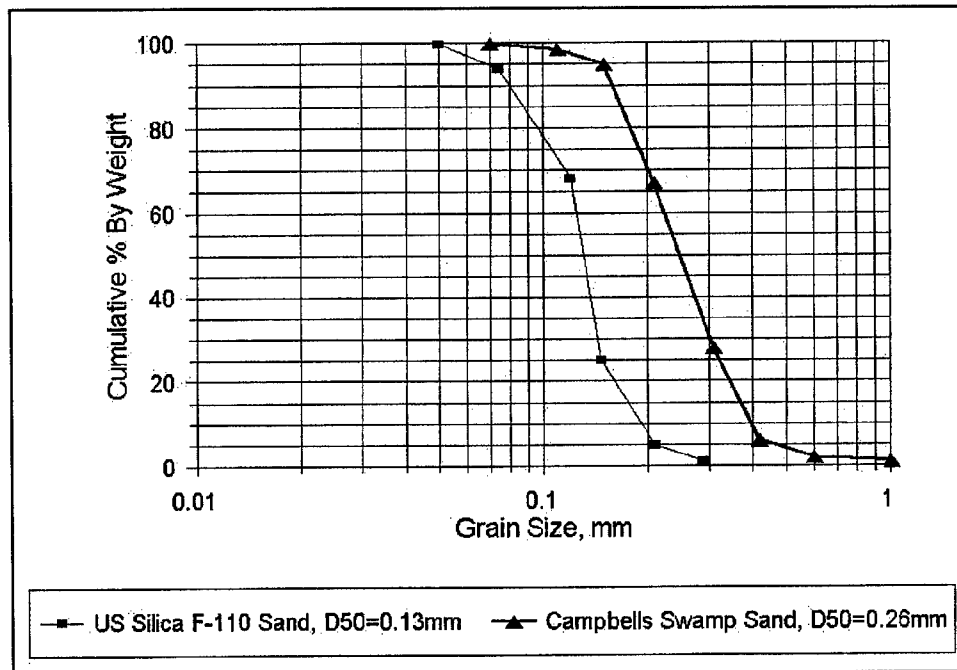


Figure 3. Grain size distributions of sands used in this study

measurements, performed by hand, measured down from a reference datum. The top of a 15-cm (6-in.) aluminum box beam was the reference. Depth measurements were made from the top of the beam to the sand bed at a variable spacing that defined breaks in slopes (horizontal spacings were as close as 1.5 cm (0.6 in.), and vertical (depth) measurements were read to 0.3 cm (0.12 in.).

At the start of a test, cross-sectional measurements were made at five locations across the inlet gorge area, spaced 0.6 m (2 ft) apart (Figure 4). Initially, for the longer tidal period, all the locations were periodically measured until a configuration of the inlet was reached where one location was the obvious minimum area, and this range was monitored from then on. Measurements were made during the test operation and were taken during slack water. For the shorter tide period, because of the short time span for slack water, measurements were usually limited to the minimum area cross section.

The tide was run without the aid of the storage tanks, so the bay area of 2,713 sq m (29,000 sq ft) contained the tidal prism. The length of the tidal waves used was much greater than the bay dimensions, so that the assumption of a uniformly rising bay could be invoked to determine the tidal prism by multiplying surface area by bay tide range.

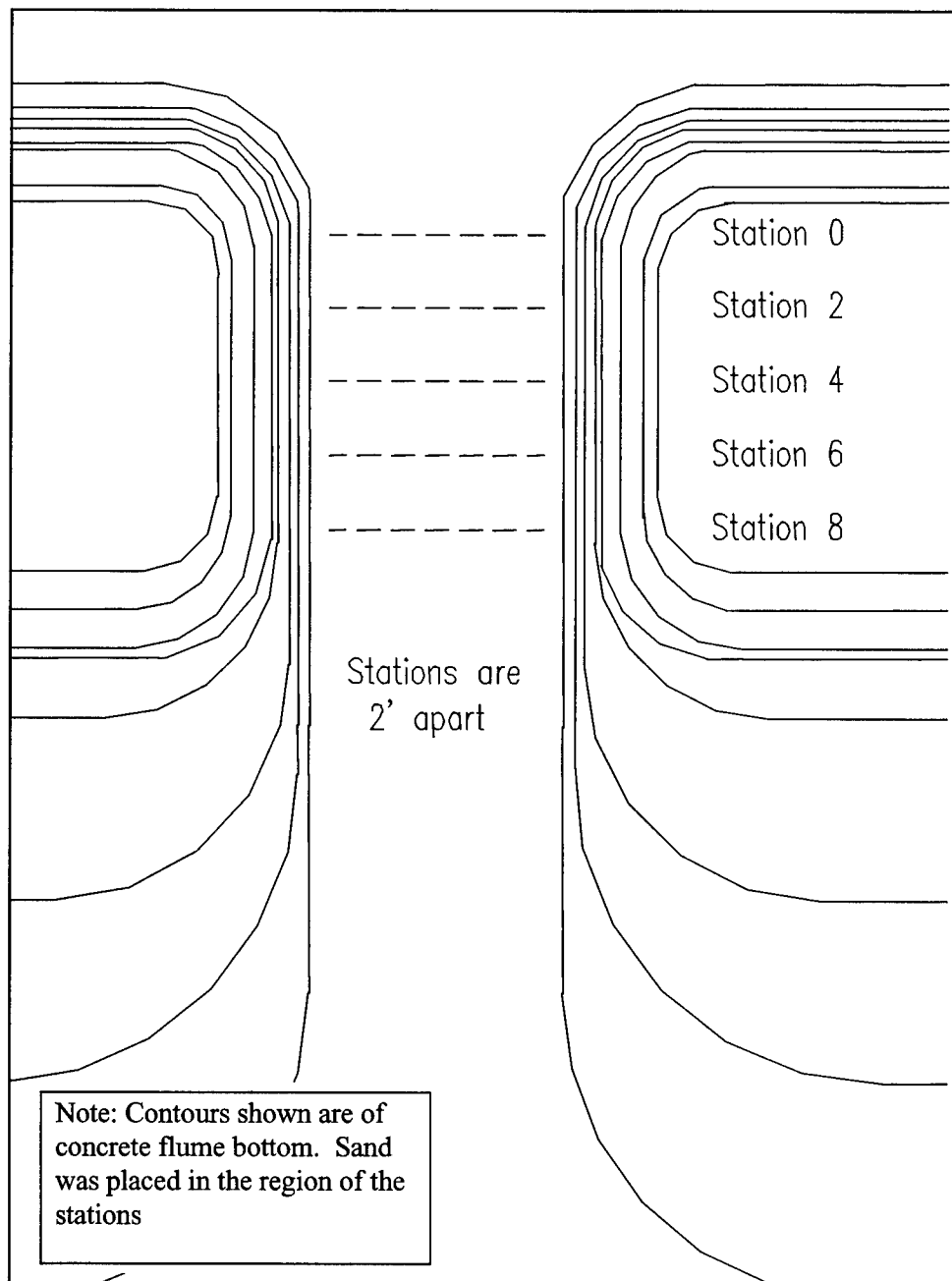


Figure 4. Location of cross-section measurement stations in the inlet. Contours are of the solid concrete bottom

4 Experiments and Results

This chapter first describes the experiments and the results achieved. The data are then compared with other laboratory and field data.

Description of Experiments

The initial sequence was a short series of runs to determine appropriate conditions for subsequent experiments. Table 2 summarizes the various runs and results. Typically a run was conducted without waves until equilibrium was reached for tidal conditions only, then waves were generated. The wave direction was perpendicular to the shoreline. Wave height at the generator (0.3-m water depth) was 3 cm with a 1-sec period. The waves were monochromatic. There was no sediment input from adjacent shorelines, so that only that sediment located on the inner shoulders and within the inlet entrance was available for transport in the inlet system. The initial experiments were performed with the fine sand (0.13 mm), and later experiments used the 0.26-mm sand. Two tidal periods, 1.76 hr (based on a Froudian scale of 1:50) and one-fourth that amount, or 0.44 hr, were run for each sand type. Measurements of channel area were made relative to mean tide level. The tide ranged ± 1.52 cm from 0.0 mean tide level. Water temperatures were in the range of 23 to 26 °C except for Run 9, where the

Appendix A provides detailed experiment information. Included are plots of minimum area, maximum velocity, maximum head difference, and bay tidal range over the test duration, typically recorded for each tidal cycle. Also included are inlet cross sections measured during and at the conclusion of the experiment. Discussion focusses primarily on Runs 4, 5, 8 and 9, which are complete experimental sets, run until an equilibrium area was obtained. Time series data for these runs are presented in Appendix B.

Run 1

This run was part of a series of preliminary experiments to determine appropriate initial operating conditions. Runs 1 to 3 involved the initial model arrangement while alterations were being made in channel depth and length, and so they were a continuum of trial experiments. An initial 4.4-m-long channel with

Table 2
Inlet Equilibrium Experiments: Conditions and Results

Run No.	Other I.D.	Sand Size, mm	Tide Period, min	Tide Cycles Start, Stop (Duration)	Wave Condition, H, T	Date	Equilibrium Area, sq m (sq ft)	Equilibrium Max Current m/sec (ft/sec)	Equilibrium Tidal Prism, cu m (cu ft)
1	Inlet 1	0.13	105	1, 1 (1)	none	7/15/96	-	-	-
	Inlet 2	0.13	mech problem	0 (0)	-	7/16/96	-	-	-
	Inlet 3	0.13	105	2, 4.5 (2.5)	none	7/16/96	-	-	-
2	Inlet 4	0.13	105	5, 7 (2)	none	7/17/96	-	-	-
3	Inlet 5	0.13	105	8, 10.5 (2.5)	(3 cm, 1 sec)	7/18/96	-	-	-
4	Inlet 6-6A	0.13	26	1, 15 (15)	none	7/19/96	0.053 (0.569)	0.396 (1.30)	9.82 (347)
	4Wav-4wav	0.13	26	16, 144 (128)	(3 cm, 1 sec)	7/24/96-8/2/96	0.061 (0.652)	0.314 (1.03)	8.20 (290)
5	5A-5E	0.13	105	1, 20 (20)	none	8/8/96-8/14/96	0.116 (1.249)	0.287 (0.94)	74.54 (2,634)
	5F-5H	0.13	105	21, 29 (8)	(3 cm, 1 sec)	8/15/96-8/19/96	0.148 (1.589)	0.271 (0.89)	71.29 (2,519)
6 (demo)	6A-6B	0.13	105	1, 4 (4)	(3 cm, 1 sec)	8/20/96-8/21/96	-	-	-
7	7A-7C	0.26	105	1.6 (6)	none	8/29/96-8/30/96	power failure		
8	8A-8B	0.26	105	1, 8 (8)	none	9/6/96-9/9/96	0.081 (0.875)	0.249 (0.82)	54.90 (1,940)
	8C-8D	0.26	105	9, 16 (8)	(3 cm, 1 sec)	9/11/96-9/12/96	0.086 (0.942)	0.274 (0.90)	57.36 (2,027)
9	9A-9H	0.26	26	1, 54 (54)	none	9/13/96-9/24/96	0.125 (1.347)	0.320 (1.05)	22.9 (811)

depth of 0.03 m (0.1 ft) and width of 0.3 m (1 ft) was carved in the sand from ocean to bay (Figure 5). One tidal cycle was run. Bay tide range was measured to be 10 percent of ocean range. The channel area was near or just greater than unstable equilibrium indicating it would most likely close, and the length/minimum area combination was judged to produce too much inlet choking. There was minimal response in the channel area.



Figure 5. Initial inlet channel at start of Run 1

Run 2

The inlet initial area was increased by mechanically deepening to 6.1 cm (0.2 ft). After 2.5 tide cycles the inlet minimum area was not appreciably changing. Maximum current had fallen to 22 cm/sec, and sediment movement was decreasing. The channel length/minimum area combination still created a strongly friction dominated inlet.

Run 3

The inlet channel was widened mechanically, and tide plus waves were run. Appreciable currents were maintained in the channel (39 cm/sec). It was judged that appropriate initial conditions were obtained.

Run 4

The tide period was changed to one-fourth the previous experiment or 26.4 min to evaluate the influence of tidal period on equilibrium area. Conditions appeared appropriate to evolve an equilibrium area, so that this became the first fully developed experiment for detailed data collection. Other initial conditions determined from the previous preliminary experiments were used. Initial minimum cross-sectional area was 0.04 sq m (0.45 sq ft). After 15 tidal cycles of tides-only condition, the minimum area had stabilized at 0.05 sq m (0.57 sq ft). The inlet width remained close to the initial width of 0.6 m (2.0 ft), with only slight slumping of its steep sides. Depths had increased from 0.07 to 0.09 m (0.22 to 0.29 ft). The sediment removed from the channel had transported both seaward and bayward initiating the creation of ebb and flood shoals, respectively. Starting with cycle 16, the 1-sec, 3-cm wave was initiated, with the generator parallel to the beach. The response was a slight widening at the oceanward side of the inlet (Figure 6, hour 31) and a bayward migration of the inlet itself as sediment was removed gradually from the inlet shoulders and introduced into the ebb and flood shoals. Figure 7 shows the inlet at the conclusion of the test at tidal cycle 144. The minimum area had migrated bayward and channel length shortened.

The bay tide range was nearly constant for the entire experiment, with a span between 0.3 and 0.33 cm (0.12 and 0.13 in.), which was one-tenth the ocean range. Figure 8 shows the ocean and bay tides. Velocity measurements were collected at one location within the inlet. Because the sensor was on a three-legged stand in the channel, it was not moved during the study. As the cross section in the channel changed, minimum area migrated. Also, a shoal developed, then moved. Therefore, a variation in velocity accompanied channel morphological variations. However, as the experiment was concluding, the velocity measurement, though not in the center of the minimum cross section, was located such that measurements representative of those in the minimum cross section were obtained. Maximum currents were 0.31 m/sec (1.03 ft/sec) at cycle 144 at a minimum area of 0.0606 sq m (0.652 sq ft).

Run 5

This experiment was conducted with the 105-min tide period. Based on results of the previous experiment, the inlet length was decreased to reduce run time. The inlet area increased from an initial minimum cross-sectional area of 0.053 sq m (0.57 sq ft) to an equilibrium area of 0.12 sq m (1.30 sq ft) by tidal cycle 16 with a maximum current of 0.29 m/sec (0.94 ft/sec). Figure 9 shows the widening of the inlet from the tide-only condition. The wave generator was then run with the standard wave condition until a new equilibrium was reached after an additional 13 tidal cycles. The minimum area increased to 0.148 sq m (1.59 sq ft), with the maximum current dropping to 0.27 m/sec (0.89 ft/sec). Figure 9 shows the widening of the channel caused by the tidal currents. It is interesting to note from Table 2 that the tidal prism is significantly larger for Run 5 due to the longer tidal period, allowing greater filling of the bay and different

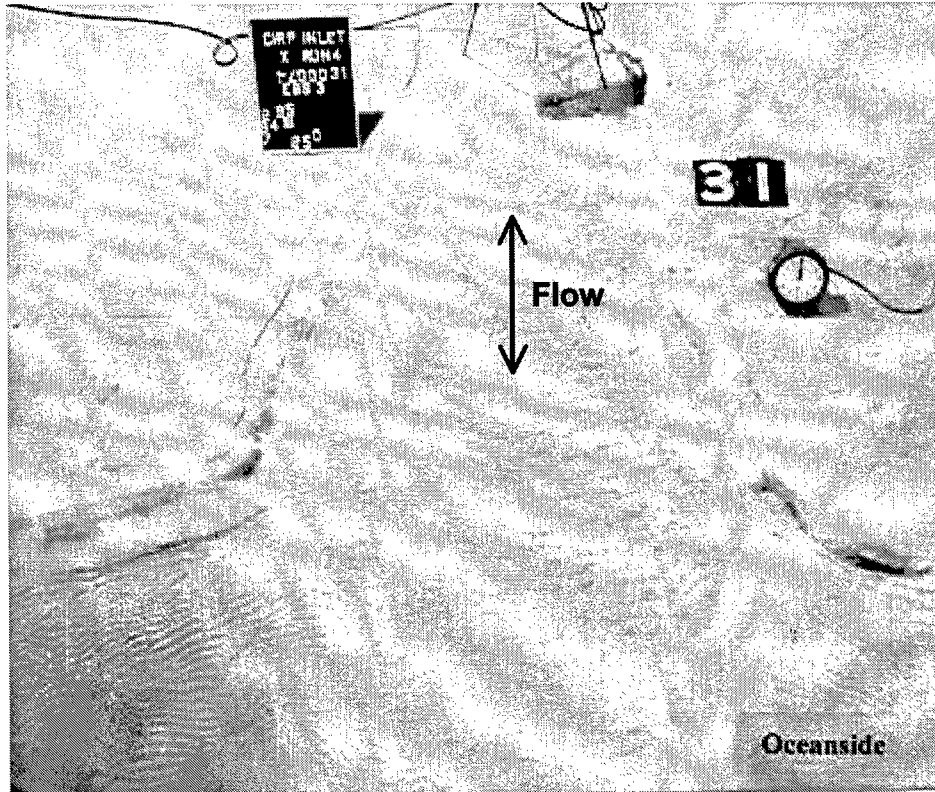


Figure 6. Hour 31 of Run 4 showing the widening of the inlet 15 hr after waves were initiated

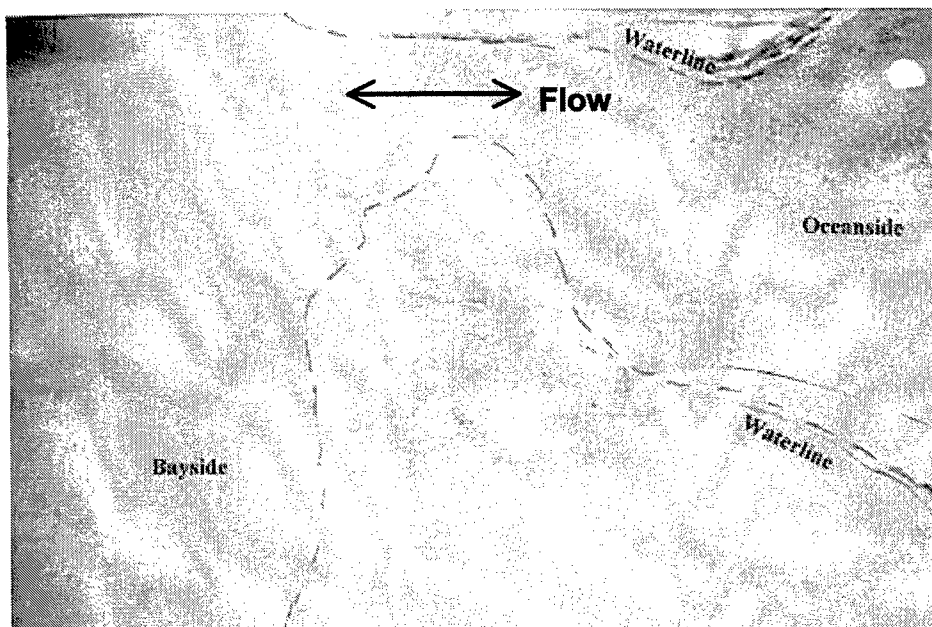


Figure 7. Hour 144 of Run 4, showing the inlet after migrating bayward and reaching equilibrium

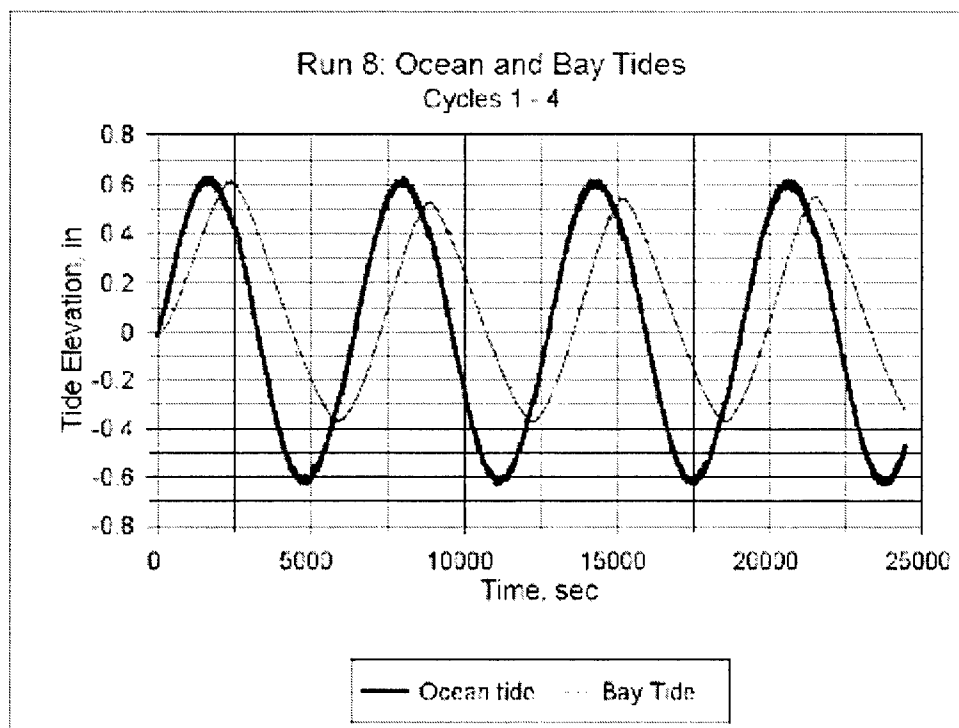
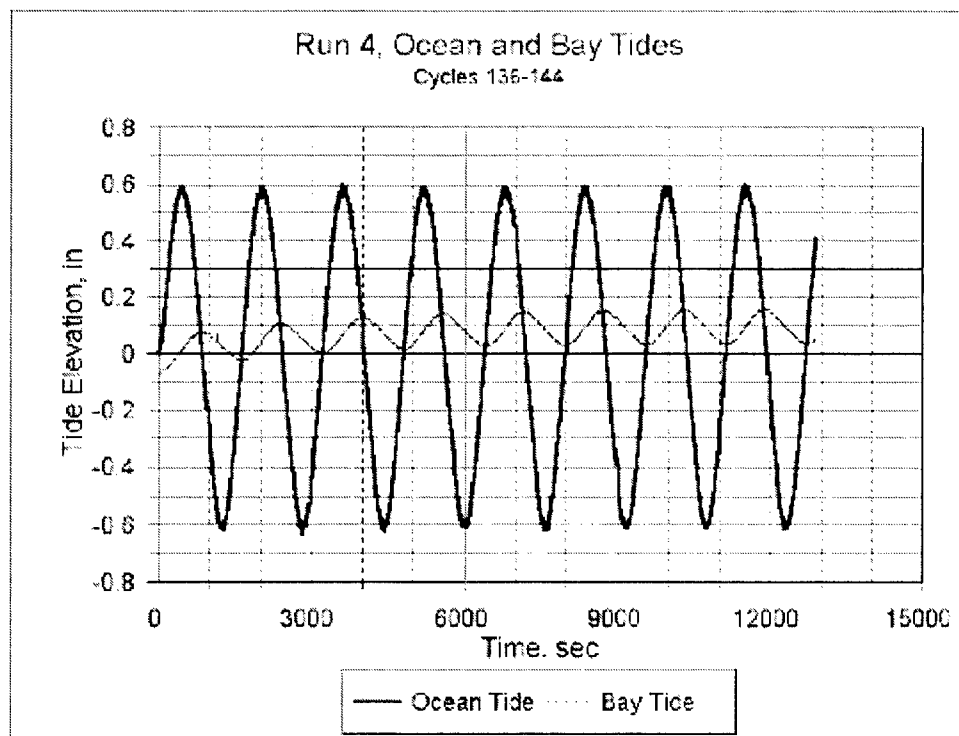


Figure 8. Ocean and bay tidal elevations for Runs 4 and 8, representing the two types of tidal conditions occurring for the 26- and 105-min tidal periods, respectively. To convert elevations to centimeters, multiply by 2.54

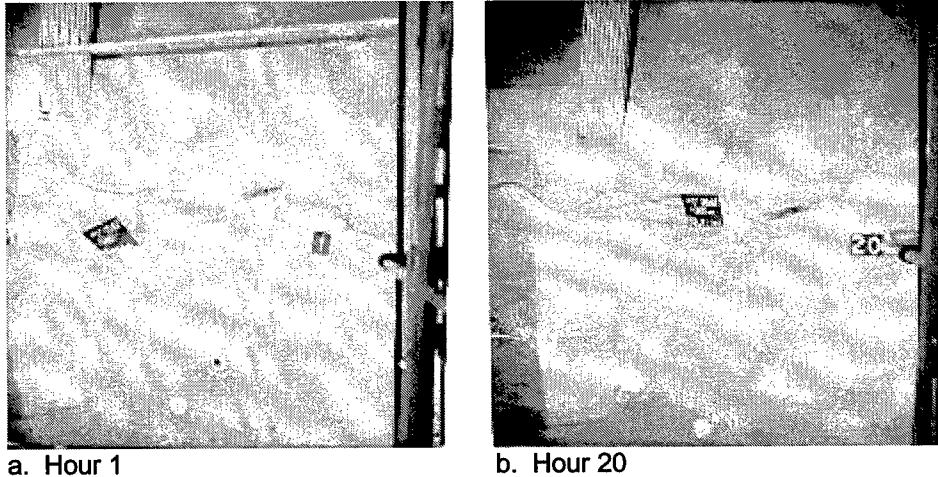


Figure 9. Hours 1 and 20 of Run 5. Hour 1 was at initiation of run, hour 20 at conclusion of tidal currents portion of run (no waves up to this point)

phasing of the tidal currents with respect to tidal elevation. The reduction in channel length reduced time to equilibrium significantly.

Run 6

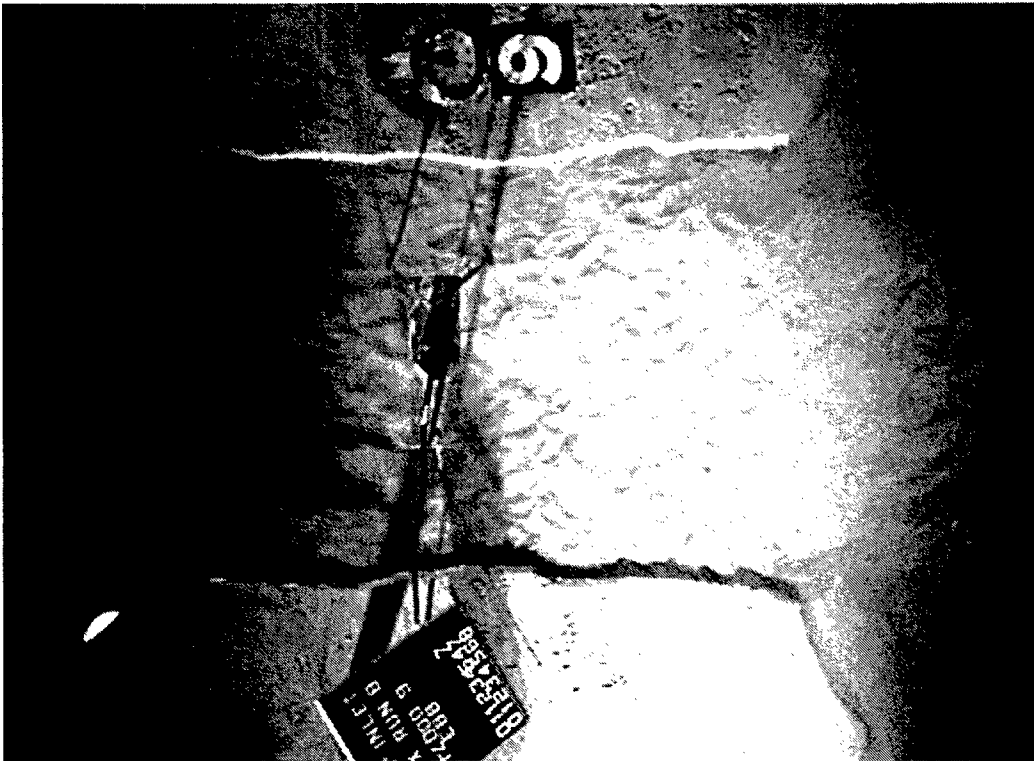
This run was a demonstration, and only a limited amount of data was collected. Conditions were similar to the previous experiment, and only four tide cycles were run.

Run 7

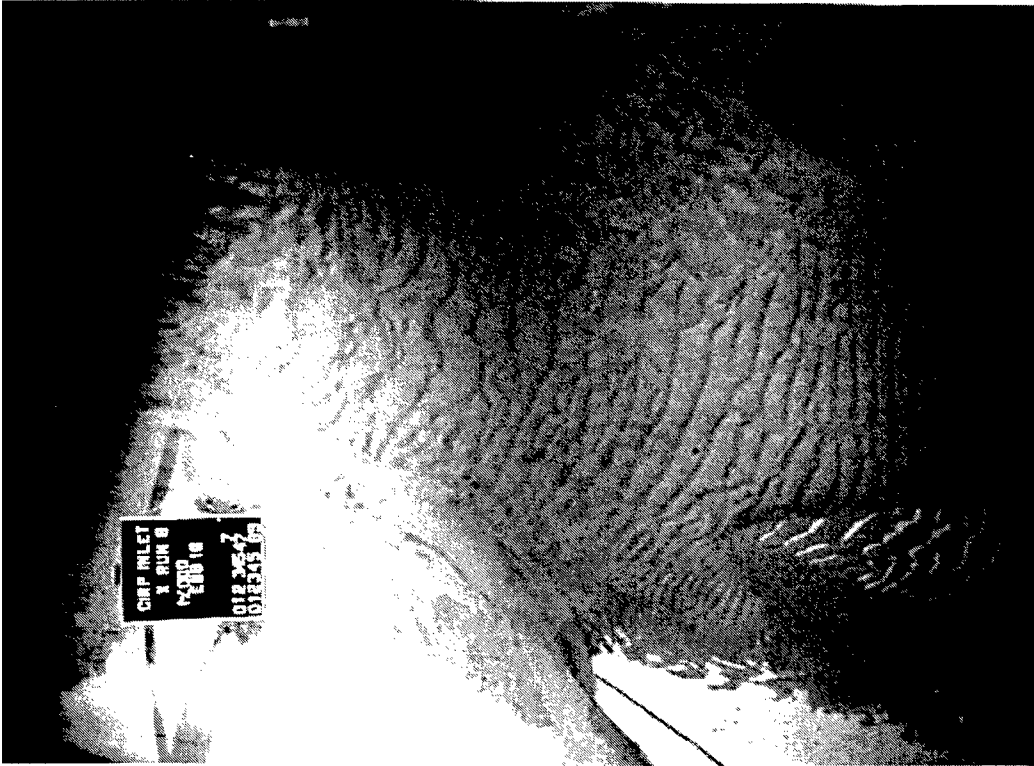
This was the first experiment with the larger grain size sand (0.26 mm) as the movable bed. A power failure limited the experiment to six tidal cycles and washed out the inlet when the pumping system was cut off.

Run 8

This was the first complete experiment with the 0.26-mm-diameter sand and the 105-min tide period. It took eight cycles of the tide-only condition to reach an equilibrium area of 0.0813 sq m (0.875 sq ft). Maximum currents at equilibrium were 0.25 m/sec (0.82 ft/sec) with a tidal prism of 55.19 cu m (1,949 cu ft). The wave generator was then run with the standard wave for eight cycles until a new equilibrium was reached. The minimum area increased slightly to 0.0875 sq m (0.942 sq ft), currents to 0.27 m/sec (0.90 ft/sec) and tidal prism to 57.39 cu m (2,027 cu ft). Figure 10 shows the inlet at the tidal current equilibrium and tidal current plus waves equilibrium. The channel sides remained straight and parallel for the tidal current equilibrium; however, following the waves and current



a. Tidal cycle 9, following eight tidal cycles of tide currents only



b. Tidal cycle 16, the end of the experiment, following eight additional cycles of tide plus waves

Figure 10. The inlet at Run 8

condition, the minimum area was pushed bayward and the inlet was progressively wider bayward and seaward from the minimum area region.

Run 9

This experiment combined the 26-min tide period and the 0.26-mm-diameter sand. After 54 tidal cycles an area of 0.125 sq m (1.347 sq ft) was reached, with 0.32-m/sec (1.05-ft/sec) maximum currents and a 22.96-cu-m (811-cu-ft) tidal prism. Figure 11 shows the inlet at the start and end of the tide-current-only test. As before, the sides of the inlet remained relatively straight and parallel to one another in the absence of waves.

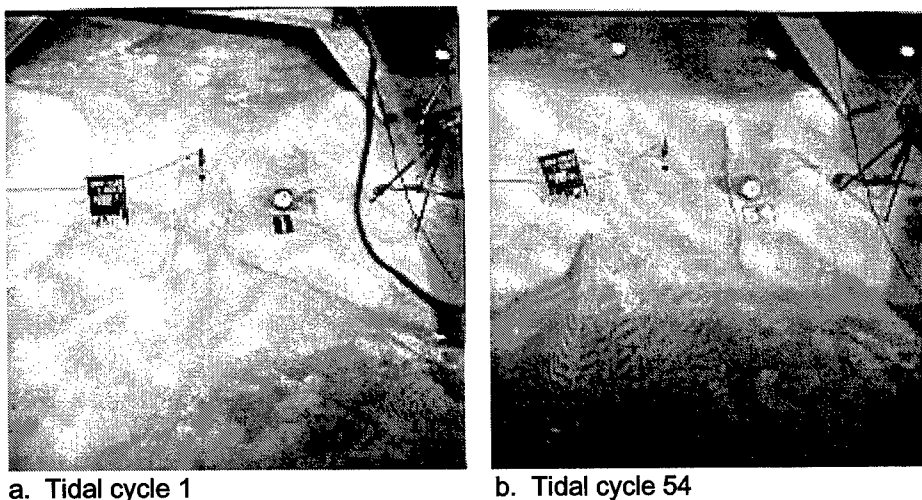


Figure 11. Tidal cycle 1 at start of Run 9 and tidal cycle 54 at the conclusion of the tidal current experiment (no waves)

Appendix A presents plots of data collected from the nine runs. Included are the minimum area versus time (elapsed time of tidal current (and wave) action), the maximum ebb and flood current in the center of the channel during the experiment, the maximum head difference between ocean and bay measured away from the influence of the inlet, the bay tidal range versus time during the experiment, and for Runs 4, 5, 8, and 9, channel cross-sectional area plots at some or all the stations shown in Figure 4.

Discussion of Results

Inlet hydraulics

The runs with tide period of 105 min produced a bay response in which the bay was nearly filled; i.e., the bay range was nearly equal to the ocean tide range. Figure 8 shows the ocean and bay water levels during Runs 4 and 8. The bay

response for the 26-min tidal period runs (Run 4, for example) was much less than that of the 105-min period of Run 8, because the shorter duration could not provide enough time to fill as much of the bay for the relatively similar geometric conditions of the inlet for both tests. The smaller amount of bay filling created significantly different hydraulic conditions, especially with regard to time for peak flows. For the longer tide period, maximum currents occurred near midtide ocean elevations, whereas for the 26-min tide, maximum ebb and flood currents occurred near times of low and high tide elevations, respectively. As a result, the two tidal wave periods provide significantly different hydraulic conditions for creation of the minimum-inlet area response.

Inlet morphology

An interesting and surprising result is no significant change in channel morphology for extremely different hydraulic conditions (compare Figure 10a (Run 8) to Figure 11b (Run 9) for tide-current-only conditions). The inlet shoulders are nearly parallel as channel width increases to an equilibrium condition. It must be remembered that there is no significant ebb shoal that might influence flow patterns for currents at different tide stages. After waves are added, the oceanward portion widens and the narrowest part of the inlet migrates bayward. The lack of littoral input from adjacent beaches may have an influence on this shape.

Table 3 shows channel width, average depth, minimum cross-section area, and channel aspect ratio ($AR = \text{width/depth at minimum width}$) for the pre-experiment, post-experiment without waves, and post-experiment with waves conditions. It should be noted that Run 4 was initially a wider, shallower inlet than the others. A comparison of Runs 5 and 8 with regard to sediment size (because tide period is common to both, 105 min) shows that the smaller sediment size developed a larger equilibrium area for both nonwave and wave areas. This result is similar to the inlet laboratory study of Delmonte and Johnson (1971) where median diameter sands of 0.52 and 0.30 mm were used. Their study

Table 3								
Widths, Depths, Areas, and Aspect Ratios for Runs 4, 5, 8, and 9								
Run No.	Tide Period min	Median Sand Size, mm	Pre-experiment		Post-tide		Post-tide and Waves	
			Width, Depth, and Area ft, ft ²	AR	Width, Depth, and Area ft, ft ²	AR	Width, Depth, and Area ft, ft ²	AR
4	26	0.13	3.1, 0.145, 0.45	22	3.8, 0.15, 0.569	25	7.6, 0.09, 0.652	88
5	105	0.13	2.15, 0.26, 0.567	8	4.25, 0.29, 1.249	15	5.7, 0.28, 1.589	20
8	105	0.26	2.3, 0.29, 0.663	8	4.5, 0.19, 0.875	24	5.3, 0.18, 0.942	29
9	26	0.26	2.2, 0.26, 0.561	9	5.5, 0.25, 1.347	22	—	—
Note: To convert width and depth to meters, multiply by 0.3048. To convert area to square meters, multiply by 0.0929.								

applied steady-state ebb flows with a parallel jetty system. A comparison of Runs 4 and 9 (26-min tide period) in a similar manner shows that the larger sediment size develops a larger equilibrium area. This difference was possibly related to the difference in initial conditions, because with Run 4, a wider, shallower channel existed at the start. Also the different hydraulic characteristics that exist for the two tidal periods may be a factor.

Substituting the current and area data from Table 2 in Equation 2 produces a calculated versus measured minimum-inlet-area plot shown in Figure 12. The run numbers are printed next to the data points, with a "w" next to a run number indicating the equilibrium area after tide plus waves. Despite the differences discussed in the previous paragraph, all the data points fall in reasonable proximity to the line of agreement. The average percentage difference between the measured and predicted areas is 14 percent. The standard error from the predicted value was 0.016 sq m (0.17 sq ft). The percentage difference for the finer sediment was 12 percent and for the coarser sediment was 18 percent. The correlation coefficient r^2 was 0.82.

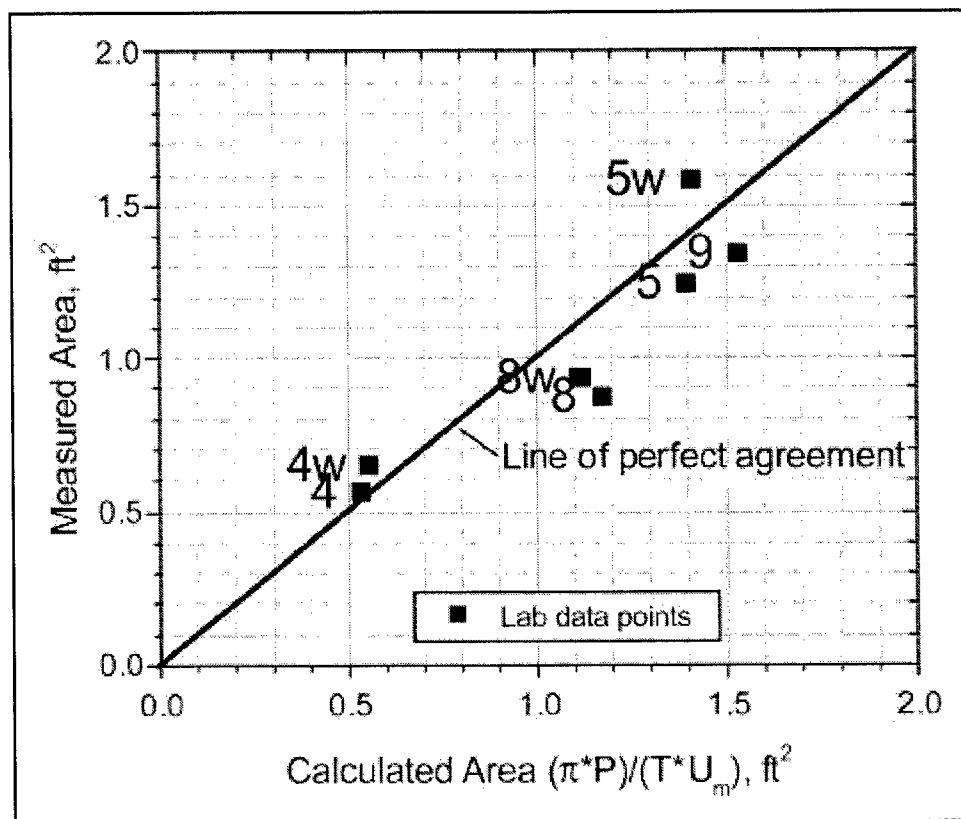


Figure 12. Comparison of measured and calculated equilibrium areas (to convert areas to square meters, multiply by 0.0929)

The equilibrium areas after waves were run are slightly larger than the areas measured after the tide without wave action runs. The larger area generated with waves might be caused by increased transport capacity after wave energy is added, thus enlarging minimum area. Because this study did not introduce littoral drift into the inlet, which might have tended to inhibit channel enlargement when wave action was added, this tendency for channel enlargement with waves and tides appears reasonable.

The relationship described by Equation 2 demonstrates its utility if a comparison is made of plots of Jarrett's (1976) relationship between tidal prism and area ($A = 5.74 \times 10^{-5} P^{0.95}$) and that of Equation 2 for both field and laboratory data (Figures 13 and 14, respectively). The agreement for small inlets (Figure 14) is much better for Equation 2; however, some of the small field inlets (Byrne, Gammisch, and Thomas 1980) fall below the line of perfect fit. For the small field inlets, this could be due to some of these inlets not being in an equilibrium state. Byrne, Gammisch, and Thomas (1980) report that these sites "are exposed to relatively weak littoral drift so disturbances from 'equilibrium' may require longer recovery times. Moreover, those systems with relatively large upland drainage basins . . . may have periodically large freshwater outflow which temporarily enlarge the channel throat area."

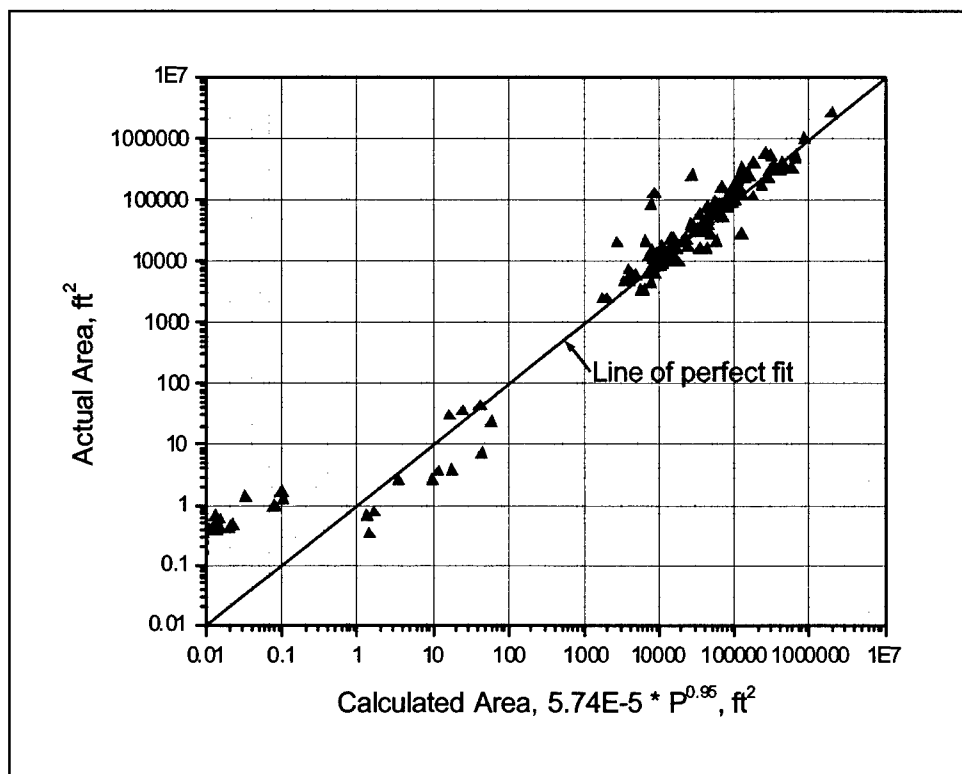


Figure 13. Actual versus calculated area for Jarrett's tidal prism minimum equilibrium area relationship

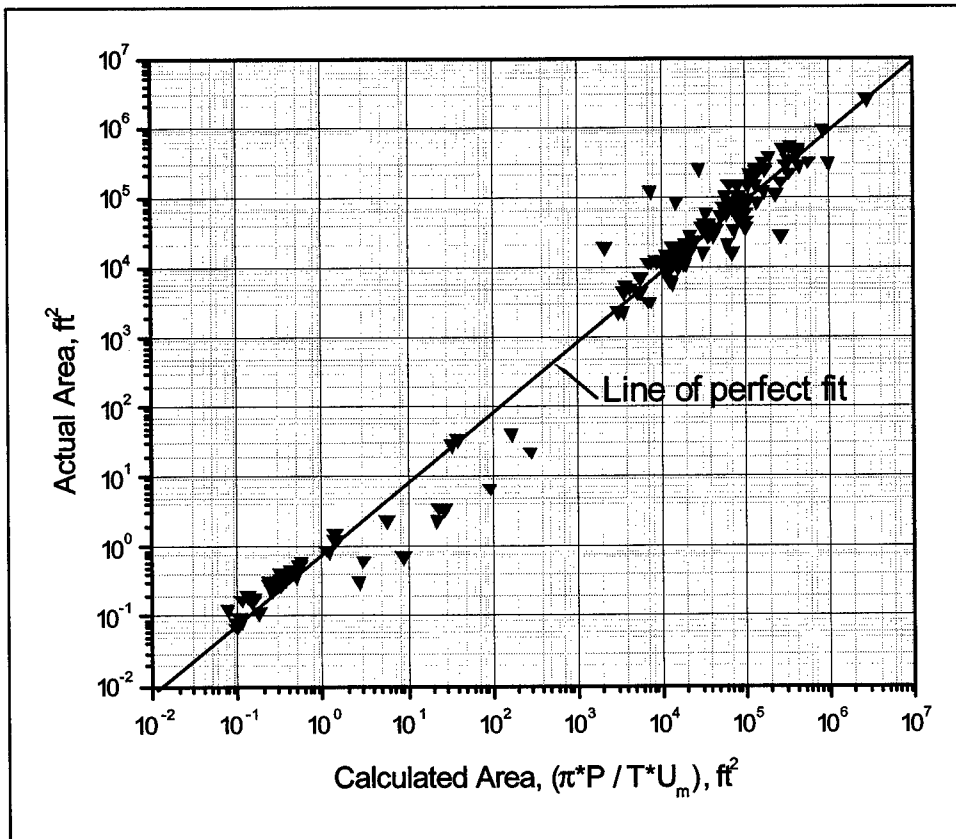


Figure 14. Actual versus calculated area for tidal prism – minimum equilibrium area relationship of this report (to convert areas to square meters, multiply by 0.0929)

The larger than equilibrium cross sections would result in weaker measured channel velocities and a larger calculated area as seen in Figure 14, because the velocity value is in the denominator of the expression for area. If the velocity measurement had been taken during the actual channel enlarging event, the data point would have been more likely to fall on the agreement line.

For relatively simple inlets, the area calculated by Equation 2 provides a good estimate of the equilibrium area, as noted by the good comparison of actual areas versus calculated area for the laboratory inlets that are truly in equilibrium (the field inlets are always in a state of flux, so a given data set from the field may not represent an equilibrium inlet).

The standard plot of tidal prism versus area is presented in Figure 15, showing data from the field (Jarrett 1976; Byrne, Gammisch, and Thomas 1980) and the laboratory (Mayor-Mora (1977) and this study). The laboratory data fall below a typical prism versus area relationship of Jarrett plotted with the field data. The relationship of Jarrett (1976), O'Brien (1931, 1969), Johnson (1972), and others has been based on the data sets of relatively large inlets. The smaller field inlet data set of Byrne, Gammisch, and Thomas (1980) falls near the regression line of Jarrett (1976) with laboratory data falling a considerable distance below the line.

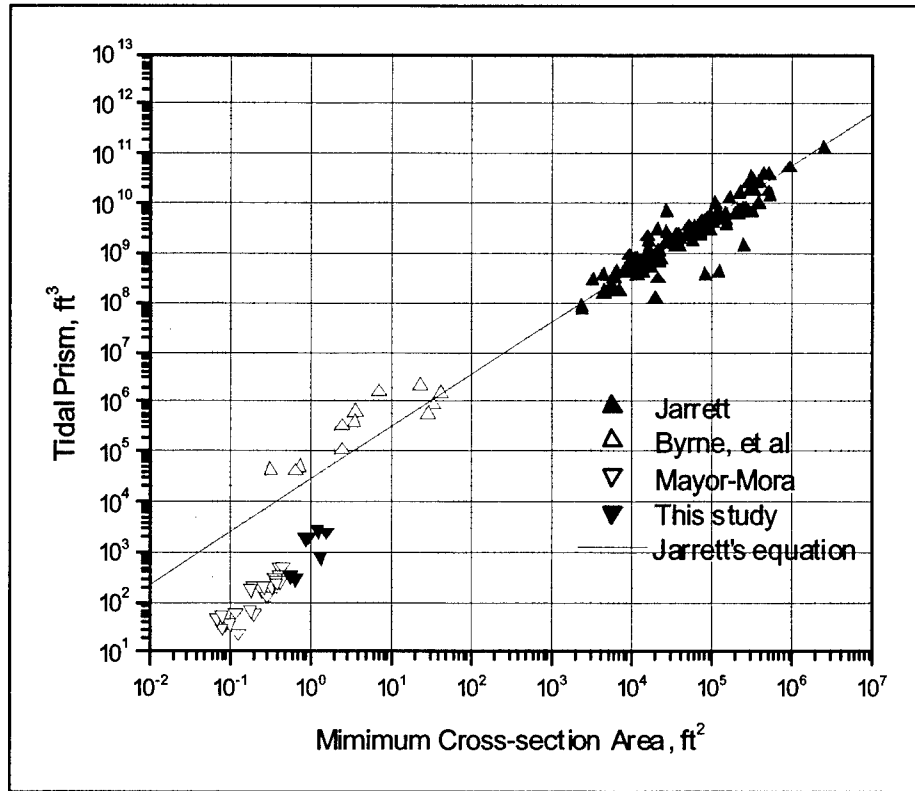


Figure 15. Field and laboratory tidal prism and inlet minimum cross-section area plotted with Jarrett's equation ($A = 5.74 \times 10^{-5} P^{0.95}$) (To convert area to square meters, multiply by 0.0929. To convert prism volume to cubic meters, multiply by 0.0283)

Based on the discussion of the previous paragraph it would seem likely that a regression relationship should be developed based on data that fall on the agreement line. This procedure with "filtered" data would more likely define a more accurate equilibrium area. There could then be a tidal prism-minimum cross-sectional area relationship for the continuum of inlets, from the large to the very small. However, this relationship would represent only inlets that satisfy the simplifying assumptions of Keulegan (1967) described in Chapter 1.

The difference between wave and nonwave conditions is illustrated by Mayor-Mora's (1973) laboratory data in Figure 16, which shows that the trend is for the nonwave tidal equilibrium-minimum areas to be larger than tide-plus-wave conditions for the same tidal prism. The smaller tide-plus-wave area would agree with the trend of the small prototype inlets falling to the right of the equality line for both Jarrett's relation and the relation discussed in this report. For the present experiments, the opposite trend occurred. That is, the tide-with-wave experiments have larger areas than tide-only experiments for a given tidal prism. The larger cross-sectional areas for the tide-and-wave condition are attributed to the lack of influx of beach sediment because only the inlet proper was molded in sand and the adjacent beaches were fixed bed. The wave energy in this case contributed to moving more sediment from the minimum area because of a deficiency of influx of sediment from the inlet, which is typically introduced from adjacent beaches.

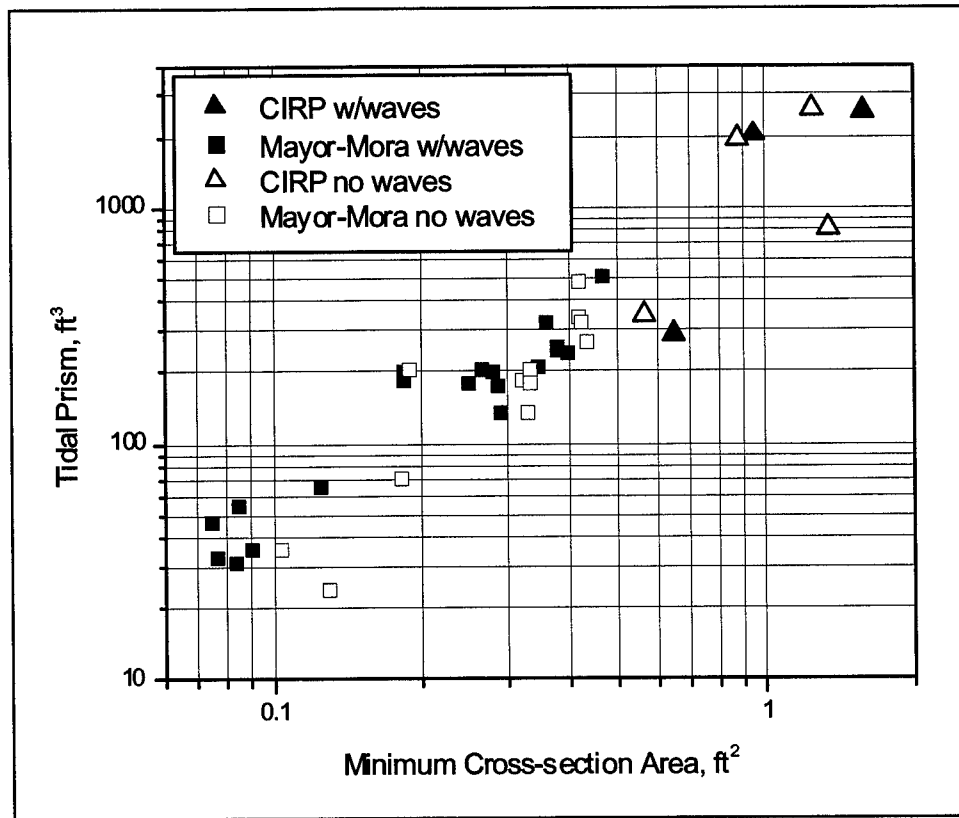


Figure 16. Laboratory data for tidal prism versus minimum cross-section area for tide-only and tide-plus-wave conditions. (To convert area to square meters, multiply by 0.0929. To convert prism volume to cubic meters, multiply by 0.0283)

Data from this study and others presented earlier indicate that Equation 2 shows good agreement with inlet data over a wide range of size scales. This could be considered surprising in light of the simplified assumptions made in deriving Equation 2 as discussed in Chapter 1. In other words, many inlets apparently fit the simplified assumptions of the derivation. Also the modeling performed in this study was distorted from larger inlets in the sense that maximum currents for equilibrium are much less than those found in the field inlets. These were only at the lower end of a decreasing progression of equilibrium velocities, i.e., thinking in terms that these inlets were small “real” inlets, not scale-model inlets. However, thinking in terms of a model, the inlets were considered undistorted models and the aspect ratios of Table 3 were reasonable to inlets of much larger dimension, indicating no real distortion of geomorphology. Currents were distorted in that sense that when using a flow equation such as Manning’s, the current is weaker because of the much smaller depth:

$$V = \frac{1.49}{n} R^{2/3} S^{1/2} \quad (6)$$

where

V = velocity

n = Manning's friction factor

R = the hydraulic radius (typically taken as the average depth for inlets, since they are shallow and wide channels)

S = water level slope across the inlet from ocean to bay

Table 4 shows an example based on realistic laboratory and field data. The table indicates that smaller inlets have smaller velocity values for equilibrium conditions. As seen in Table 2, equilibrium velocity values were in the range of 0.249 to 0.396 m/sec (0.82 to 1.30 ft/sec). Interesting to note from Table 4 is that the ratio of the velocities between large field inlet and small laboratory inlet was about the same as the velocity scale shown in Table 1. The Manning's n values in Table 4 for the field inlet represent a typical value used in many field calculations, and for the laboratory, were calculated from data collected in this study (values for equilibrium conditions varied from 0.012 to 0.025). The model movable bed was covered with ripples. For example at depths of about 0.11 m (0.35 ft), ripple lengths of about 0.076 to 0.122 m (0.25 to 0.40 ft) and heights of 0.012 to 0.018 m (0.04 to 0.06 ft) occurred. These would scale roughly to be about one-half the wavelength of sand waves in a large inlet. Ripple heights in the laboratory experiments would scale approximately to dune heights in a field inlet.

Table 4
Calculation of Velocity in Laboratory and Field Inlet with Manning's Equation

Inlet	n	R , m (ft)	S	V , m/sec (ft/sec)
Large field inlet	0.025	3.048 (10.0)	0.0005	1.856 (6.09)
Laboratory inlet	0.017	0.09 (0.3)	0.0005	0.262 (0.86)

5 Conclusions

This study was designed to examine a relationship between channel area, tidal period, tidal prism, and maximum channel velocity through the inlet. Movable-bed model experiments were conducted to define an equilibrium area for two different tidal periods and two sand grain sizes. The magnitude of the areas measured provided additional data for the tidal prism versus minimum channel area relationship in a size range slightly larger than previous laboratory data in the continuum to very large field inlets. These data may help define the tidal prism-minimum channel cross-sectional area in the midrange region of channel size.

The following conclusions were reached:

- a. Physical model simulations in the idealized inlet model facility and other laboratory data and field data support a relationship, initially derived analytically, between an inlet equilibrium area, maximum inlet velocity, tidal period, and tidal prism as:

$$A_c = \frac{\delta}{T U_m} P \quad (2 \text{ bis})$$

- b. Equation 2 is applicable to define equilibrium inlets that meet the assumptions entering its derivation; namely, an inlet with a bay or lagoon that fills uniformly (i.e., the tidal wavelength is much greater than bay length); a sinusoidal bay tide, or nearly so; and a channel cross-sectional area that does not change significantly during the tidal cycle. This conclusion was reached from noting how well the laboratory data (which represent true equilibrium inlets) was equivalent to the calculated area of Equation 2.
- c. The relationship could be applied to field data to evaluate data points that do not define an equilibrium relationship between minimum cross-sectional area and tidal prism. These filtered data may then be used to define new, more accurate tidal prism versus equilibrium area relationships among all sizes of inlets, from laboratory to large field inlets.
- d. Laboratory experiments conducted in this study indicate that Equation 2 is maintained for various inlet hydraulic conditions (e.g., inlet bays that nearly fill and those so large that they have a tidal range much less than

that of the adjacent sea) and various geomorpologic conditions, such as an inlet with a long tidally dominated channel or a short wave-dominated inlet channel.

- e.* Equilibrium area channels for tide-only conditions retained their original length and widened and deepened upon approaching equilibrium cross-sectional area.
- f.* Equilibrium area channels following tide-plus-wave conditions migrated bayward as they approached equilibrium and shortened in length.
- g.* The equilibrium area experimental results will be useful in the design of other experiments relating to ebb and flood shoals and spit migration in the CIRP Idealized Inlet.

References

- Byrne, R. J., Gammisch, R. A., and Thomas, G. R. (1980). "Tidal prism-inlet area relationships for small tidal inlets." *Proceedings, 17th Coastal Engineering Conference*, Sydney, Australia, March 23-28, 1980. American Society of Civil Engineers, New York, III, 2517-2533.
- Dean, R. G. (1977). "Equilibrium beach profiles: U.S. Atlantic and Gulf Coasts," Ocean Engineering Technical Report No. 12, Department of Civil Engineering and College of Marine Studies, University of Delaware, Newark.
- Delmonte, R. C., and Johnson, J. W. (1971). "The influence of bed material size on the tidal prism-area relationship in a tidal inlet," Report No. HEL 24-8, University of California at Berkeley, Hydraulic Engineering Laboratory, Berkeley, CA.
- Hughes, S. A. (1993). *Physical models and laboratory techniques in Coastal Engineering*. World Scientific, Singapore, 568 pp.
- Hughes, S. A. (1999). "Equilibrium scour depth at tidal inlets," Coastal Engineering Technical Note CETN-IV-18, March 1999. U.S. Army Engineer Research and Development Center, Vicksburg, MS.
<http://chl.wes.army.mil/library/publications/chetn/>
- Jarrett, J. T. (1976). "Tidal prism-inlet area relationships," GITI Report 3, General Investigation of Tidal Inlets, U.S. Army Coastal Engineering Research Center, Ft. Belvoir, VA, and U.S. Army Engineer Waterways Experiment Station, Vicksburg, MS.
- Johnson, J. W. (1972). "Tidal inlets on the California, Oregon, and Washington Coasts," Technical Report HEL 24-12, University of California at Berkeley, Hydraulic Engineering Laboratory, Berkeley, CA.
- Keulegan, G. H. (1967). "Tidal flow in entrances, water-level fluctuations of basins in communication with seas," Technical Bulletin No.14, Committee on Tidal Hydraulics, U.S. Army Corps of Engineers, U.S. Army Engineer Waterways Experiment Station, Vicksburg, MS.

- Kraus, N. C. (1998). "Inlet cross-sectional area calculated by process-based model." *Proceedings 26th Coastal Engineering Conference*, Copenhagen, Denmark, June 22-26, 1998. American Society of Civil Engineers, New York, 3, 265-3,278.
- LeConte, L. J. (1905). "Discussion of 'Notes on the improvement of river and harbor outlets in the United States,' by D. A. Watts," Paper No. 1009, *Transactions, American Society of Civil Engineers* LV, December, 306-308.
- Mayor-Mora, R. (1973). "Hydraulics of tidal inlets on sandy coasts," Report HEL-24-16, University of California at Berkeley, Hydraulic Engineering Laboratory, Berkeley, CA.
- Mayor-Mora, R. (1977). "Laboratory investigation of tidal inlets on sandy coasts," GITI Report 11, General Investigation of Tidal Inlets, U.S. Army Coastal Engineering Research Center, Ft. Belvoir, VA, and U.S. Army Engineer Waterways Experiment Station, Vicksburg, MS.
- McDowell, D. M. (1955). "The vertical distribution of water velocities in tidal streams and in models of tidal regions." *Proceedings, 6th General Meeting of the International Association for Hydraulic Research* I, Paper A-1.
- McNair, E. C. (1976). "Model materials evaluation, sand tests, Hydraulic Laboratory Investigation," GITI Report 7, General Investigation of Tidal Inlets, U.S. Army Coastal Engineering Research Center, Ft. Belvoir, VA, and U.S. Army Engineer Waterways Experiment Station, Vicksburg, MS.
- O'Brien, M. P. (1931). "Estuary tidal prisms related to entrance areas," *Civil Engineering* 1(8), 738-739.
- O'Brien, M. P. (1969). "Equilibrium flow areas of inlets on sandy coasts," *Journal of Waterways and Harbors Division* 95(WW1), 43-52.
- Riedel, H. P., and Gourlay, M. R. (1980). "Inlets/estuaries discharging into sheltered waters." *Proceedings, 17th Coastal Engineering Conference*, Sydney, Australia, March 23-28, 1980. American Society of Civil Engineers, New York, III, 2550-2564.
- Seabergh, W. C. (1999). "Physical model for coastal inlet entrance studies," Coastal Engineering Technical Note IV-19, U.S. Army Engineer Research and Development Center, Vicksburg, MS.
<http://chl.wes.army.mil/library/publications/chetn/>
- Stevens, J. C. (1942). "Hydraulic models," *Manuals of Engineering Practice* 25, American Society of Civil Engineers, New York.
- Van de Kreeke, J. (1992). "Stability of tidal inlets; Escoffier's analysis," *Shore and Beach* 60(1), 9-12.

Appendix A

Detailed Experiment Data

This appendix contains plots of the variation with time of minimum area, maximum ebb and flood velocities, maximum head difference across the inlet, and bay tide range. Also included are inlet cross-section plots at selected locations (see Figure 4 for station locations). Chapter 3 discusses experiment measurement procedures.

To convert measurements in this appendix given in feet to meters, multiply by 0.3048. To convert measurements given in inches to centimeters, multiply by 2.54. To convert measurements given in square feet to square meters, multiply by 0.09290304.

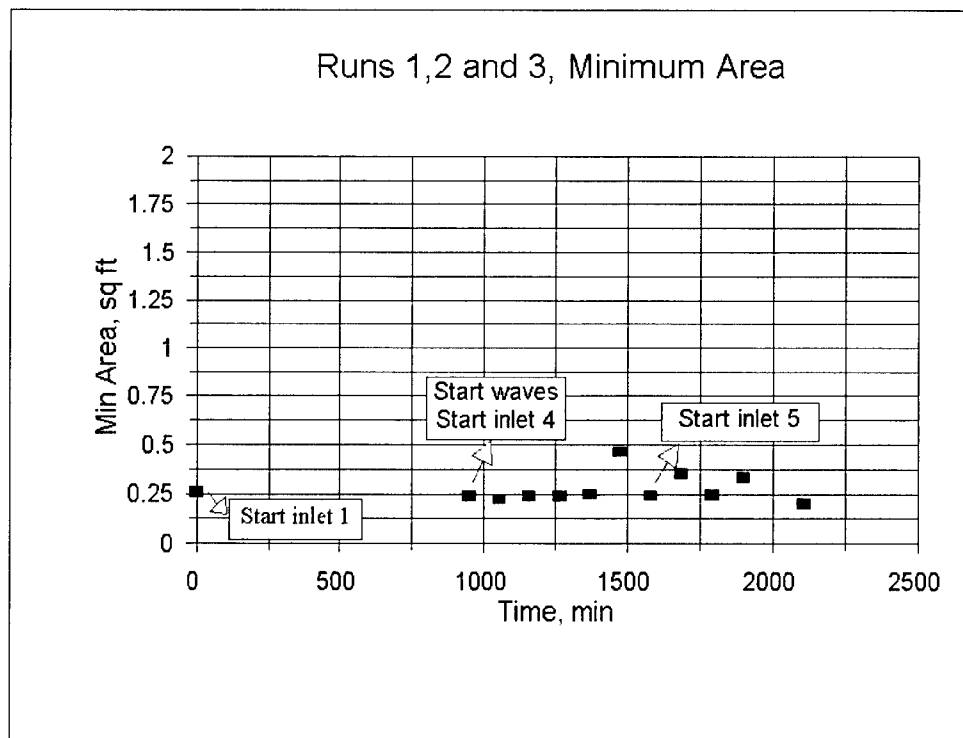


Plate A1

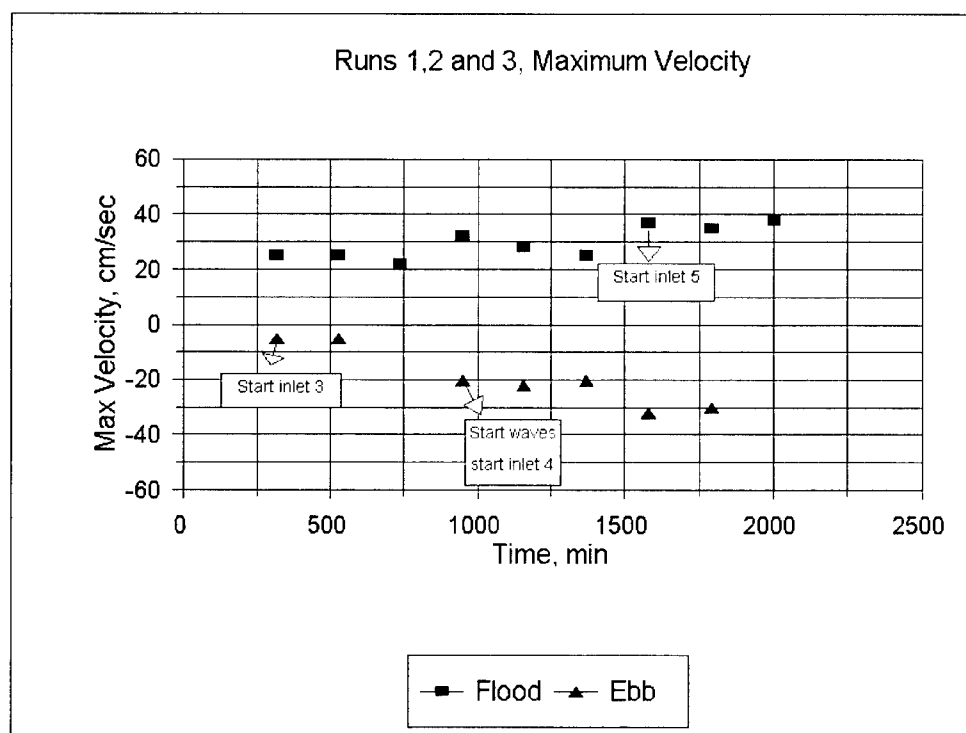


Plate A2

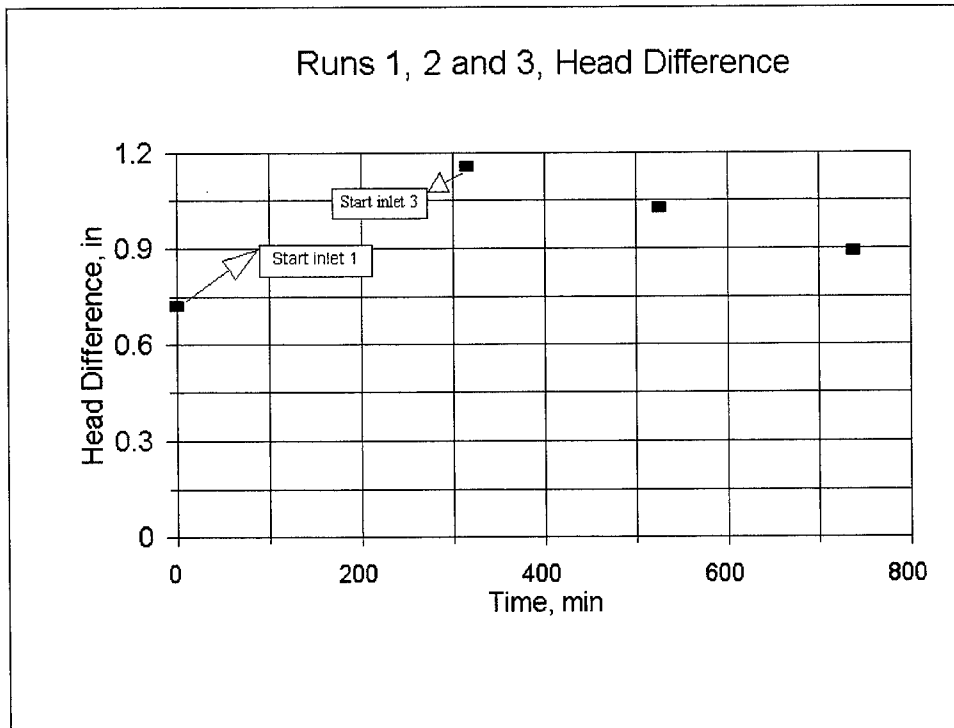


Plate A3

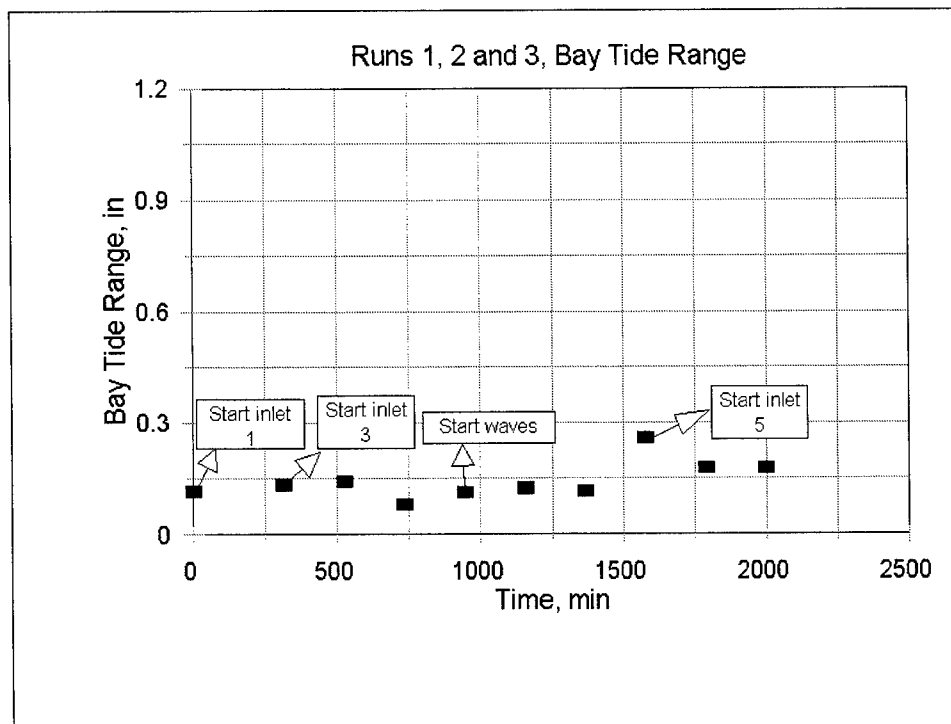


Plate A4

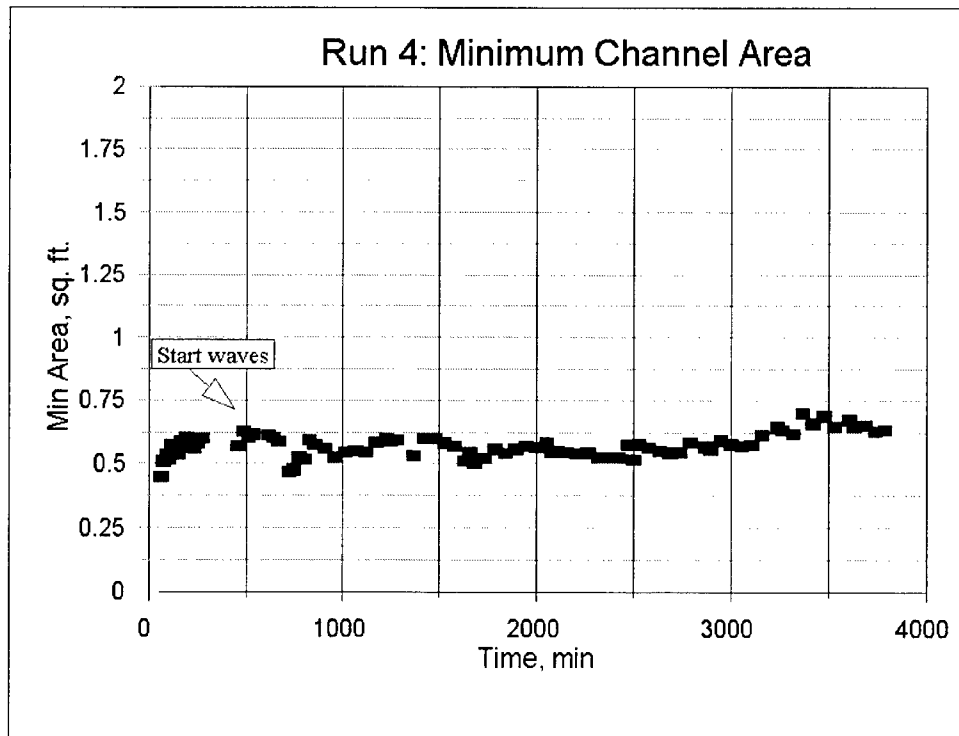


Plate A5

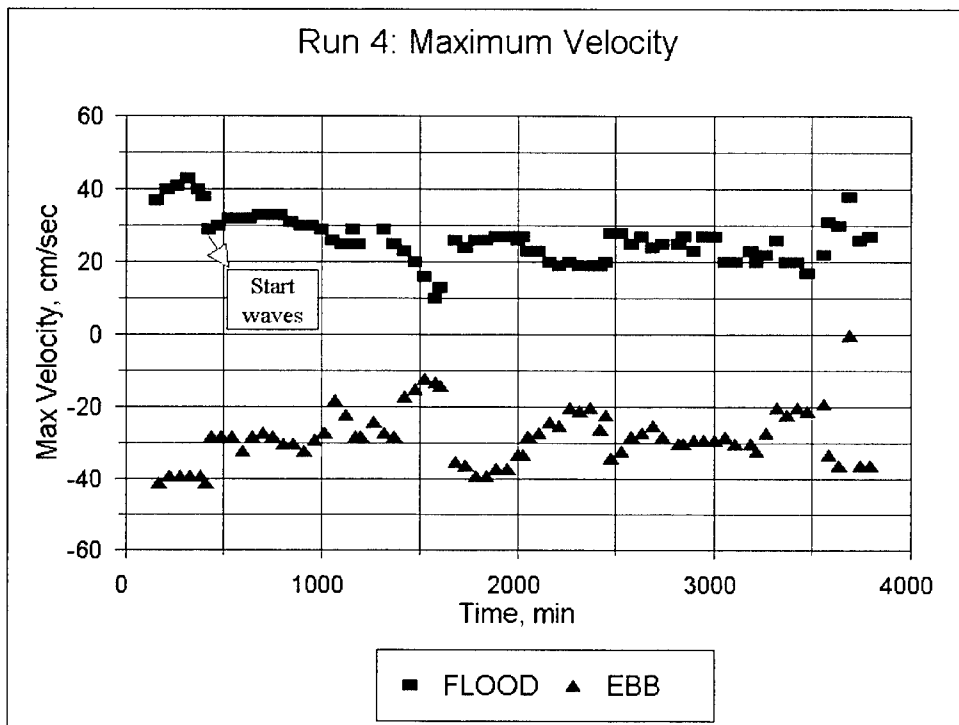


Plate A6

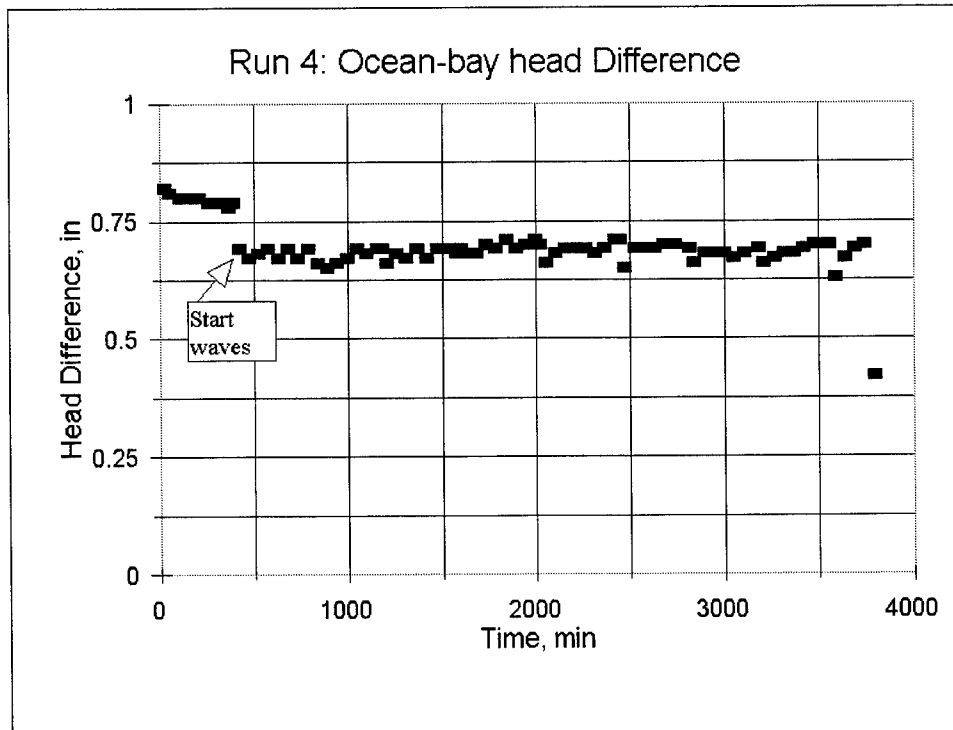


Plate A7

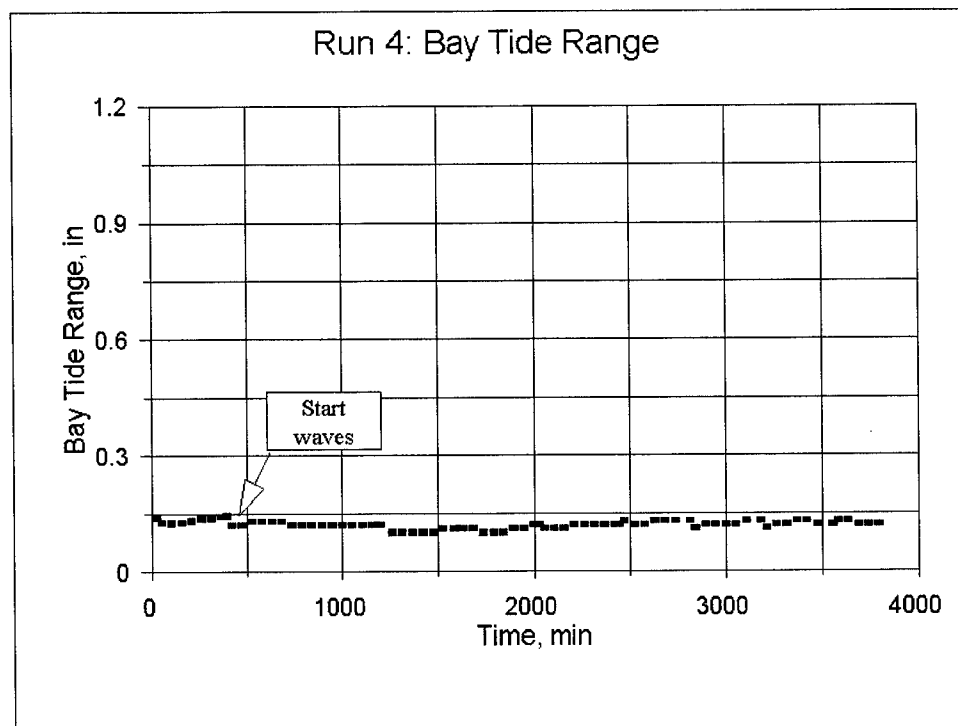


Plate A8

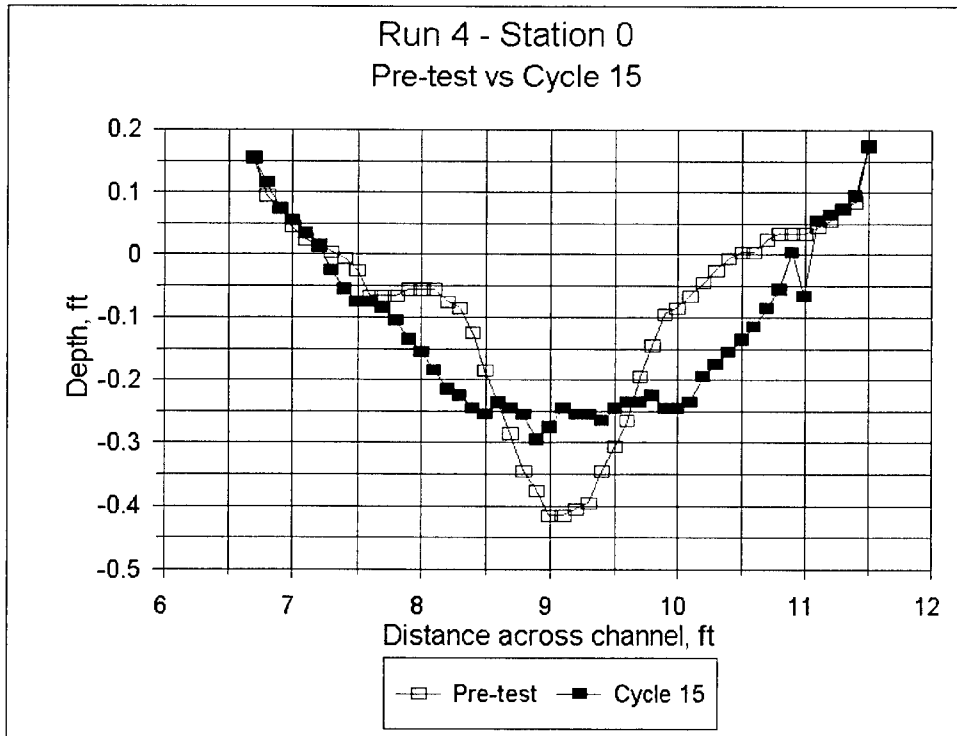


Plate A9

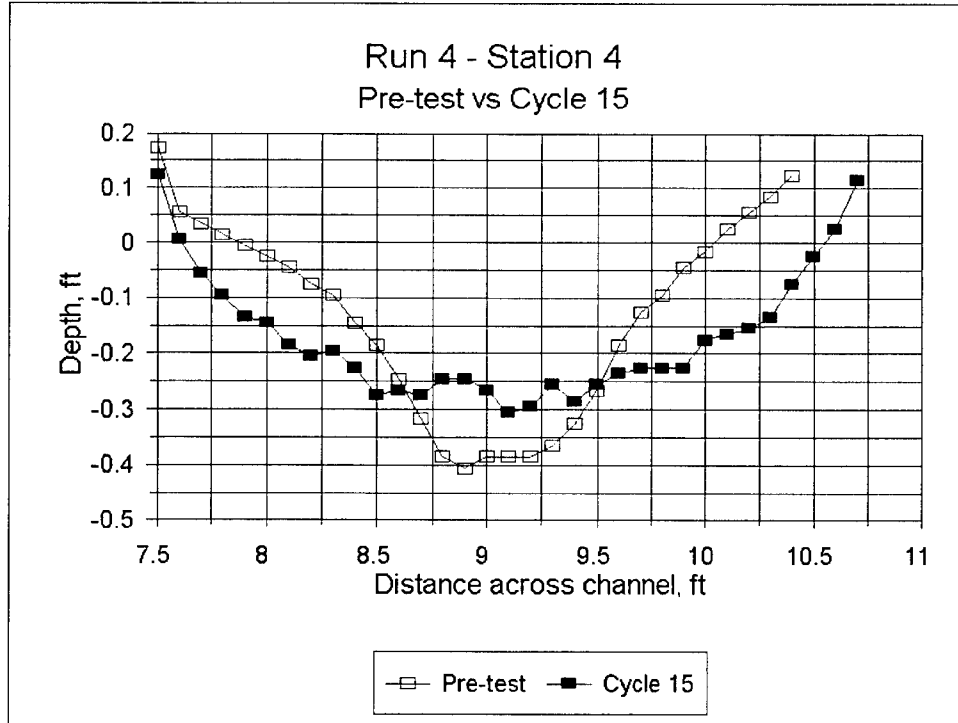


Plate A10

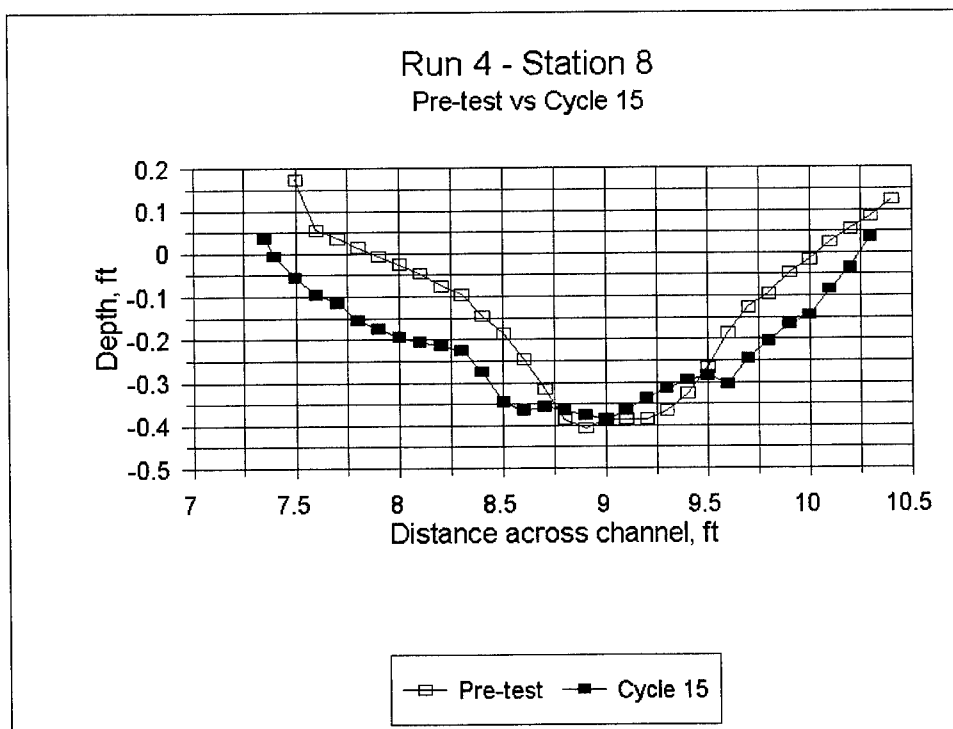


Plate A11

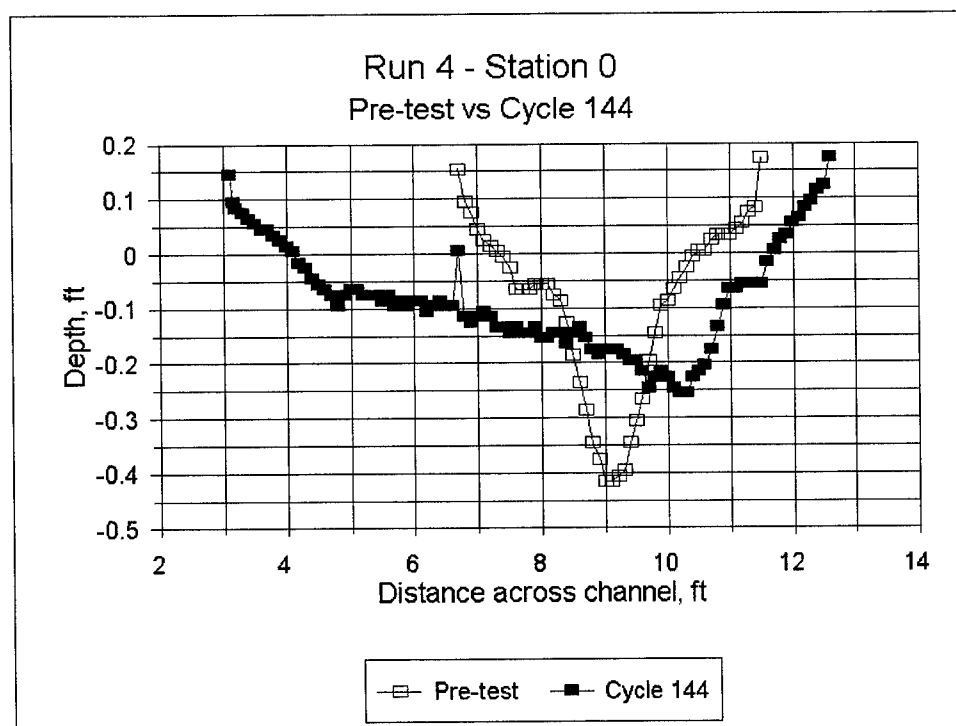


Plate A12

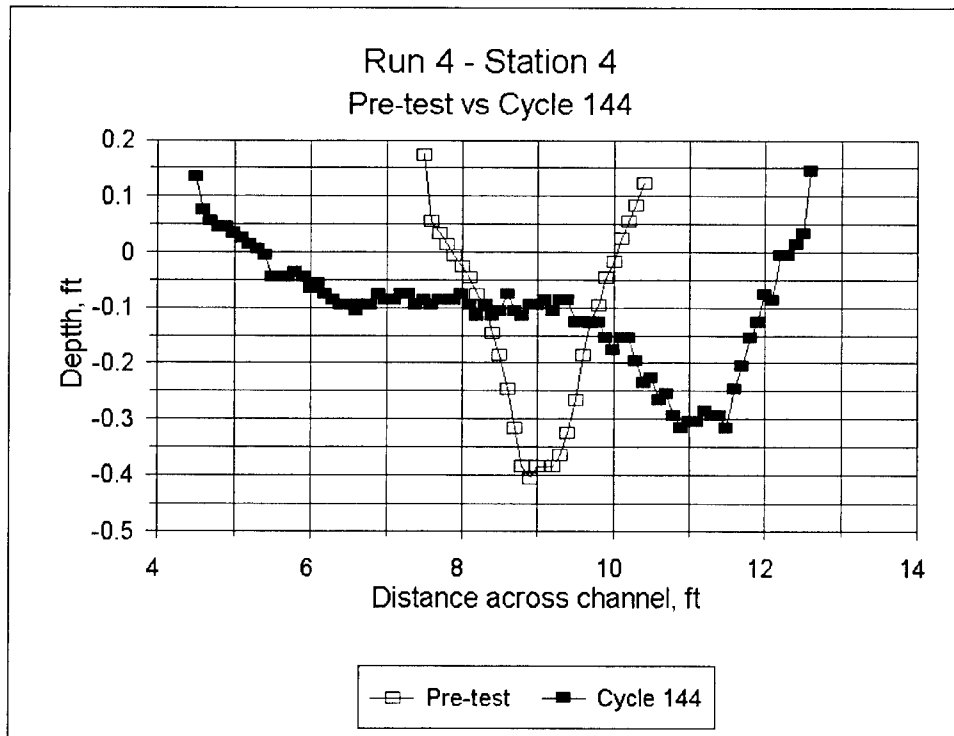


Plate A13

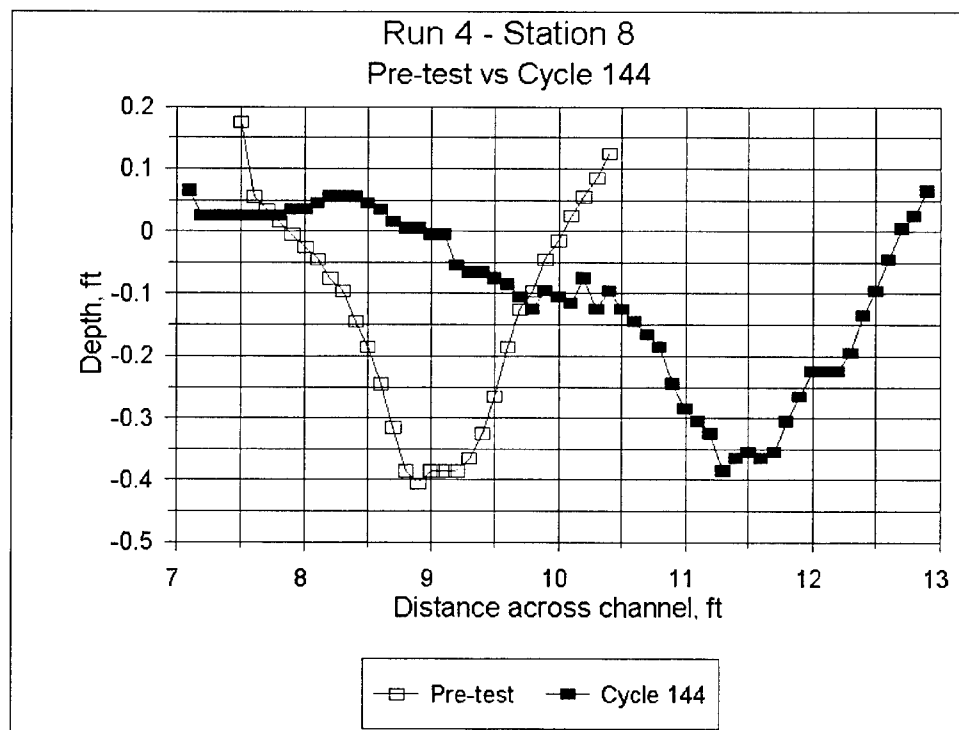


Plate A14

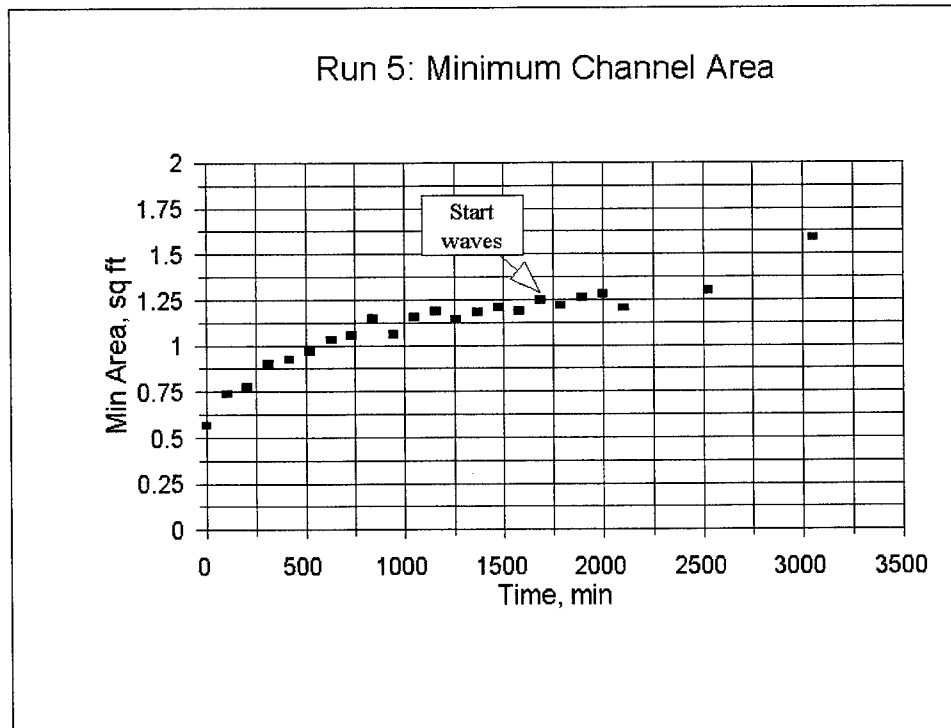


Plate A15

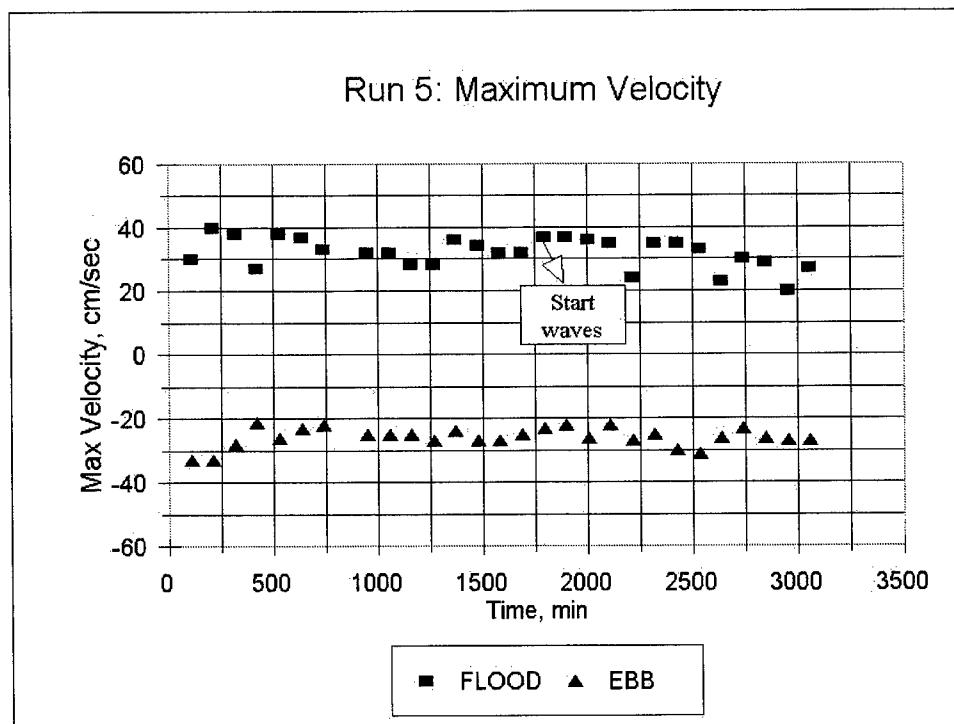


Plate A16

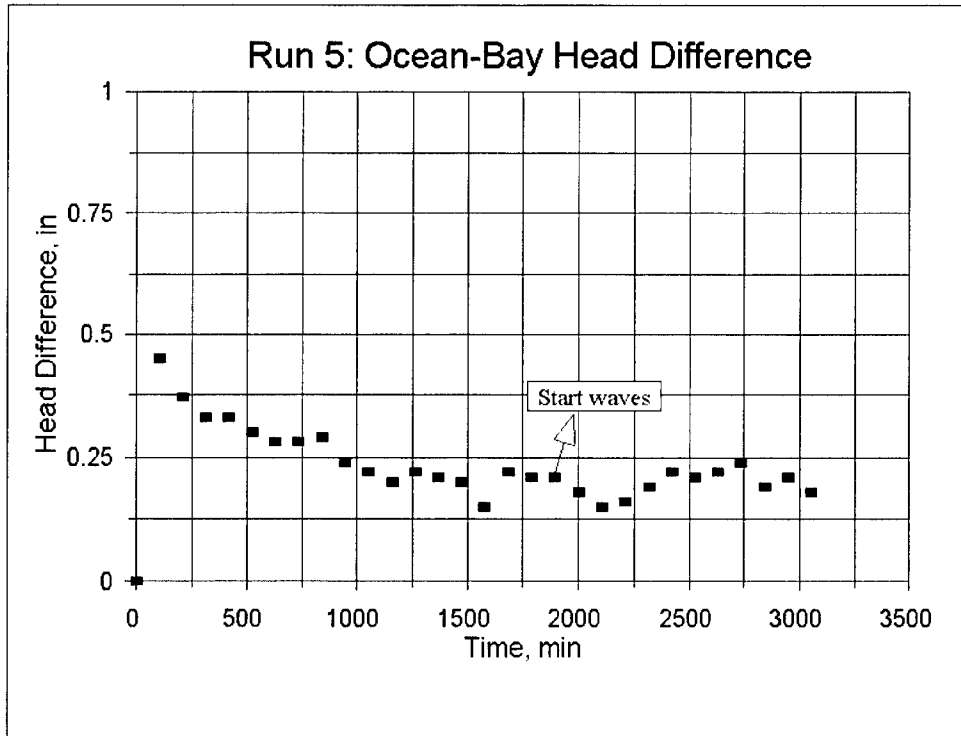


Plate A17

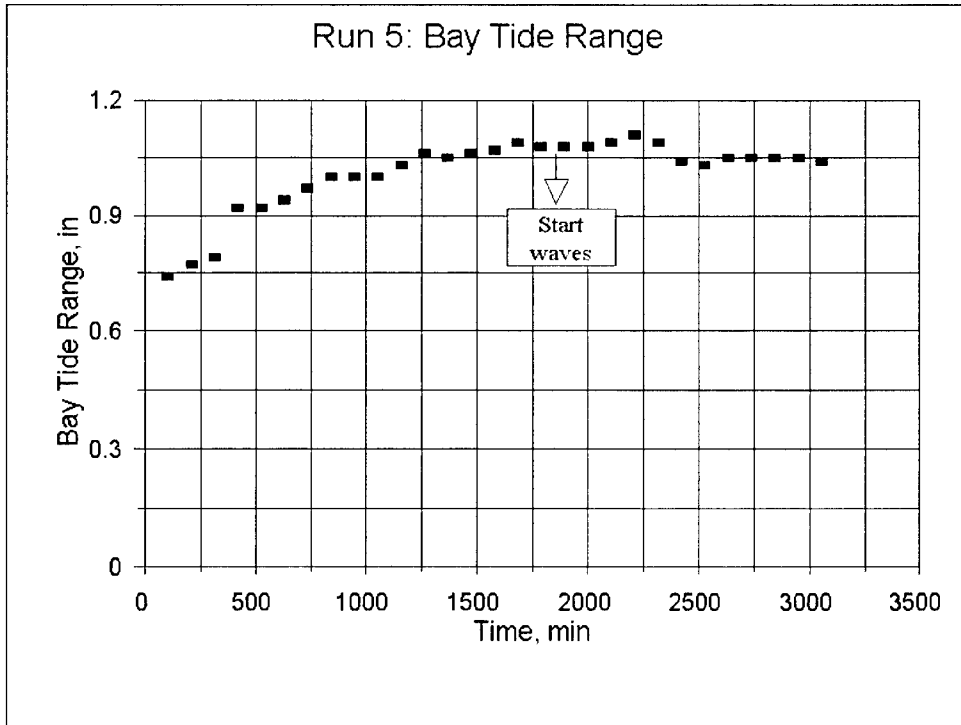


Plate A18

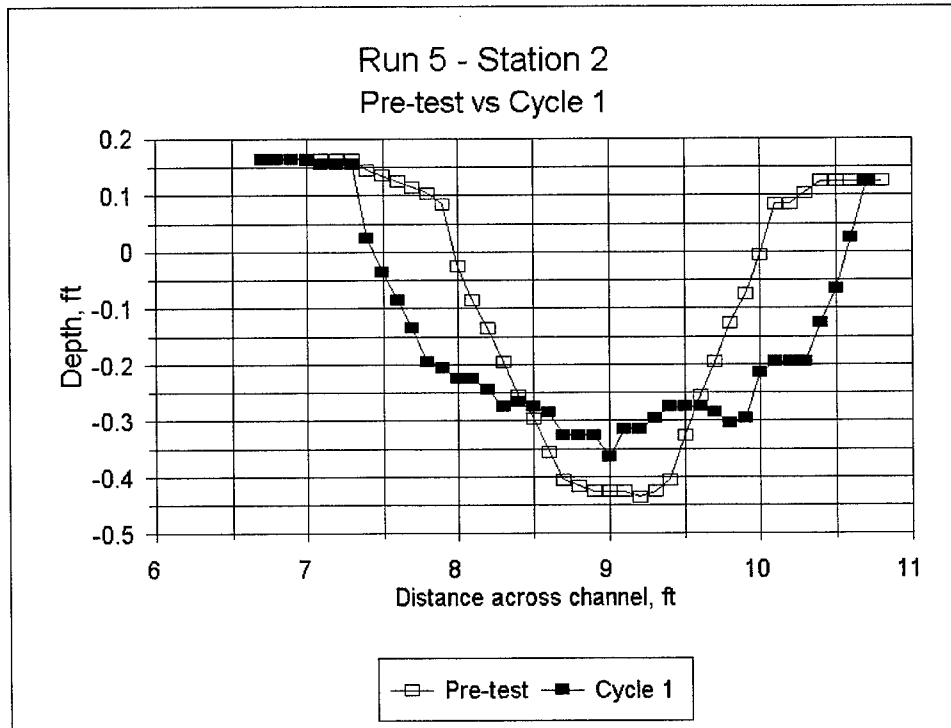


Plate A19

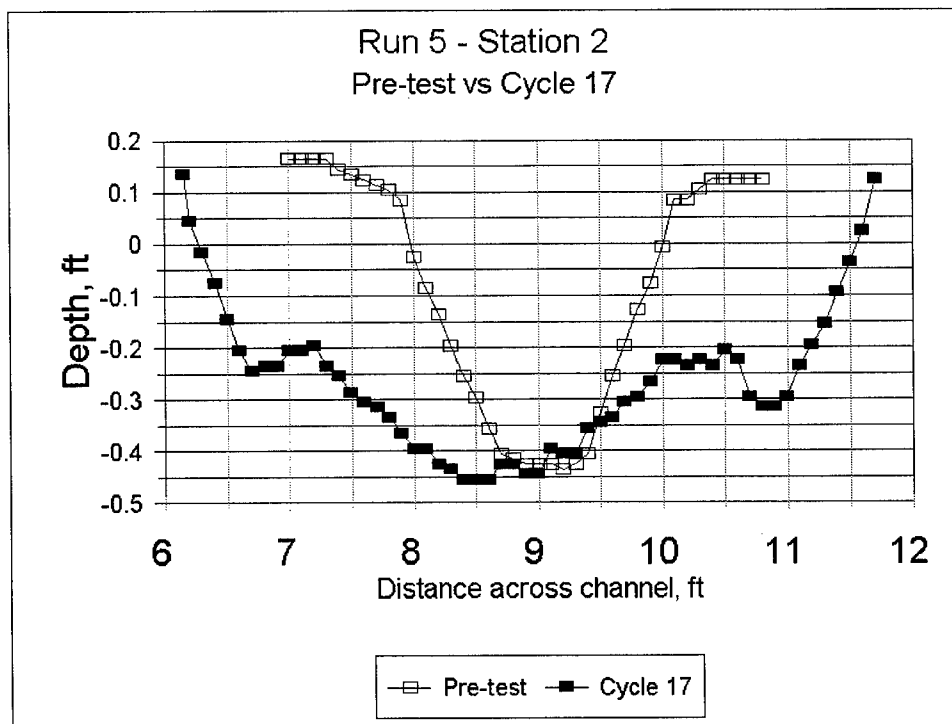


Plate A20

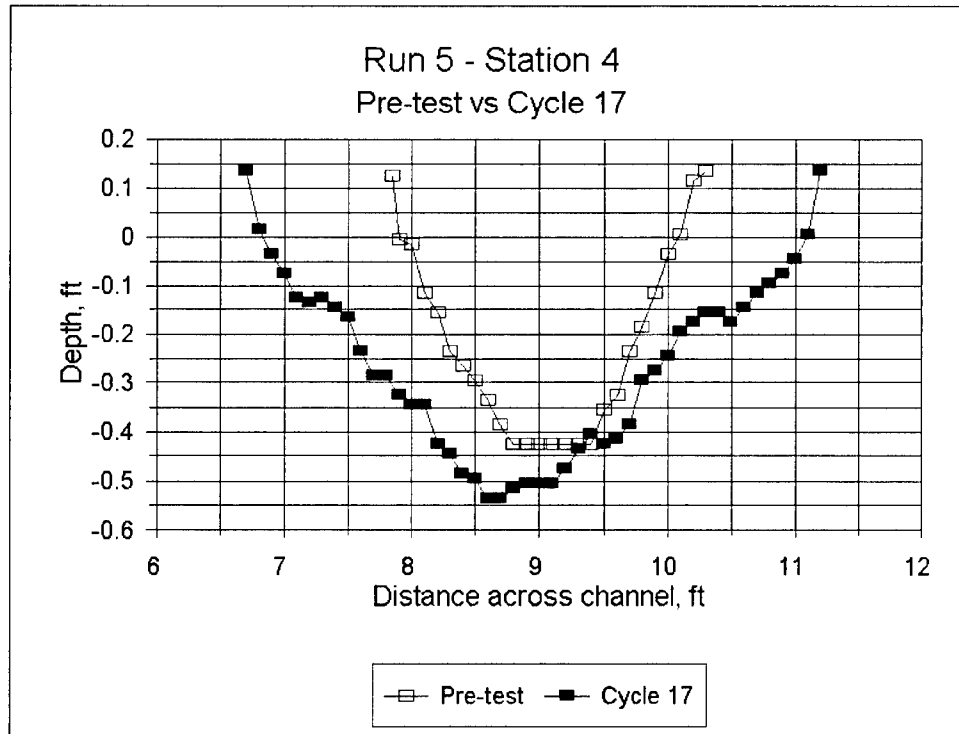


Plate A21

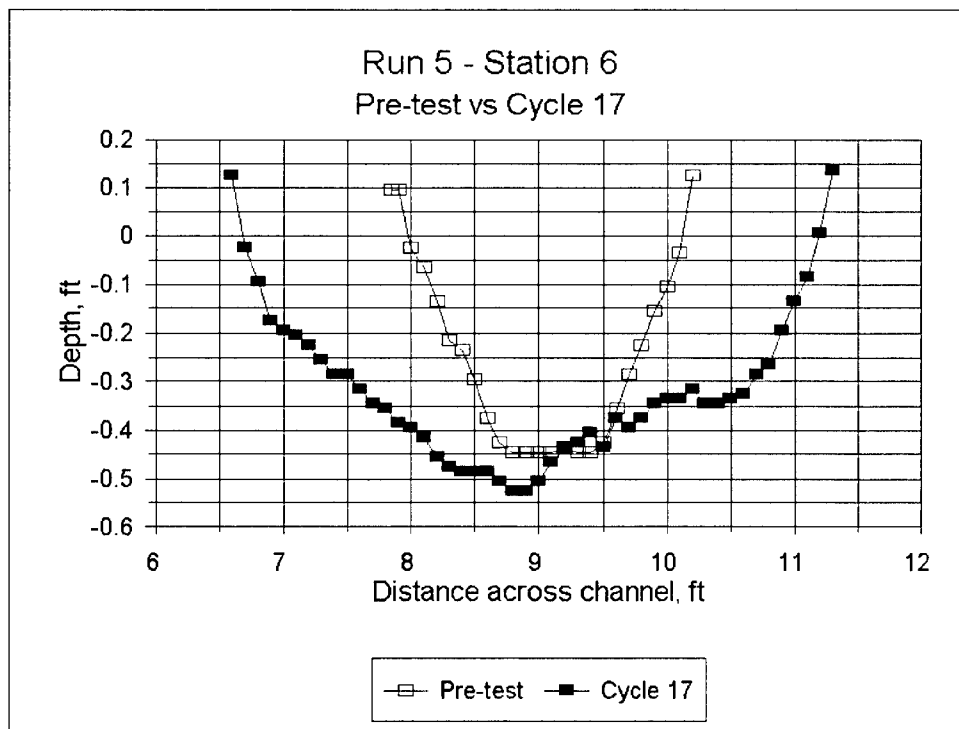


Plate A22

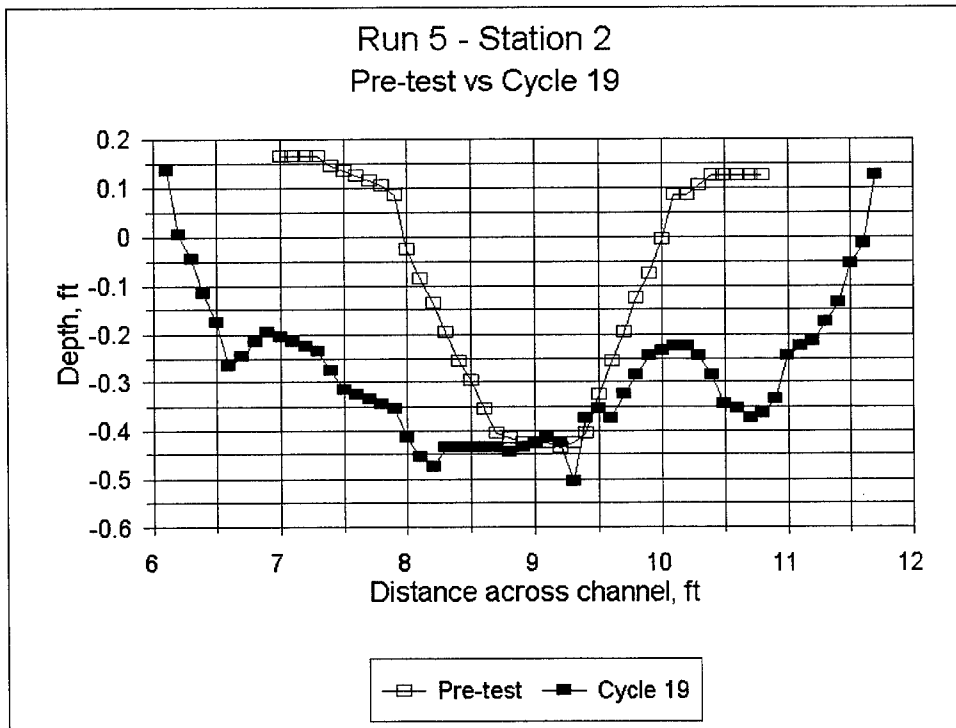


Plate A23

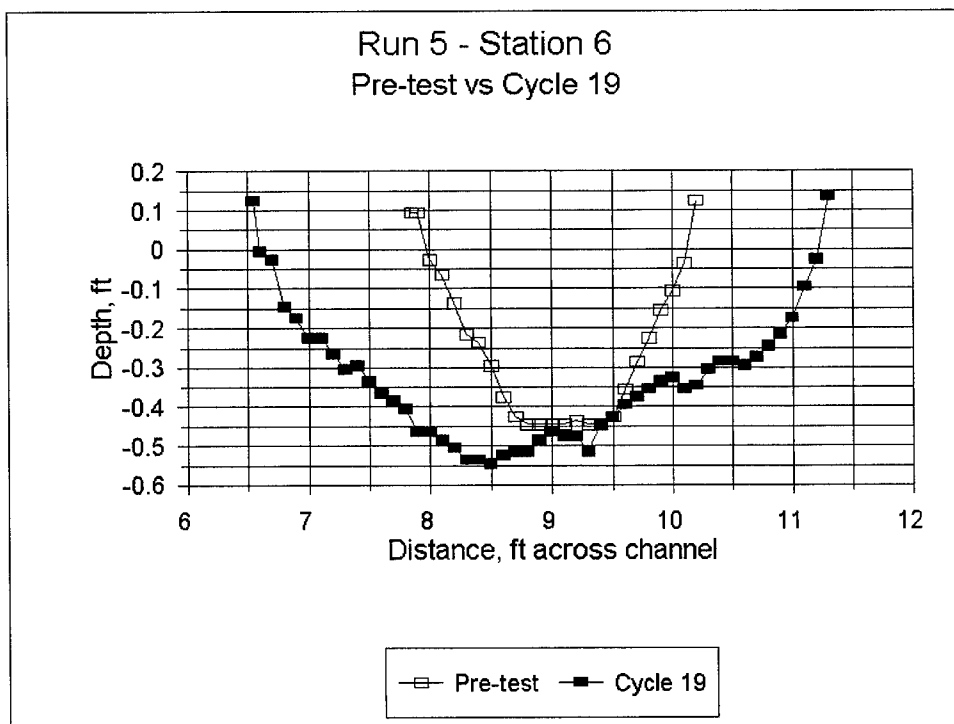


Plate A24

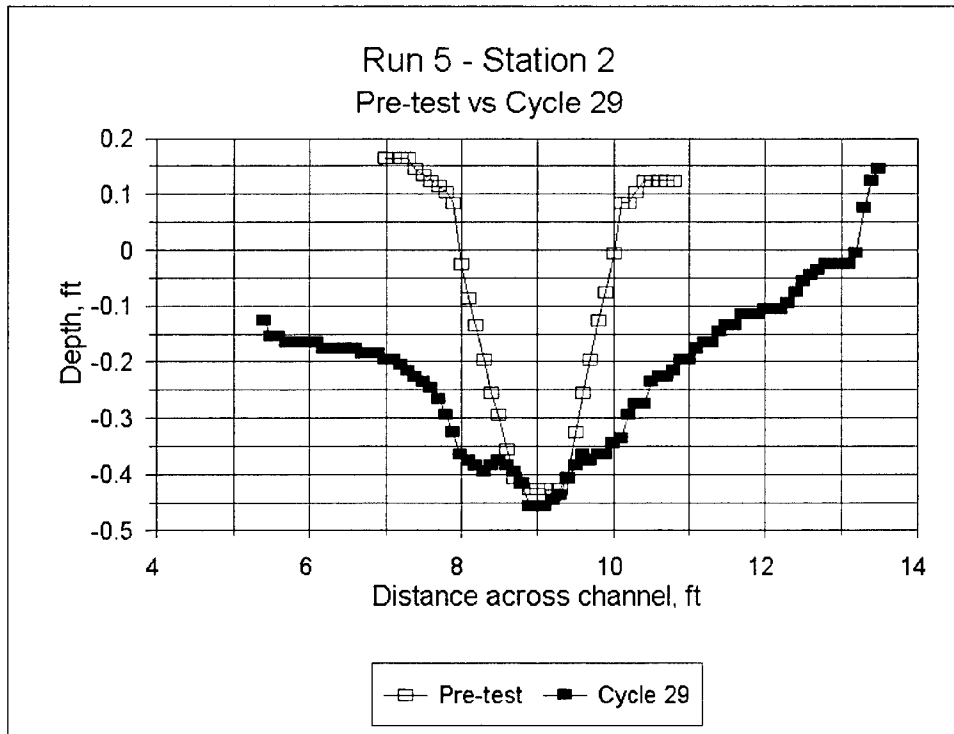


Plate A25

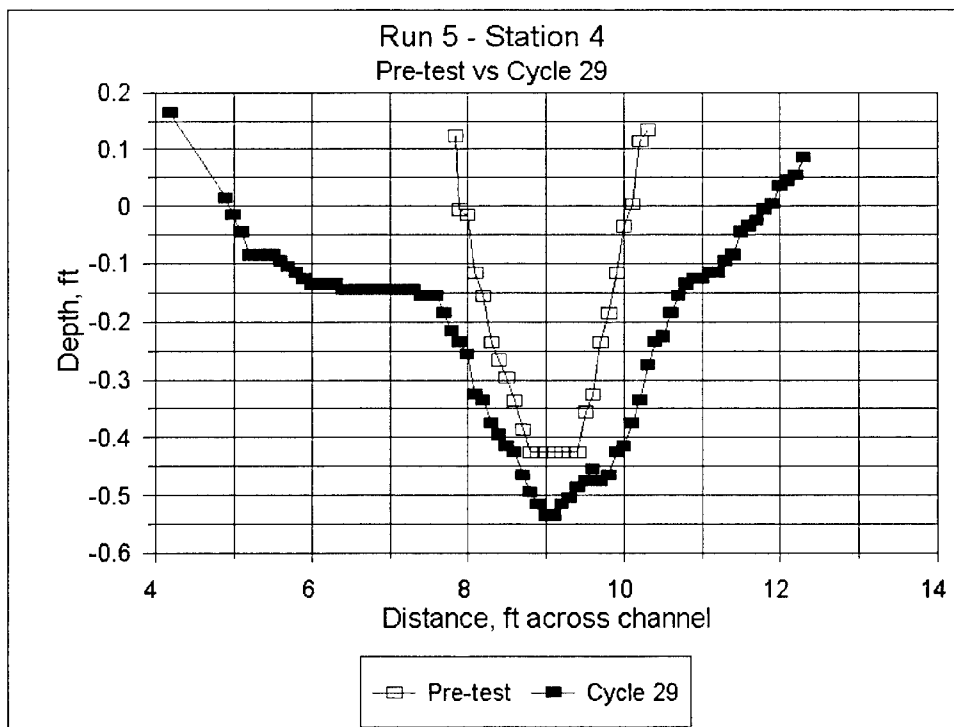


Plate A26

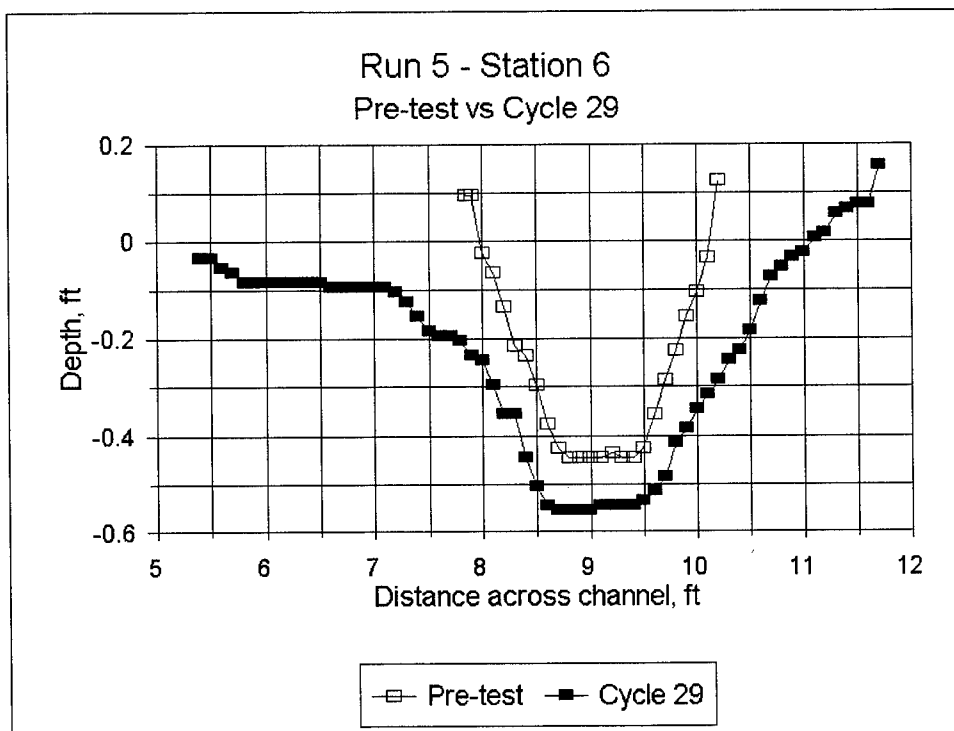


Plate A27

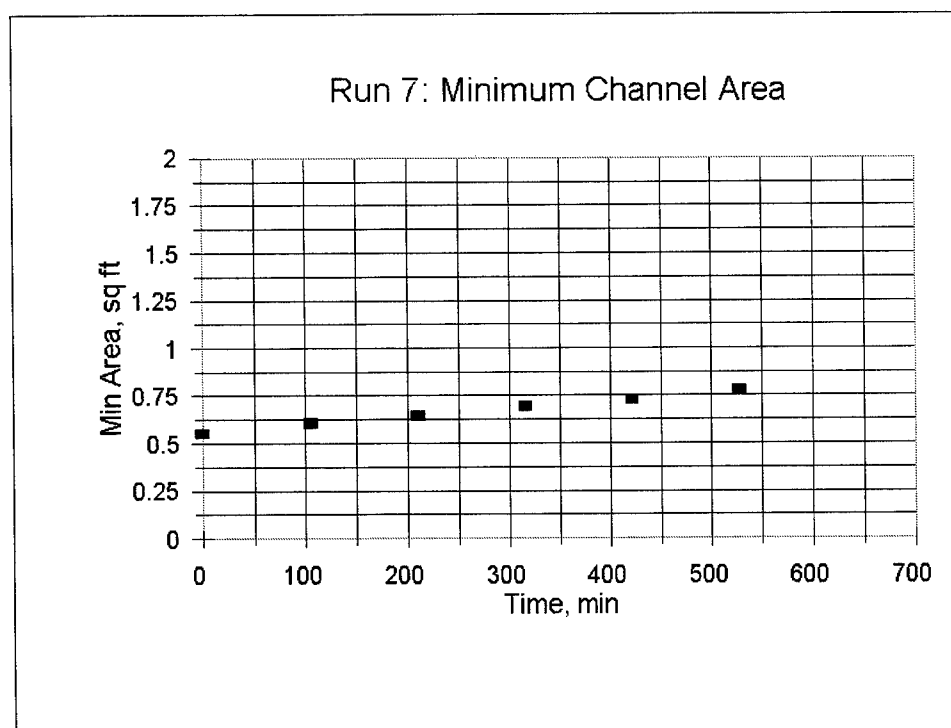


Plate A28

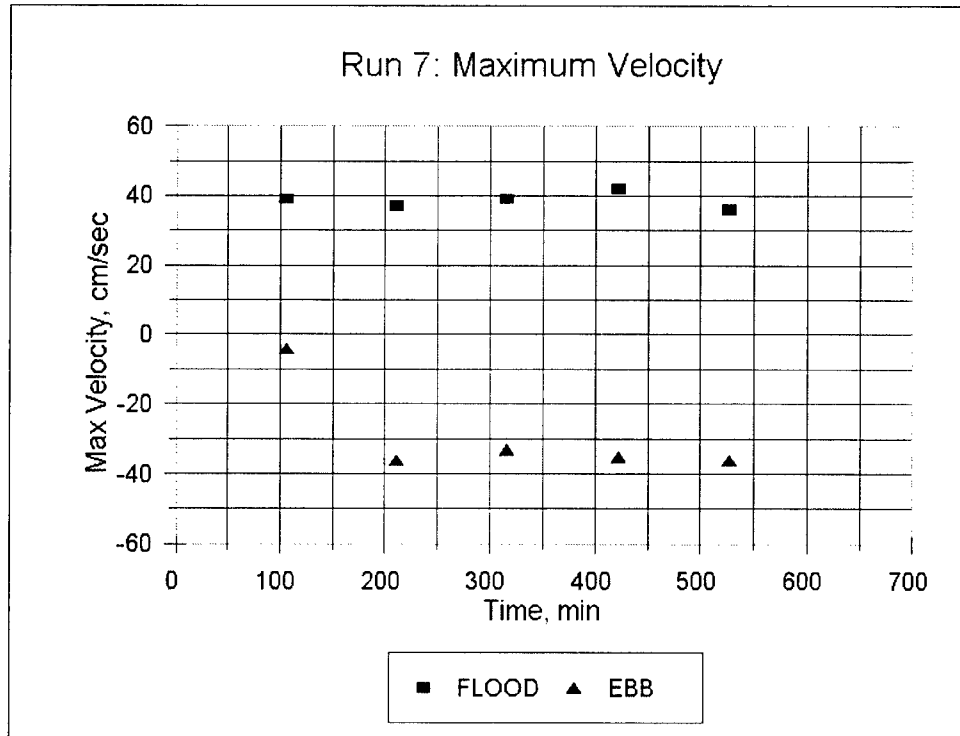


Plate A29

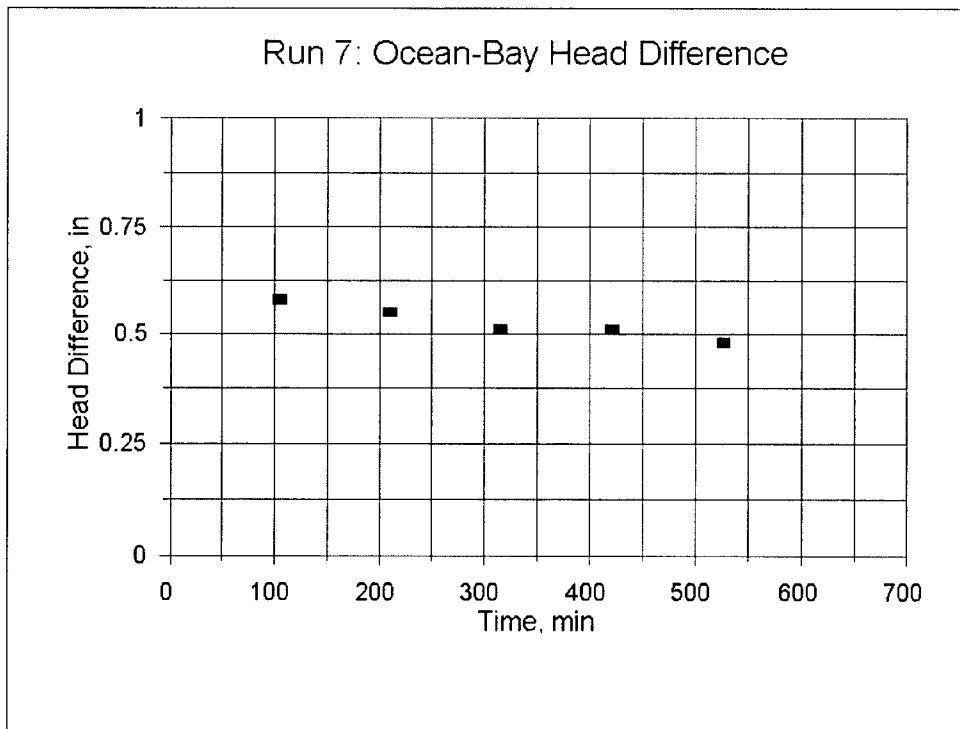


Plate A30

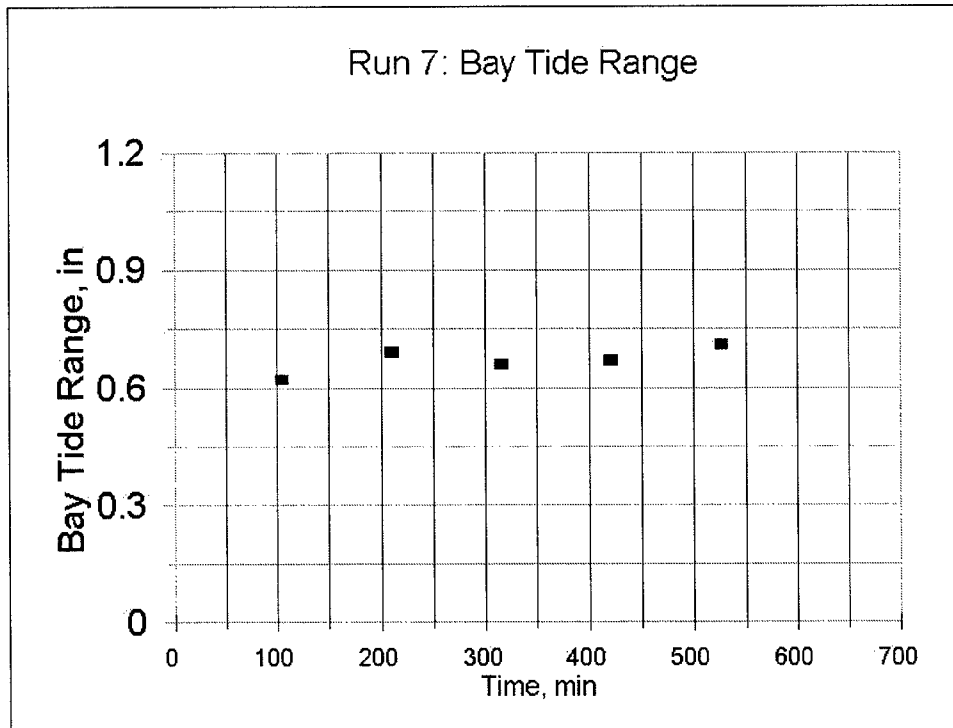


Plate A31

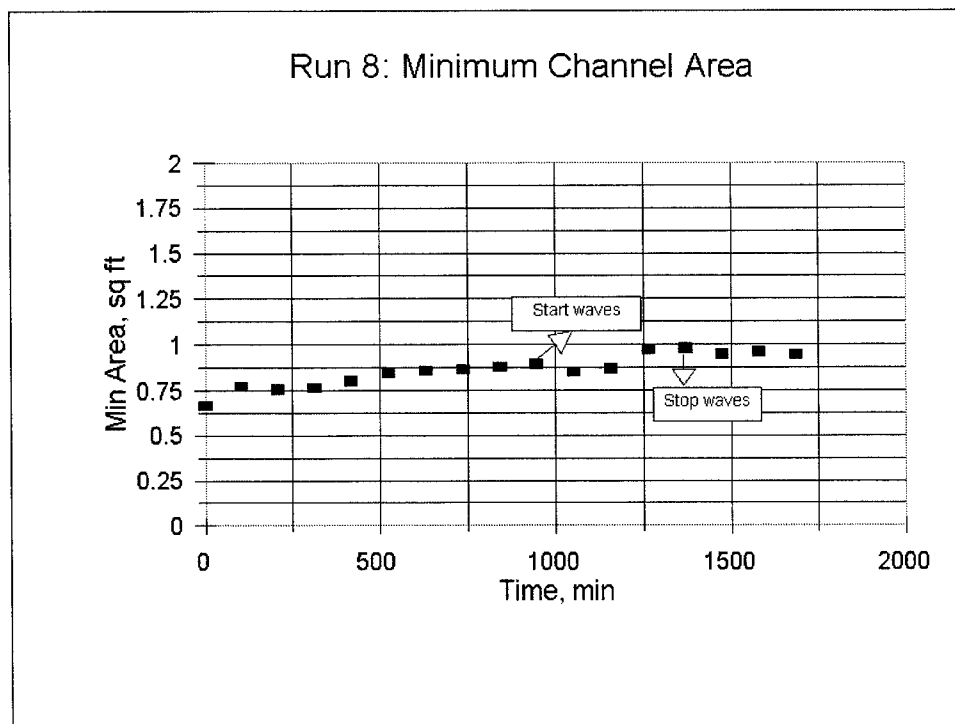


Plate A32

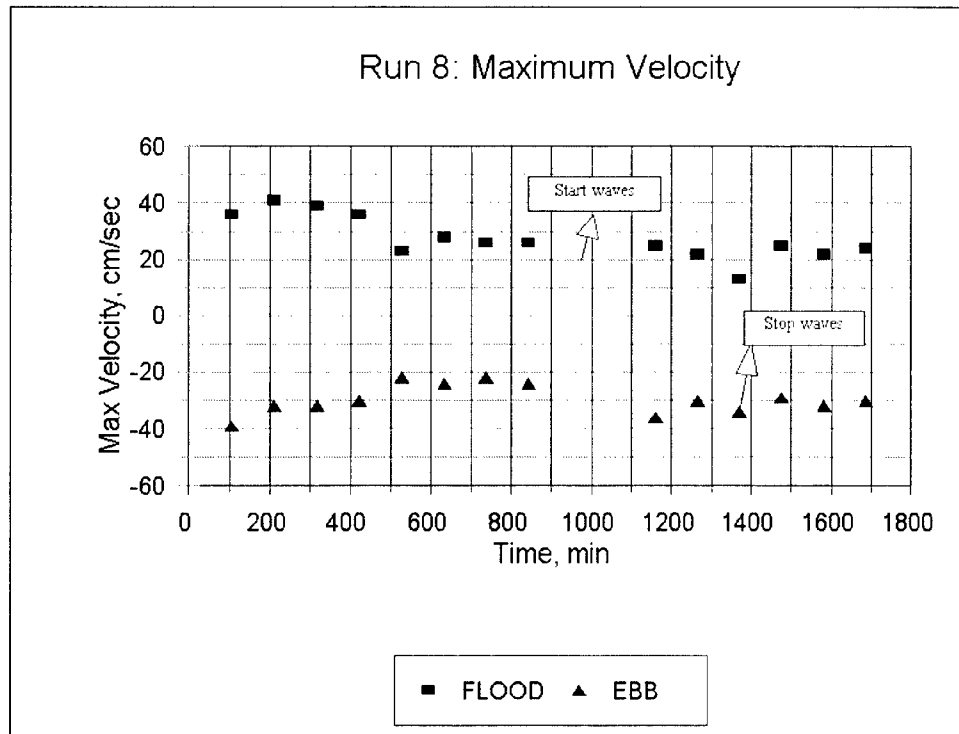


Plate A33

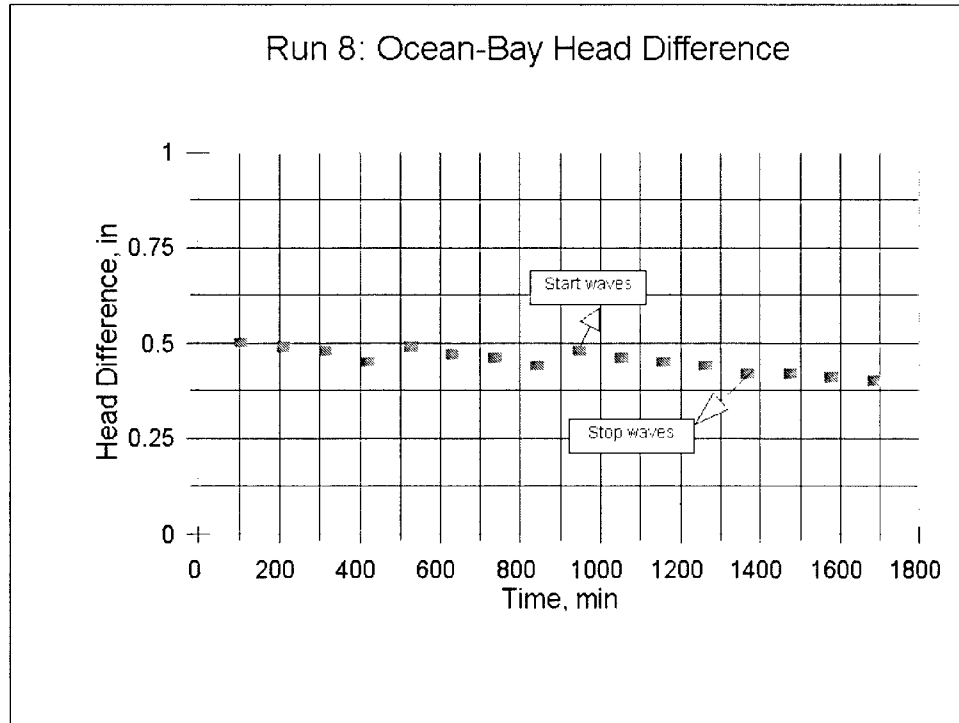


Plate A34

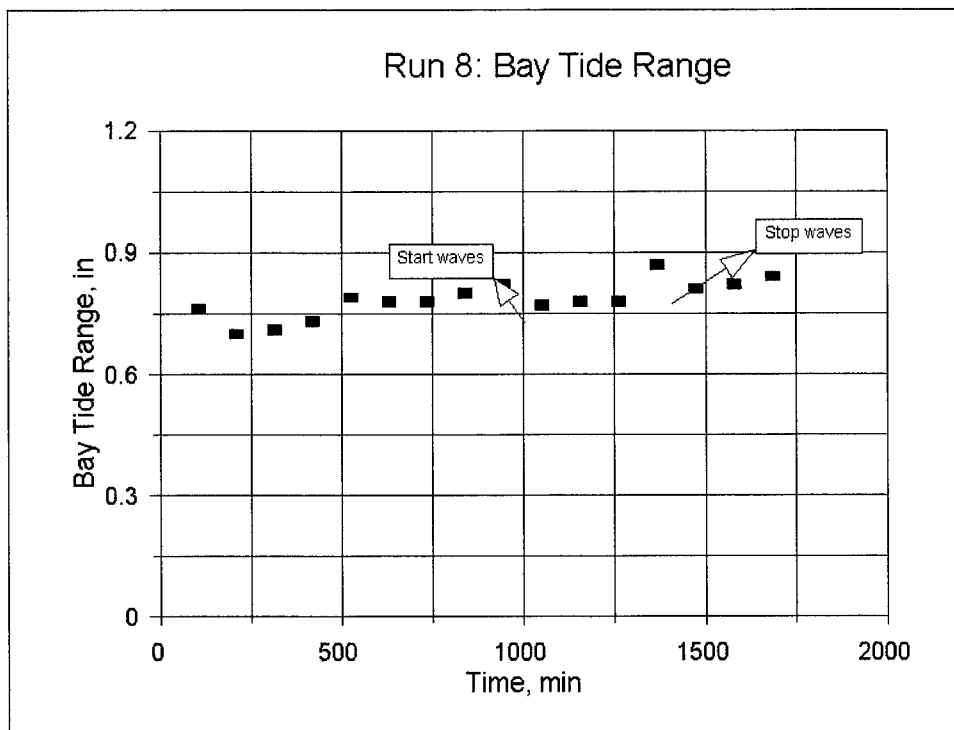


Plate A35

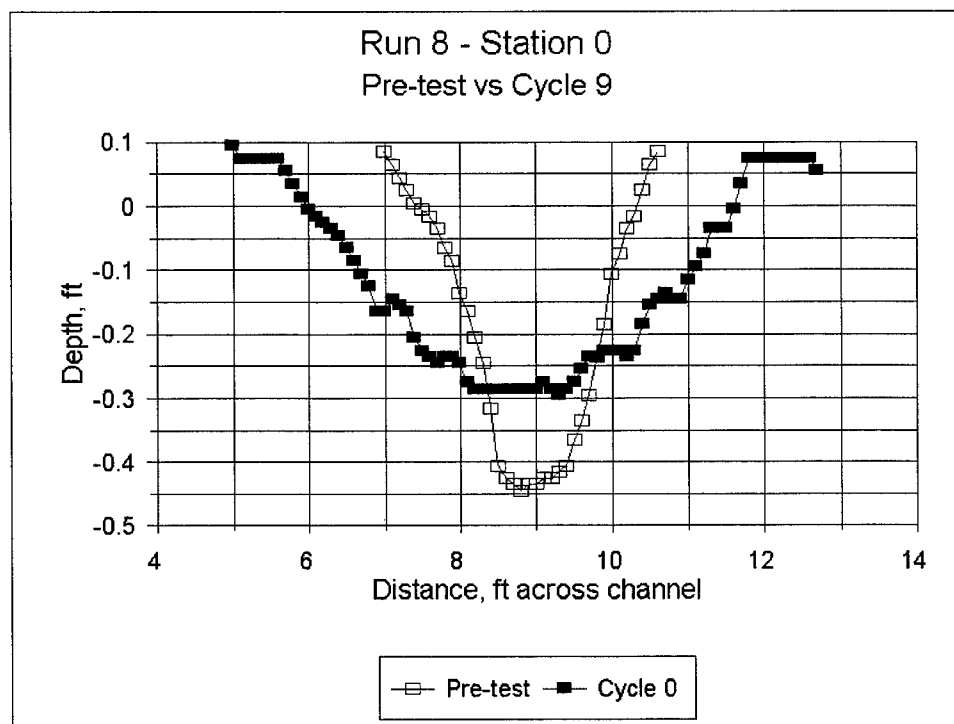


Plate A36

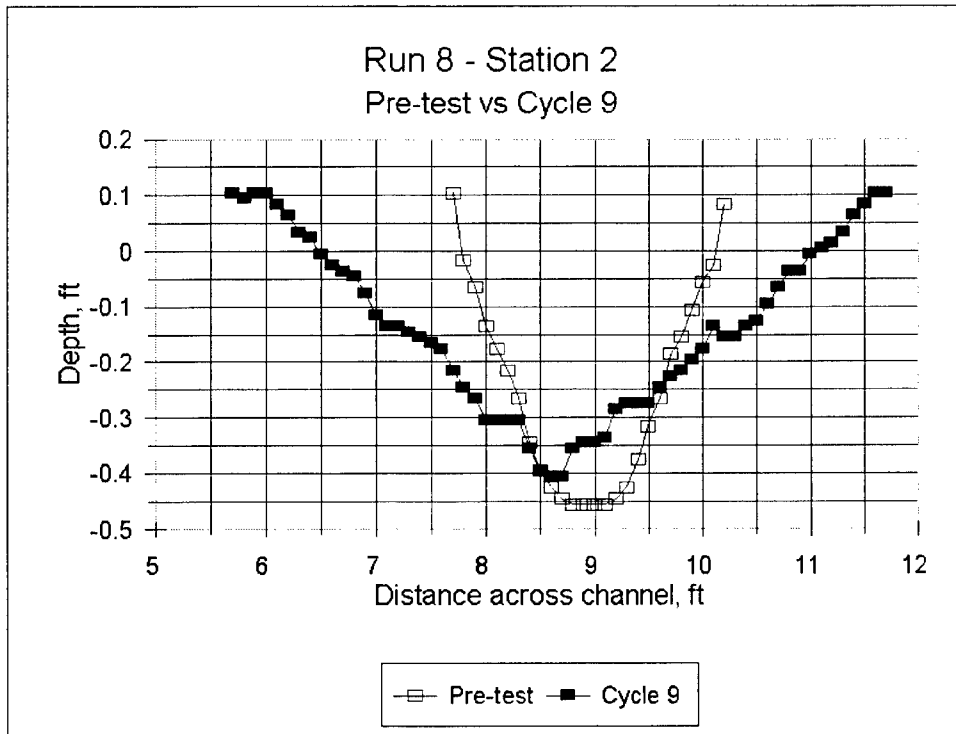


Plate A37

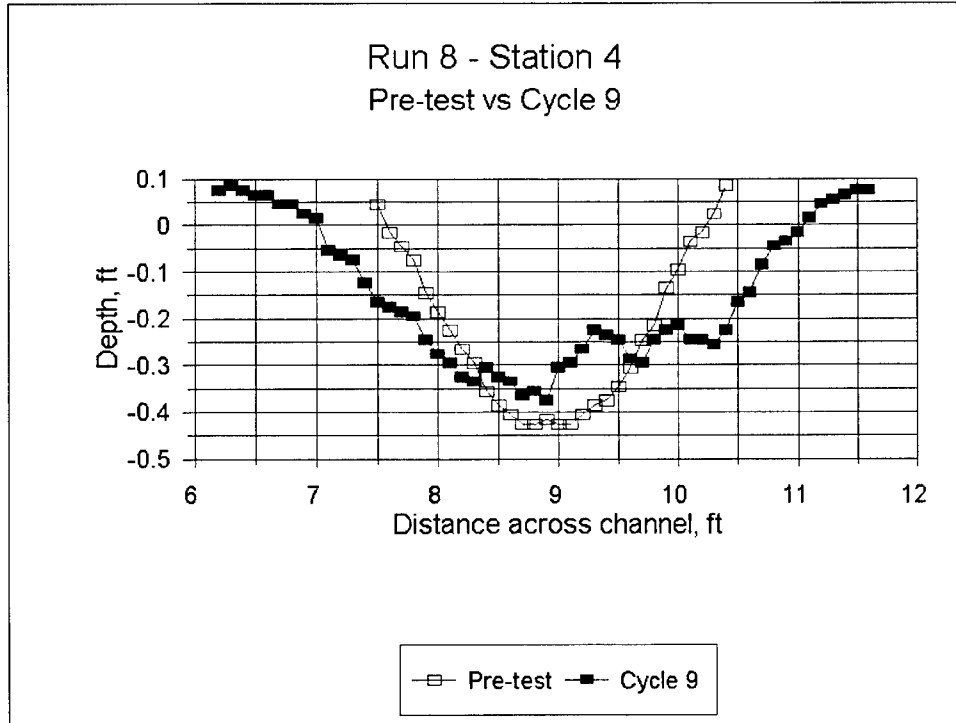


Plate A38

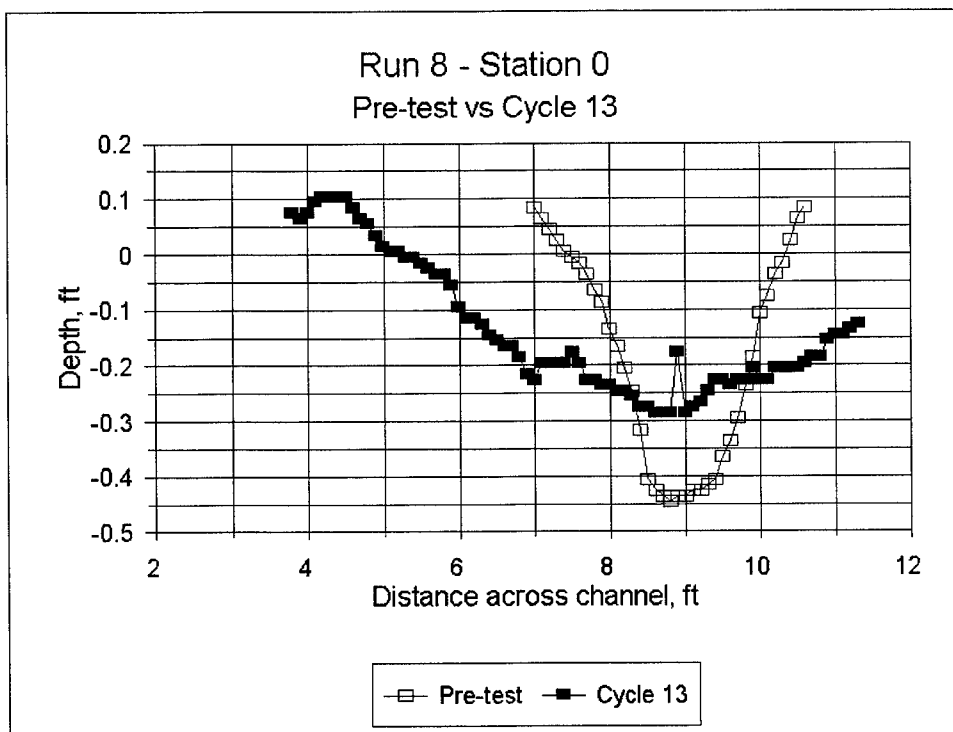


Plate A39

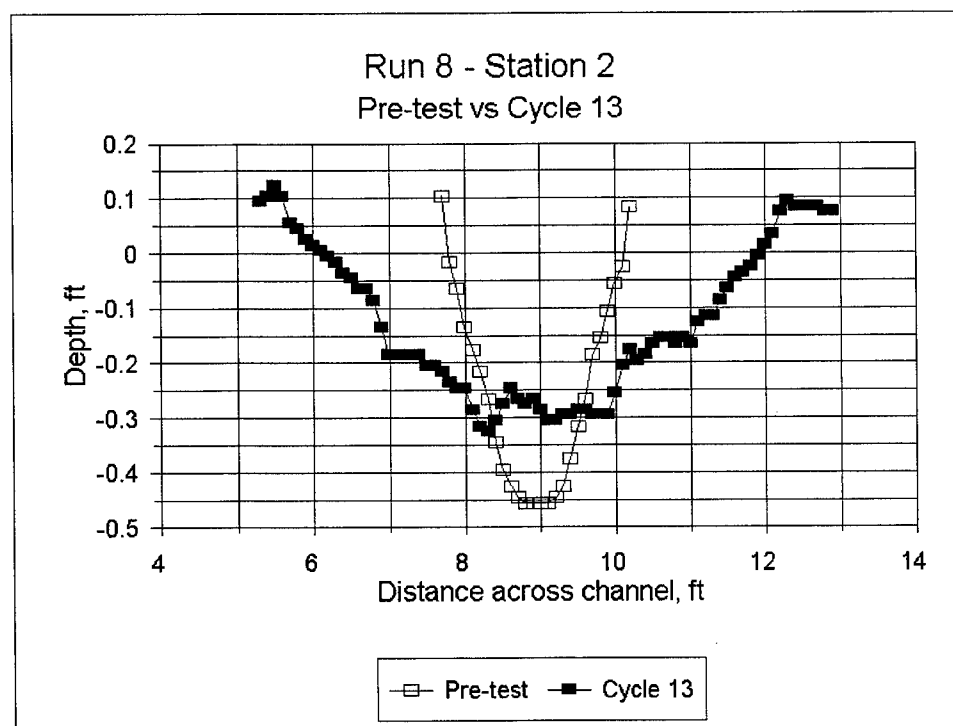


Plate A40

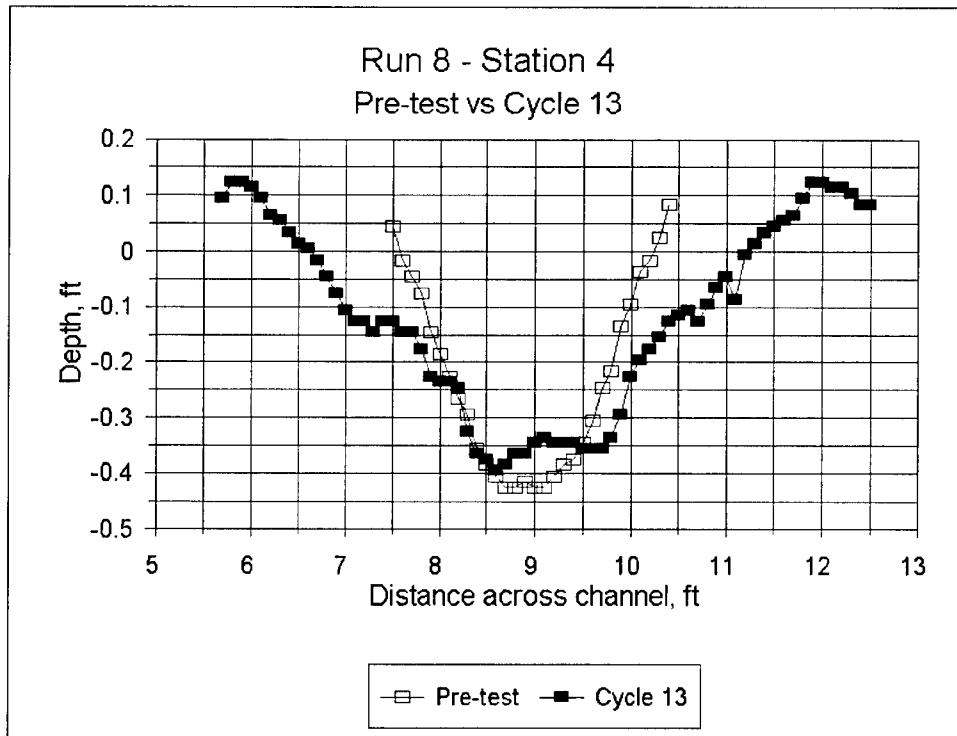


Plate A41

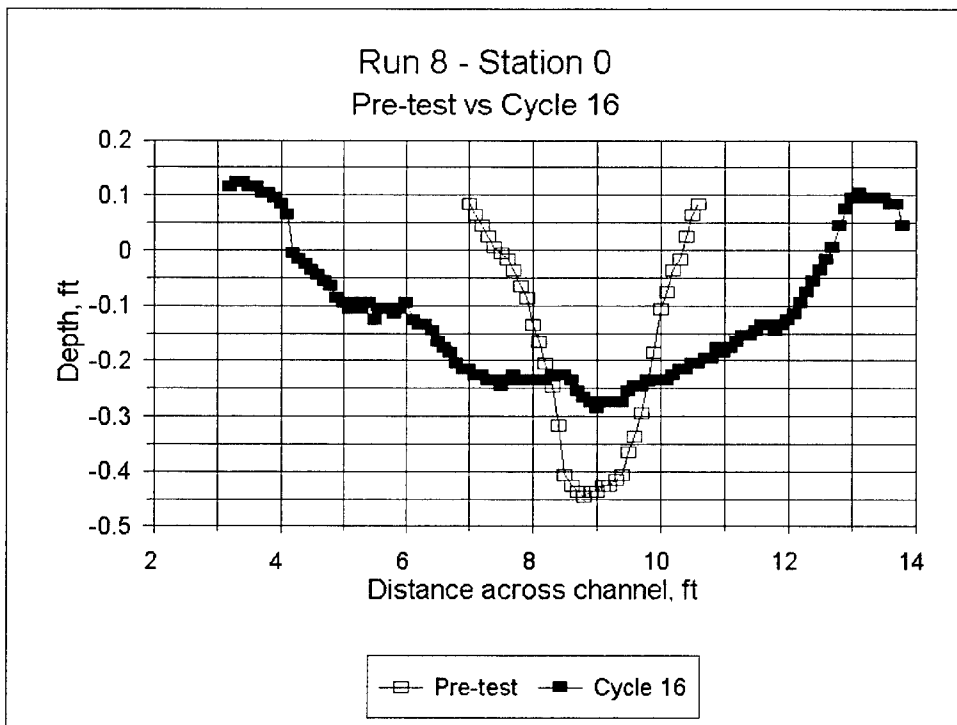


Plate A42

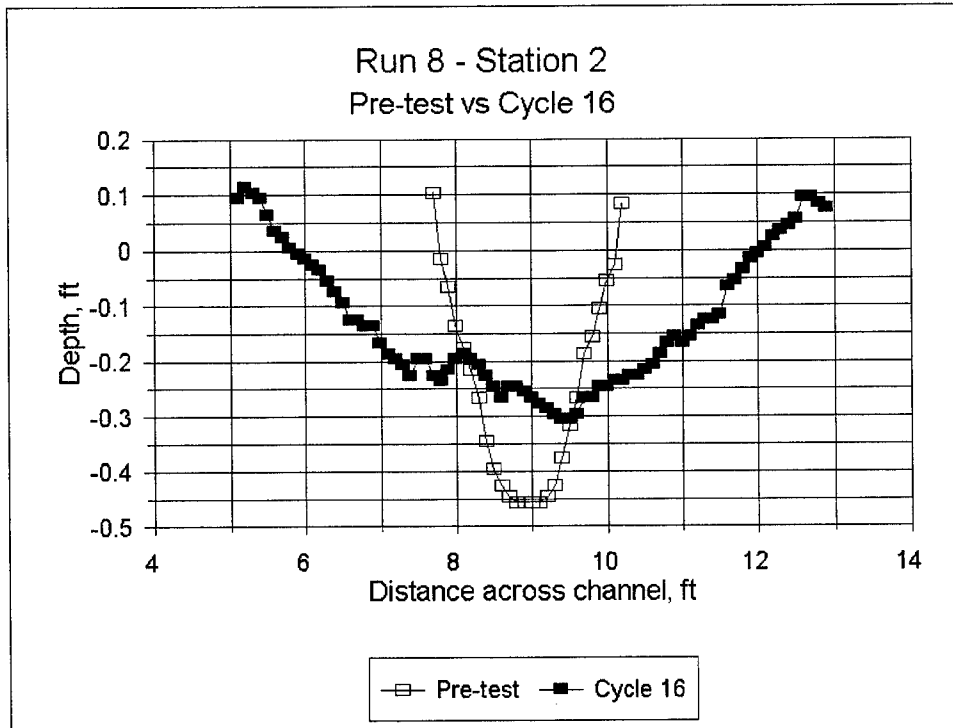


Plate A43

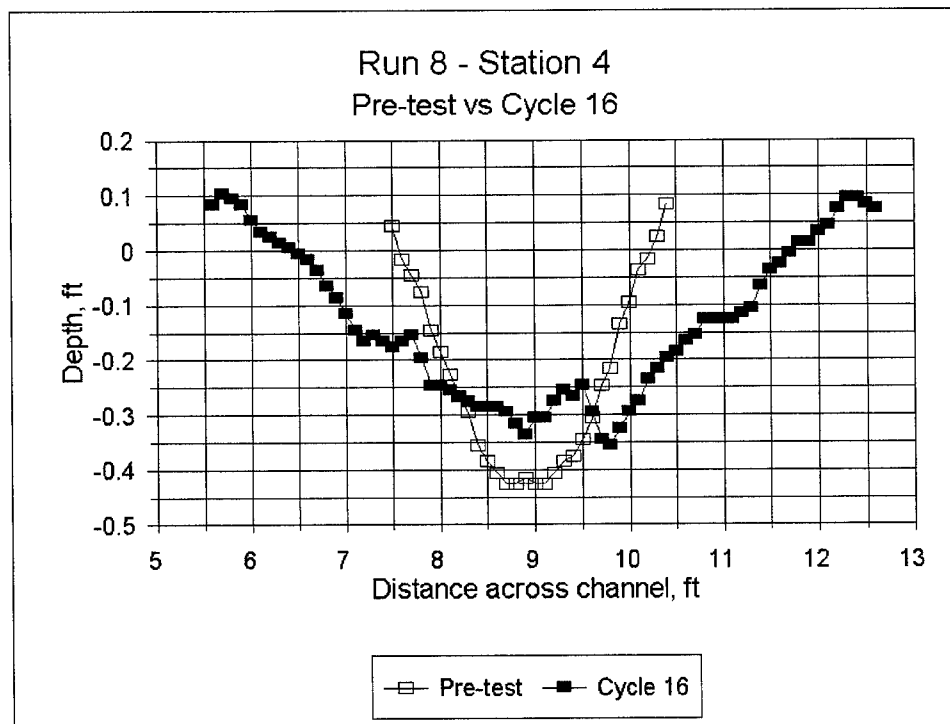


Plate A44

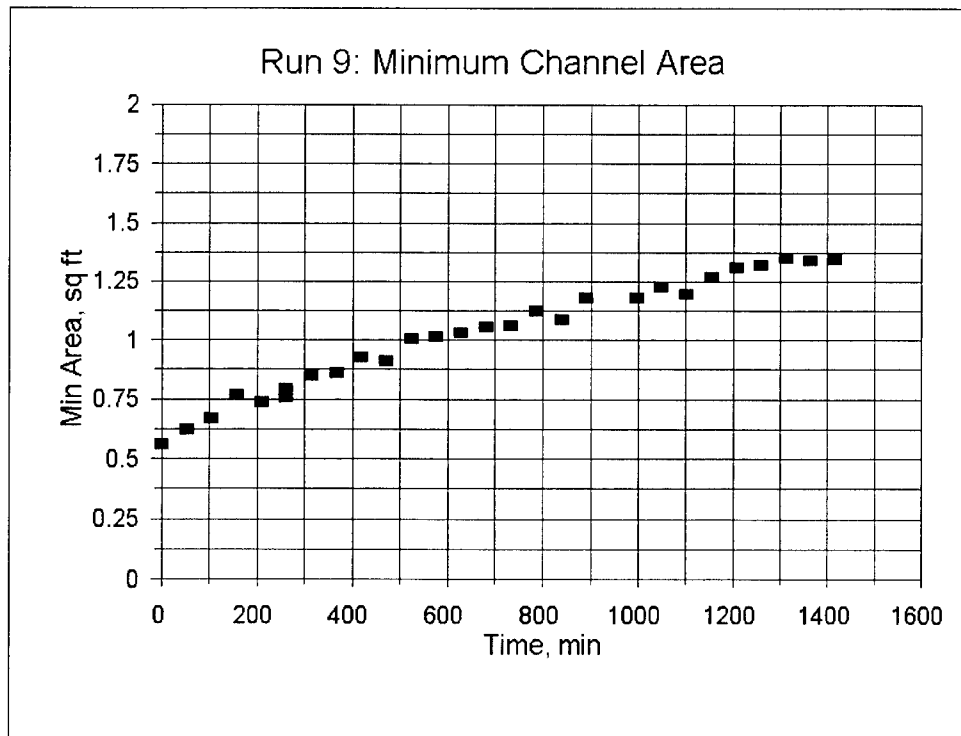


Plate A45

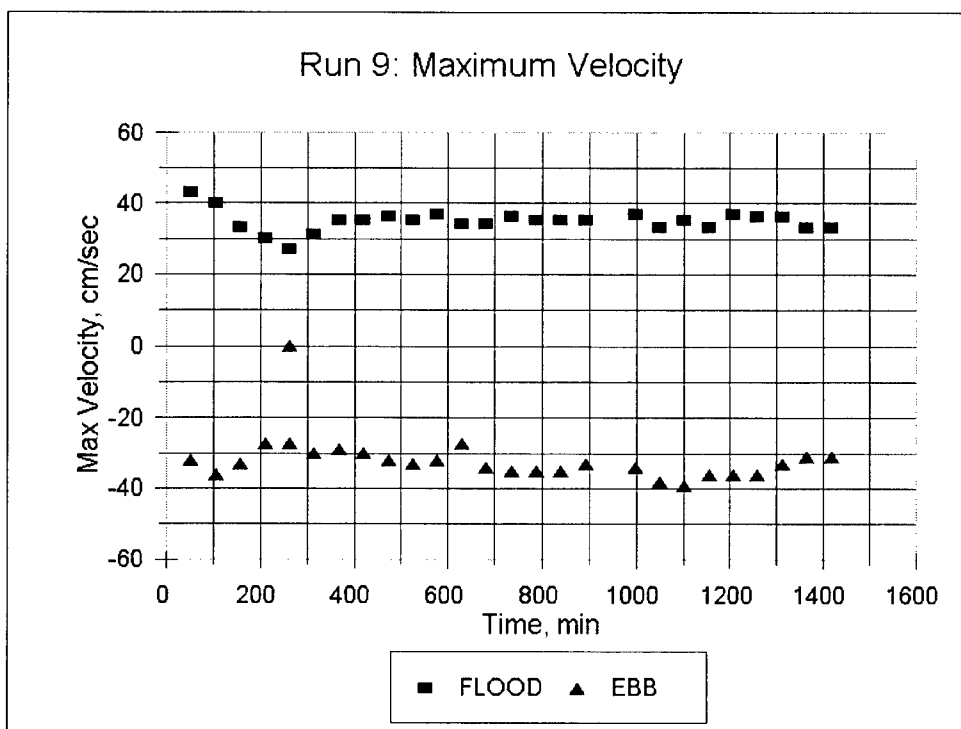


Plate A46

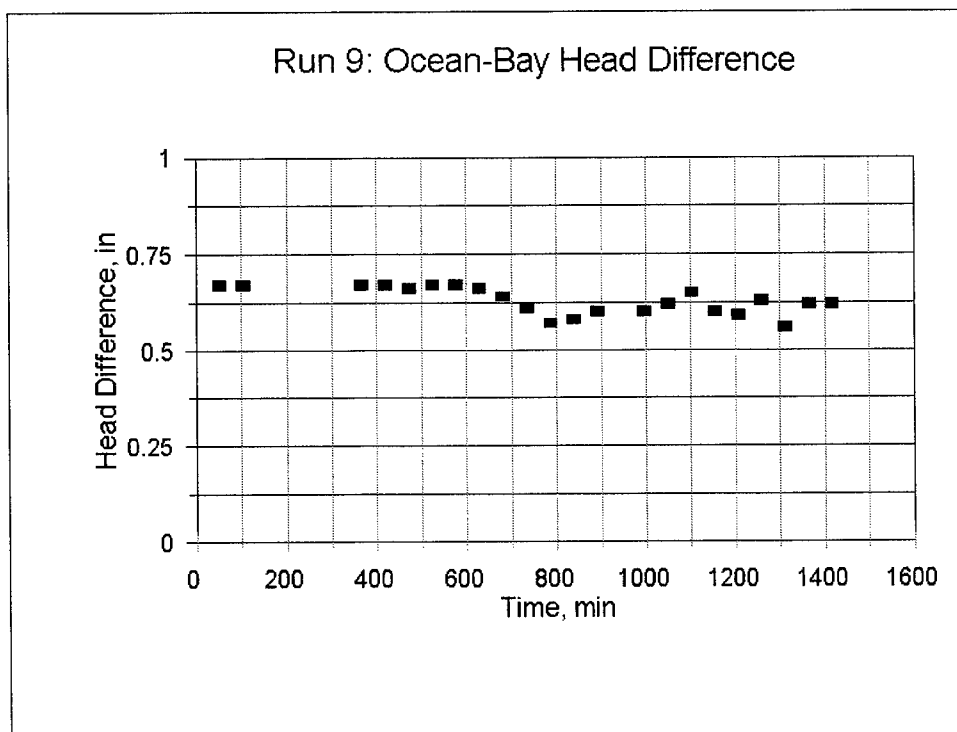


Plate A47

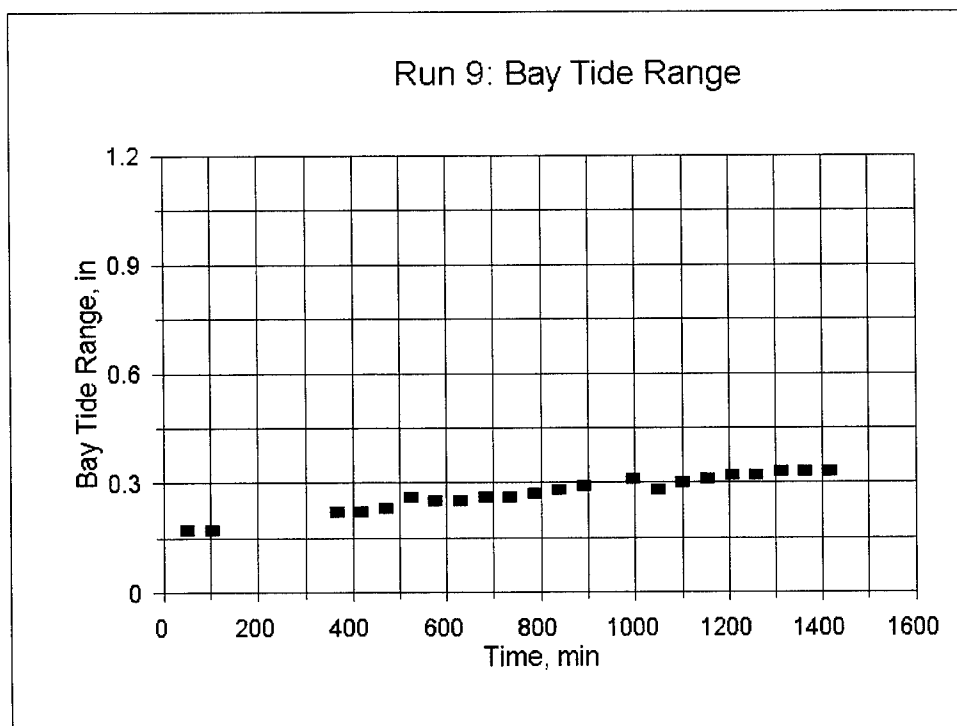


Plate A48

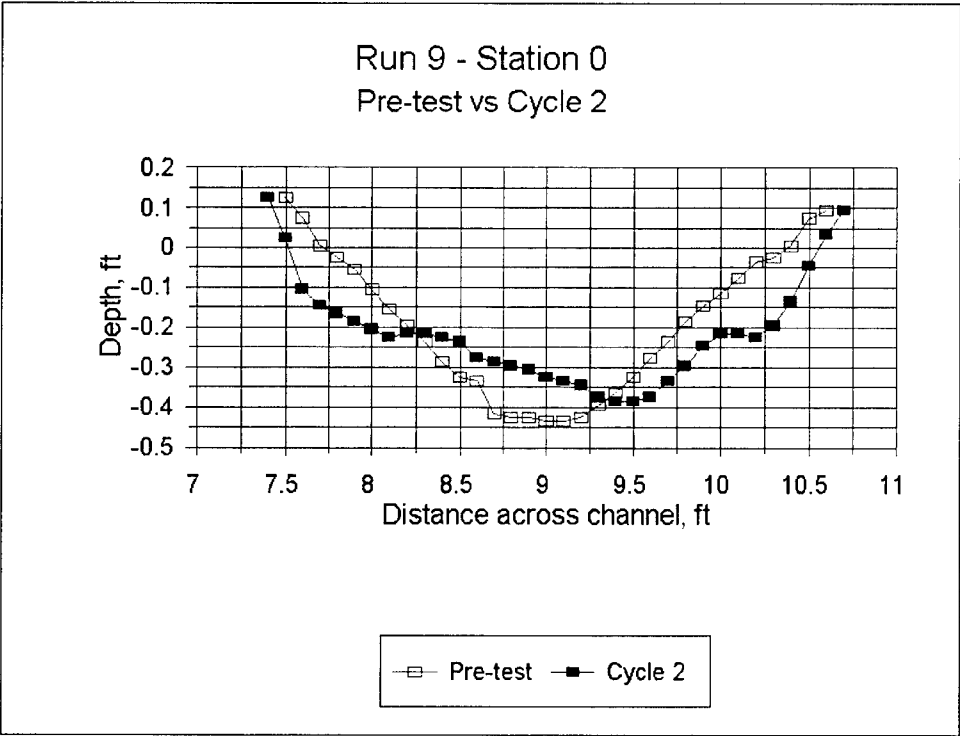


Plate A49

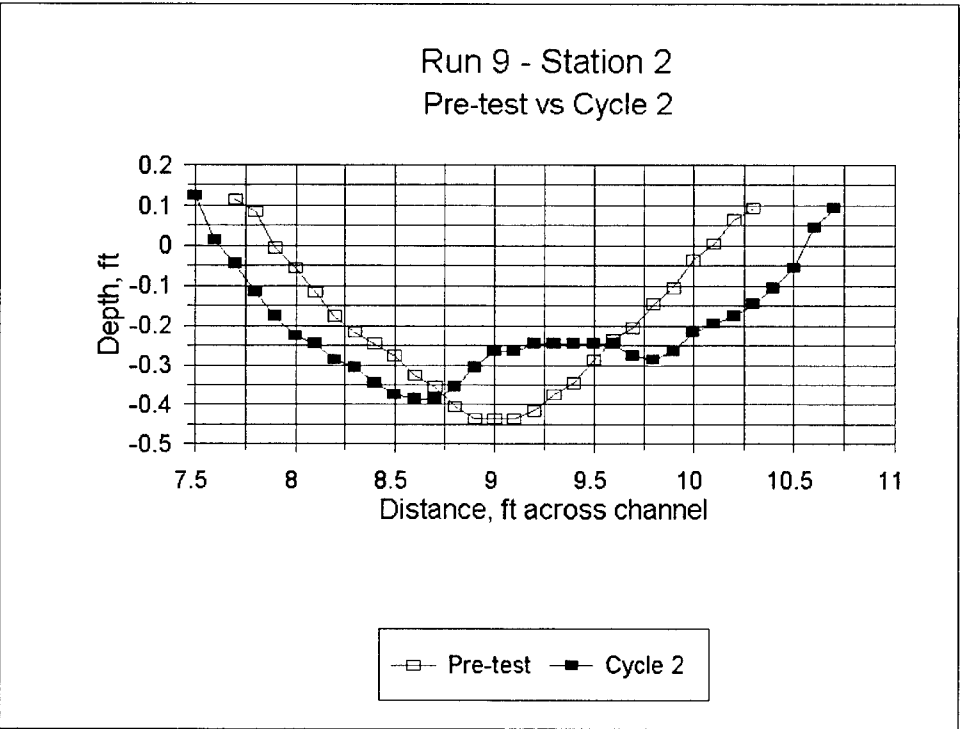


Plate A50

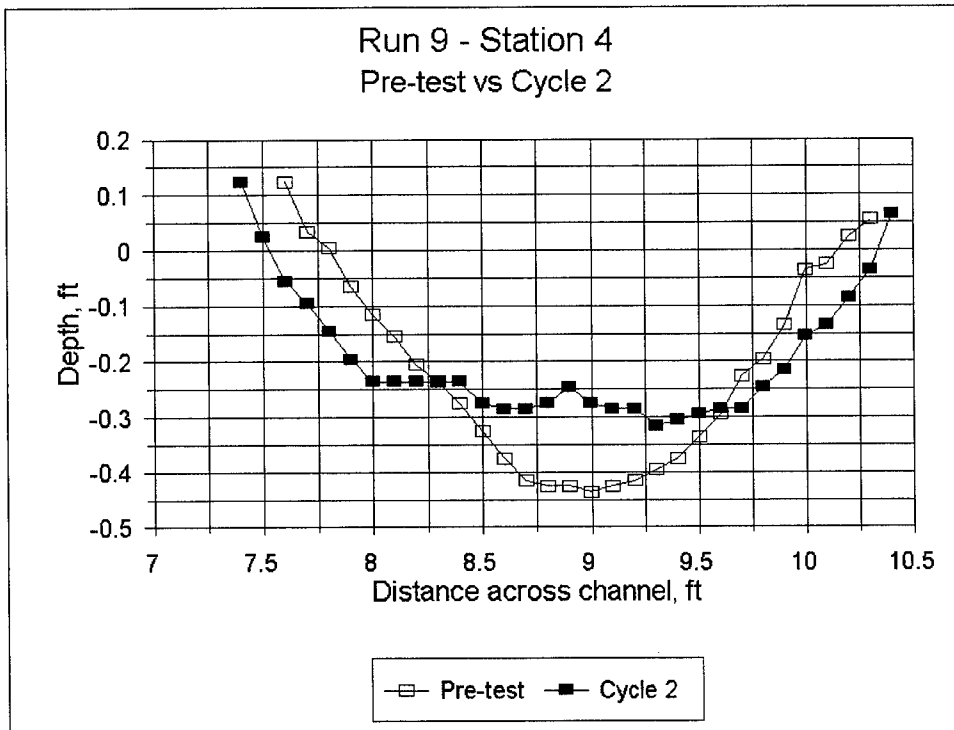


Plate A51

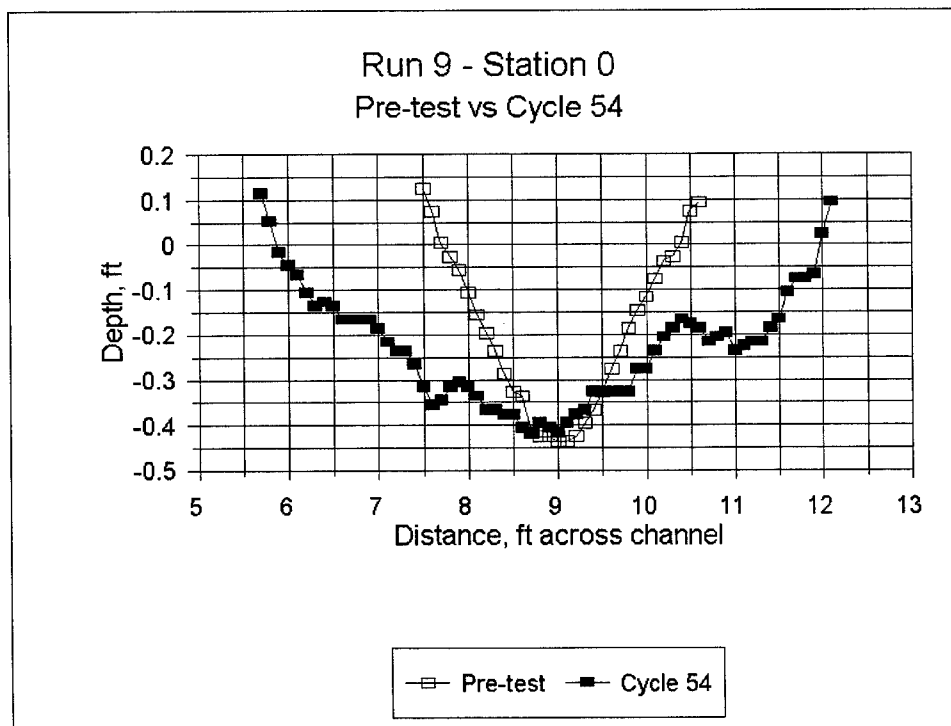


Plate A52

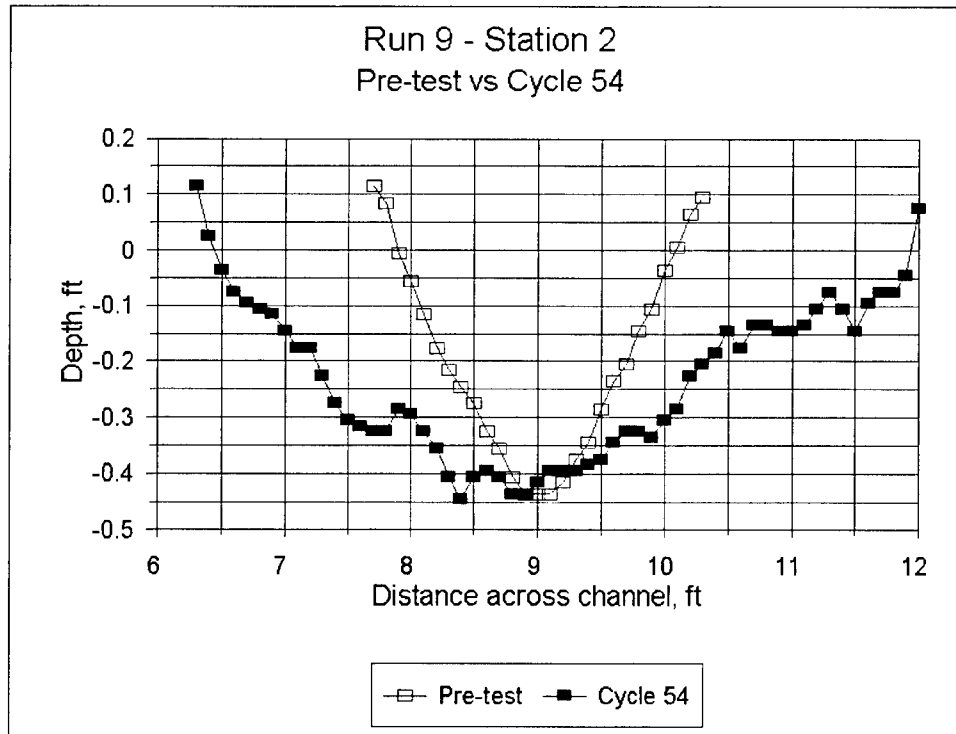


Plate A53

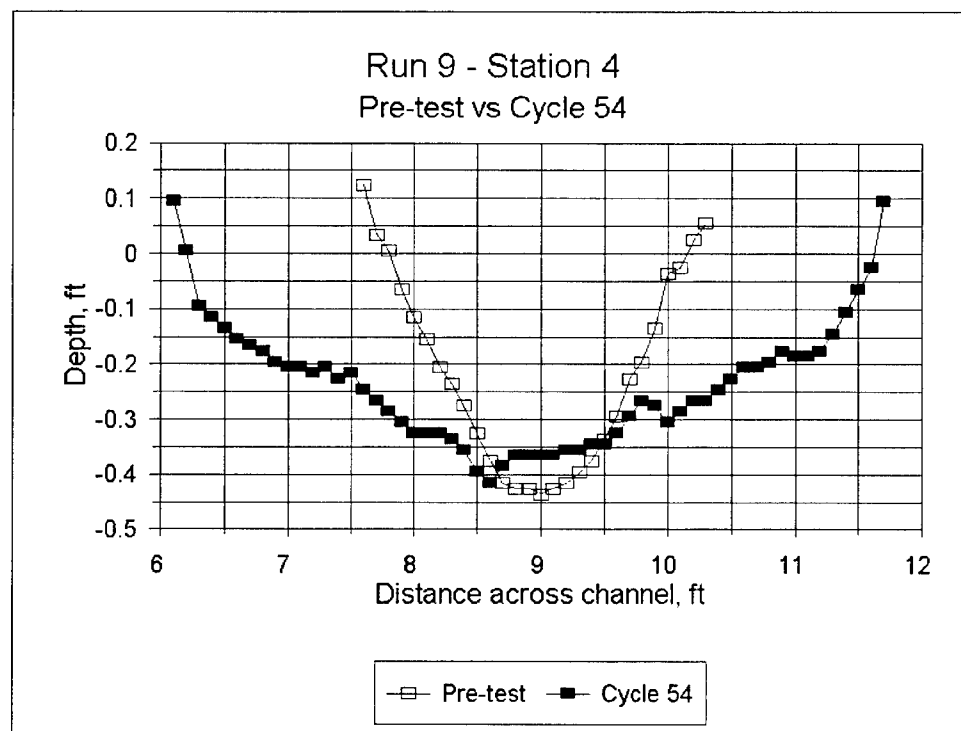


Plate A54

Appendix B

Data Time Series

This appendix contains time series data of maximum inlet velocity (ebb and flood flow), bay tide range, maximum head difference between ocean and bay for ebb and flood flow, and the minimum cross-sectional area. These data are for Runs 4, 5, 7, 8, and 9. Chapter 3 discusses experiment measurement procedures.

To convert measurements in this appendix given in inches to centimeters, multiply by 2.54. To convert measurements given in square feet to square meters, multiply by 0.09290304.

Table B1
CIRP Run 4

Cycle	Run Time min	Max Inlet Velocity, cm/sec		Bay Tide Range inches	Head Difference inches	Minimum Cross-Section Area, sq ft
		Flood	Ebb			
0	0					0.449
1	26.35			0.139	0.82	0.508
1.5	39.525					0.534
2	52.7			0.125	0.81	0.518
2.5	65.875					0.573
3	79.05					0.542
3.5	92.225					0.552
4	105.4			0.124	0.8	0.536
4.5	118.575					0.587
5	131.75					0.567
5.5	144.925					0.604
6	158.1	37		0.126	0.8	0.566
6.5	171.275		-41			0.594
7	184.45					0.562
7.5	197.625					0.58
8	210.8	40		0.131	0.8	
8.5	223.975		-39			0.599
9	237.15					
9.5	250.325					
10	263.5	41		0.136	0.79	
10.5	276.675		-39			
11	289.85					
11.5	303.025					
12	316.2	43		0.137	0.79	
12.5	329.375		-39			
13	342.55					
13.5	355.725					
14	368.9	40		0.141	0.78	
14.5	382.075		-39			
15	395.25	38		0.143	0.79	
15.5	408.425		-41			0.569
16	421.6	29		0.12	0.69	
16.5	434.775		-28			0.626
17	447.95					
17.5	461.125					0.604
18	474.3	30		0.12	0.67	
18.5	487.475		-28			0.615
19	500.65					

(Sheet 1 of 8)

Table B1 (Continued)						
Cycle	Run Time min	Max Inlet Velocity, cm/sec		Bay Tide Range Inches	Head Difference Inches	Minimum Cross-Section Area, sq ft
		Flood	Ebb			
19.5	513.825					
20	527	32		0.13	0.68	
20.5	540.175		-28			
21	553.35					
21.5	566.525					0.612
22	579.7	32		0.13	0.69	
22.5	592.875		-32			0.602
23	606.05					
23.5	619.225					0.588
24	632.4	32		0.13	0.67	
24.5	645.575		-28			
25	658.75					
25.5	671.925					0.468
26	685.1	33		0.13	0.69	
26.5	698.275		-27			0.474
27	711.45					
27.5	724.625					0.527
28	737.8	33		0.12	0.67	
28.5	750.975		-28			0.515
29	764.15					
29.5	777.325					0.592
30	790.5	33		0.12	0.69	
30.5	803.675		-30			0.575
31	816.85					
31.5	830.025					
32	843.2	31		0.12	0.66	
32.5	856.375		-30			0.559
33	869.55					
33.5	882.725					
34	895.9	30		0.12	0.65	
34.5	909.075		-32			0.525
35	922.25					
35.5	935.425					
36	948.6	30		0.12	0.66	
36.5	961.775		-29			0.546
37	974.95					
37.5	988.125					
38	1001.3	29		0.12	0.67	
(Sheet 2 of 8)						

Table B1 (Continued)						
Cycle	Run Time min	Max Inlet Velocity, cm/sec		Bay Tide Range Inches	Head Difference Inches	Minimum Cross-Section Area, sq ft
		Flood	Ebb			
38.5	1014.475		-27			0.55
39	1027.65					
39.5	1040.825					
40	1054	26		0.12	0.69	
40.5	1067.175		-18			0.546
41	1080.35					
41.5	1093.525					
42	1106.7	25		0.12	0.68	
42.5	1119.875		-22			0.584
43	1133.05					
43.5	1146.225					
44	1159.4	29		0.12	0.69	
44.5	1172.575		-28			0.597
45	1185.75	25			0.69	
45.5	1198.925		-28	0.12		0.59
46	1212.1				0.66	
46.5	1225.275					0.592
47	1238.45					
47.5	1251.625					
48	1264.8		-24	0.1	0.68	
48.5	1277.975					
49	1291.15					
49.5	1304.325					
50	1317.5	29	-27	0.1	0.67	0.531
50.5	1330.675					
51	1343.85					
51.5	1357.025					
52	1370.2	25	-28	0.1	0.69	0.599
52.5	1383.375					
53	1396.55					
53.5	1409.725					
54	1422.9	23	-17	0.1	0.67	0.599
54.5	1436.075					
55	1449.25					
55.5	1462.425					
56	1475.6	20	-15	0.1	0.69	0.58
56.5	1488.775					
57	1501.95					
(Sheet 3 of 8)						

Table B1 (Continued)						
Cycle	Run Time min	Max Inlet Velocity, cm/sec		Bay Tide Range inches	Head Difference inches	Minimum Cross-Section Area, sq ft
		Flood	Ebb			
57.5	1515.125					
58	1528.3	16	-12	0.11	0.69	0.569
58.5	1541.475					
59	1554.65					
59.5	1567.825					
60	1581	10	-13	0.11	0.68	0.509
60.5	1594.175					
61	1607.35	13	-14	0.11	0.69	0.545
61.5	1620.525					
62	1633.7			0.11	0.68	0.5
62.5	1646.875					
63	1660.05					
63.5	1673.225					
64	1686.4	26	-35	0.11	0.68	0.519
64.5	1699.575					
65	1712.75					
65.5	1725.925					
66	1739.1	24	-36	0.1	0.7	0.558
66.5	1752.275					
67	1765.45					
67.5	1778.625					
68	1791.8	26	-39	0.1	0.69	0.538
68.5	1804.975					
69	1818.15					
69.5	1831.325					
70	1844.5	26	-39	0.1	0.71	0.558
70.5	1857.675					
71	1870.85					
71.5	1884.025					
72	1897.2	27	-37	0.11	0.69	0.568
72.5	1910.375					
73	1923.55					
73.5	1936.725					
74	1949.9	27	-37	0.11	0.7	0.563
74.5	1963.075					
75	1976.25					
75.5	1989.425					
76	2002.6	26	-33	0.12	0.71	0.583
76.5	2015.775					
(Sheet 4 of 8)						

Table B1 (Continued)						
Cycle	Run Time min	Max Inlet Velocity, cm/sec		Bay Tide Range Inches	Head Difference Inches	Minimum Cross-Section Area, sq ft
		Flood	Ebb			
77	2028.95	27	-33	0.12	0.7	0.545
77.5	2042.125					
78	2055.3	23	-28	0.11	0.66	0.55
78.5	2068.475					
79	2081.65					
79.5	2094.825					
80	2108	23	-27	0.11	0.68	0.544
80.5	2121.175					
81	2134.35					
81.5	2147.525					
82	2160.7	20	-24	0.11	0.69	0.542
82.5	2173.875					
83	2187.05					
83.5	2200.225					
84	2213.4	19	-25	0.12	0.69	0.543
84.5	2226.575					
85	2239.75					
85.5	2252.925					
86	2266.1	20	-20	0.12	0.69	0.526
86.5	2279.275					
87	2292.45					
87.5	2305.625					
88	2318.8	19	-21	0.12	0.68	0.524
88.5	2331.975					
89	2345.15					
89.5	2358.325					
90	2371.5	19	-20	0.12	0.69	0.525
90.5	2384.675					
91	2397.85					
91.5	2411.025					
92	2424.2	19	-26	0.12	0.71	0.575
92.5	2437.375					
93	2450.55	20	-22	0.12	0.71	0.516
93.5	2463.725					
94	2476.9	28	-34	0.13	0.65	0.576
94.5	2490.075					
95	2503.25					
95.5	2516.425					
96	2529.6	28	-32	0.12	0.69	0.563
(Sheet 5 of 8)						

Table B1 (Continued)						
Cycle	Run Time min	Max Inlet Velocity, cm/sec		Bay Tide Range Inches	Head Difference inches	Minimum Cross-Section Area, sq ft
		Flood	Ebb			
96.5	2542.775					
97	2555.95					
97.5	2569.125					
98	2582.3	25	-28	0.12	0.69	0.549
98.5	2595.475					
99	2608.65					
99.5	2621.825					
100	2635	27	-27	0.13	0.69	0.543
100.5	2648.175					
101	2661.35					
101.5	2674.525					
102	2687.7	24	-25	0.13	0.7	0.546
102.5	2700.875					
103	2714.05					
103.5	2727.225					
104	2740.4	25	-28	0.13	0.7	0.584
104.5	2753.575					
105	2766.75					
105.5	2779.925					
106	2793.1					
106.5	2806.275					
107	2819.45	25	-30	0.13	0.69	0.566
107.5	2832.625					
108	2845.8	27	-30	0.11	0.66	0.557
108.5	2858.975					
109	2872.15					
109.5	2885.325					
110	2898.5	23	-29	0.12	0.68	0.591
110.5	2911.675					
111	2924.85					
111.5	2938.025					
112	2951.2	27	-29	0.12	0.68	0.577
112.5	2964.375					
113	2977.55					
113.5	2990.725					
114	3003.9	27	-29	0.12	0.68	0.569
114.5	3017.075					
115	3030.25					
115.5	3043.425					
(Sheet 6 of 8)						

Table B1 (Continued)						
Cycle	Run Time min	Max Inlet Velocity, cm/sec		Bay Tide Range inches	Head Difference inches	Minimum Cross-Section Area, sq ft
		Flood	Ebb			
116	3056.6	20	-28	0.12	0.67	0.574
116.5	3069.775					
117	3082.95					
117.5	3096.125					
118	3109.3	20	-30	0.13	0.68	0.613
118.5	3122.475					
119	3135.65					
119.5	3148.825					
120	3162					
120.5	3175.175					
121	3188.35	23	-30	0.13	0.69	0.645
121.5	3201.525					
122	3214.7	20	-32	0.11	0.66	0.633
122.5	3227.875					
123	3241.05					
123.5	3254.225					
124	3267.4	22	-27	0.12	0.67	0.619
124.5	3280.575					
125	3293.75					
125.5	3306.925					
126	3320.1	26	-20	0.12	0.68	0.699
126.5	3333.275					
127	3346.45					
127.5	3359.625					
128	3372.8	20	-22	0.13	0.68	0.659
128.5	3385.975					
129	3399.15					
129.5	3412.325					
130	3425.5	20	-20	0.13	0.69	0.688
130.5	3438.675					
131	3451.85					
131.5	3465.025					
132	3478.2	17	-21	0.12	0.7	0.646
132.5	3491.375					
133	3504.55					
133.5	3517.725					
134	3530.9					
134.5	3544.075					
135	3557.25	22	-19	0.12	0.7	0.674
(Sheet 7 of 8)						

Table B1 (Concluded)						
Cycle	Run Time min	Max Inlet Velocity, cm/sec		Bay Tide Range inches	Head Difference inches	Minimum Cross-Section Area, sq ft
		Flood	Ebb			
135.5	3570.425					
136	3583.6	31	-33	0.13	0.63	0.649
136.5	3596.775					
137	3609.95					
137.5	3623.125					
138	3636.3	30	-36	0.13	0.67	0.65
138.5	3649.475					
139	3662.65					
139.5	3675.825					
140	3689	38	-0.12	0.12	0.69	0.629
140.5	3702.175					
141	3715.35					
141.5	3728.525					
142	3741.7	26	-36	0.12	0.7	0.632
142.5	3754.875					
143	3768.05					
143.5	3781.225					
144	3794.4	27	-36	0.12	0.42	0.652
144.5	3807.575					
(Sheet 8 of 8)						

Table B2
CIRP Run 5

Cycle	Run Time min	Max Inlet Velocity, cm/sec		Bay Tide Range Inches	Head Difference Inches	Minimum Cross-Section Area, sq ft
		Flood	Ebb			
0	0	0	0	0	0	0.567
1	105.4	30	-33	0.74	0.45	0.739
2	210.8	40	-33	0.77	0.37	0.775
3	316.2	38	-28	0.79	0.33	0.902
4	421.6	27	-21	0.92	0.33	0.927
5	527	38	-26	0.92	0.3	0.971
6	632.4	37	-23	0.94	0.28	1.031
7	737.8	33	-22	0.97	0.28	1.054
8	843.2			1	0.29	1.148
9	948.6	32	-25	1	0.24	1.061
10	1054	32	-25	1	0.22	1.154
11	1159.4	28	-25	1.03	0.2	1.19
12	1264.8	28	-27	1.06	0.22	1.141
13	1370.2	36	-24	1.05	0.21	1.181
14	1475.6	34	-27	1.06	0.2	1.209
15	1581	32	-27	1.07	0.15	1.19
16	1686.4	32	-25	1.09	0.22	1.249
17	1791.8	37	-23	1.08	0.21	1.217
18	1897.2	37	-22	1.08	0.21	1.258
19	2002.6	36	-26	1.08	0.18	1.279
20	2108	35	-22	1.09	0.15	1.202
21	2213.4	24	-27	1.11	0.16	
22	2318.8	35	-25	1.09	0.19	
23	2424.2	35	-30	1.04	0.22	
24	2529.6	33	-31	1.03	0.21	1.3
25	2635	23	-26	1.05	0.22	
26	2740.4	30	-23	1.05	0.24	
27	2845.8	29	-26	1.05	0.19	
28	2951.2	20	-27	1.05	0.21	
29	3056.6	27	-27	1.04	0.18	1.589

Table B3 CIRP Run 7						
Cycle	Run Time min	Max Inlet Velocity, cm/sec		Bay Tide Range Inches	Head Difference Inches	Minimum Cross-Section Area, sq ft
		Flood	Ebb			
0	0					0.552
1	105.4	39	-4	0.62	0.58	0.605
2	210.8	37	-36	0.69	0.55	0.644
3	316.2	39	-33	0.66	0.51	0.695
4	421.6	42	-35	0.67	0.51	0.731
5	527	36	-36	0.71	0.48	0.78
6	632.4					

Table B4						
CIRP Run 8						
Cycle	Run Time min	Max Inlet Velocity, cm/sec		Bay Tide Range Inches	Head Difference Inches	Minimum Cross-Section Area, sq ft
		Flood	Ebb			
0	0					0.663
1	105.4	36	-39	0.76	0.5	0.769
2	210.8	41	-32	0.7	0.49	0.752
3	316.2	39	-32	0.71	0.48	0.765
4	421.6	36	-30	0.73	0.45	0.8
5	527	23	-22	0.79	0.49	0.842
6	632.4	28	-24	0.78	0.47	0.858
7	737.8	26	-22	0.78	0.46	0.862
8	843.2	26	-24	0.8	0.44	0.875
9	948.6			0.82	0.48	0.892
10	1054			0.77	0.46	0.851
11	1159.4	25	-36	0.78	0.45	0.866
12	1264.8	22	-30	0.78	0.44	0.969
13	1370.2	13	-34	0.87	0.42	0.979
14	1475.6	25	-29	0.81	0.42	0.946
15	1581	22	-32	0.82	0.41	0.959
16	1686.4	24	-30	0.84	0.4	0.942

Table B5
CIRP Run 9

Cycle	Run Time min	Max Inlet Velocity, cm/sec		Bay Tide Range Inches	Head Difference Inches	Minimum Cross-Section Area, sq ft
		Flood	Ebb			
0	0					0.562
2	52.5	43	-32	0.17	0.67	0.62
4	105	40	-36	0.17	0.67	0.672
6	157.5	33	-33		-0	0.766
8	210	30	-27		-0	0.735
10	262.5	27	-27		-0	0.758
12	315	31	-30		-0	0.851
14	367.5	35	-29	0.22	0.67	0.862
16	420	35	-30	0.22	0.67	0.926
18	472.5	36	-32	0.23	0.66	0.911
20	525	35	-33	0.26	0.67	1.003
22	577.5	37	-32	0.25	0.67	1.017
24	630	34	-27	0.25	0.66	1.032
26	682.5	34	-34	0.26	0.64	1.059
28	735	36	-35	0.26	0.61	1.063
30	787.5	35	-35	0.27	0.57	1.123
32	840	35	-35	0.28	0.58	1.089
34	892.5	35	-33	0.29	0.6	1.178
38	997.5	37	-34	0.31	0.6	1.182
40	1050	33	-38	0.28	0.62	1.226
42	1103	35	-39	0.3	0.65	1.196
44	1155	33	-36	0.31	0.6	1.266
46	1208	37	-36	0.32	0.59	1.308
48	1260	36	-36	0.32	0.63	1.322
50	1313	36	-33	0.33	0.56	1.353
52	1365	33	-31	0.33	0.62	1.341
54	1418	33	-31	0.33	0.62	1.347

REPORT DOCUMENTATION PAGE

Form Approved
OMB No. 0704-0188

Public reporting burden for this collection of information is estimated to average 1 hour per response, including the time for reviewing instructions, searching existing data sources, gathering and maintaining the data needed, and completing and reviewing this collection of information. Send comments regarding this burden estimate or any other aspect of this collection of information, including suggestions for reducing this burden to Department of Defense, Washington Headquarters Services, Directorate for Information Operations and Reports (0704-0188), 1215 Jefferson Davis Highway, Suite 1204, Arlington, VA 22202-4302. Respondents should be aware that notwithstanding any other provision of law, no person shall be subject to any penalty for failing to comply with a collection of information if it does not display a currently valid OMB control number. **PLEASE DO NOT RETURN YOUR FORM TO THE ABOVE ADDRESS.**

1. REPORT DATE (DD-MM-YYYY) September 2001		2. REPORT TYPE Final report		3. DATES COVERED (From - To)	
4. TITLE AND SUBTITLE Tidal Inlet Equilibrium Area Experiments, Inlet Laboratory Investigations				5a. CONTRACT NUMBER	
				5b. GRANT NUMBER	
				5c. PROGRAM ELEMENT NUMBER	
6. AUTHOR(S) William C. Seabergh, David B. King, Jr., Bettye E. Stephens				5d. PROJECT NUMBER	
				5e. TASK NUMBER	
				5f. WORK UNIT NUMBER WU 32935	
7. PERFORMING ORGANIZATION NAME(S) AND ADDRESS(ES) U.S. Army Engineer Research and Development Center Coastal and Hydraulics Laboratory 3909 Halls Ferry Road, Vicksburg, MS 39180-6199				8. PERFORMING ORGANIZATION REPORT NUMBER ERDC/CHL TR-01-20	
9. SPONSORING / MONITORING AGENCY NAME(S) AND ADDRESS(ES) U.S. Army Corps of Engineers Washington, DC 20314-1000				10. SPONSOR/MONITOR'S ACRONYM(S)	
				11. SPONSOR/MONITOR'S REPORT NUMBER(S)	
12. DISTRIBUTION / AVAILABILITY STATEMENT Approved for public release; distribution is unlimited.					
13. SUPPLEMENTARY NOTES					
14. ABSTRACT <p>This study was designed to examine the relationship among channel area, tidal period, tidal prism, and maximum channel velocity. Movable-bed model experiments were run to define an equilibrium area for different tidal periods and sediments. The magnitude of the areas measured provided additional data for the relationship of the tidal prism versus minimum channel area in a size range slightly larger than previous laboratory data in the continuum to very large field inlets. These data may help define the tidal prism-minimum channel cross-sectional area relationship in the midrange channel size.</p> <p>The study determined that physical model simulations in the idealized inlet model facility, other laboratory data, and field data support a relationship, initially derived analytically, between an inlet equilibrium area A_c, maximum inlet velocity U_m, tidal period T, and tidal prism P as $A_c = \frac{\pi P}{T U_m}$</p> <p style="text-align: right;">(Continued)</p>					
15. SUBJECT TERMS <div style="display: flex; justify-content: space-between;"> <div>Inlet equilibrium cross-sectional area</div> <div>Movable-bed model</div> </div> <div style="display: flex; justify-content: space-between;"> <div>Inlet physical model</div> <div>Tidal inlet</div> </div>					
16. SECURITY CLASSIFICATION OF:			17. LIMITATION OF ABSTRACT	18. NUMBER OF PAGES 80	19a. NAME OF RESPONSIBLE PERSON
a. REPORT UNCLASSIFIED	b. ABSTRACT UNCLASSIFIED	c. THIS PAGE UNCLASSIFIED			19b. TELEPHONE NUMBER (include area code)

14. (Concluded).

This relationship may be used to define equilibrium inlets that meet the assumptions used in its derivation, namely, an inlet with a bay or lagoon that fills uniformly (i.e., the tidal wavelength is much greater than bay length), has a sinusoidal bay tide, or nearly so, and a channel cross-sectional area that does not change significantly during the tidal cycle. This was noted from how well the laboratory data (which represent true equilibrium inlets) were equivalent to the calculated areas of this equation. The relationship could be applied to field data to evaluate data points that do not define an equilibrium relationship between minimum cross-sectional area and tidal prism. These filtered data may then be used to define new, more accurate, tidal prism versus equilibrium area relationships among all sizes of inlets, from laboratory to large field inlets.

Other observations indicated equilibrium area channels for tide-only conditions retained their original length and widened and deepened upon approaching equilibrium cross-sectional area. Equilibrium area channels following tide-plus-wave conditions migrated bayward as they approached equilibrium and shortened in length.